# Discovery and Optimization of the First PqsR Antagonists as Anti-virulence Agents Combating *Pseudomonas aeruginosa* Infections

## Dissertation

zur Erlangung des Grades des Doktors der Naturwissenschaften
der Naturwissenschaftlich-Technischen Fakultät III
Chemie, Pharmazie, Bio- und Werkstoffwissenschaften
der Universität des Saarlandes

von

**MMed Cenbin LU**

Saarbrücken, 2014

Die vorliegende Arbeit wurde von September 2009 bis März 2014 unter Anleitung von Herrn Prof. Dr. Rolf W. Hartmann am Helmholtz Institut für pharmazeutische Forschung und in der Fachrichtung 8.2 Pharmazeutische und Medizinische Chemie der Naturwissenschaftlich-Technischen Fakultät III der Universität des Saarlandes angefertigt.

| | |
|---|---|
| Tag des Kolloquiums: | 04. 09. 2014 |
| Dekan: | Prof. Dr. Volkhard Helms |
| Berichterstatter: | Prof. Dr. Rolf W. Hartmann |
| | Prof. Dr. Rolf Müller |
| Vorsitz: | Prof. Dr. Claus-Michael Lehr |
| Akad. Mitarbeiter: | Dr. André Schäftlein |

# Abstract

Antibiotic resistance is emerging as a tremendous medical burden worldwide. The mode of action of antibiotics is based on killing or growth inhibition, thus leading to an inevitable selection of resistant strains. The predicament obliges human beings to explore novel therapeutic concepts. Quorum sensing (QS) communication system stringently regulates the bacterial pathogenicity without affecting viability making QS an ideal target for development of new anti-infectives being less prone to resistance (QS inhibitors, QSIs). For *P. aeruginosa*, we started to develop QSIs blocking its crucial QS receptor PqsR, and discovered the first PqsR antagonist **I-20/II-1** by modification of the natural agonist HHQ. However, the antagonist suffered from ineffectiveness in *P. aerugnosa* due to an unexpected functional inversion mediated by a bacterial enzyme. Overcoming the undesired biotransformation resulted in the most potent anti-infective PqsR antagonist discovered so far (**II-3**) that fully protects *Galleria mellonella* from *P. aeruginosa* infections at a low nanomolar concentration, thus providing the first proof-of-concept for PqsR as a therapeutic target. To improve the druglikeness, the compounds were further optimized, and a second promising compound **III-16** with enhanced solubility was identified. Overall, this work describes the discovery of inhibitors for a novel anti-infective target, a rational procedure for rescuing ineffective compounds, and a reasonable process to improve drug-like properties. This research may illuminate a promising avenue for combating antibiotic-resistant *P. aeruginosa* infections.

# Zusammenfassung

Antibiotikaresistenz stellt weltweit eine enorme medizinische Herausforderung dar. Da Antibiotika durch Abtötung der Krankheitserreger oder Hemmung des Zellwachstums wirken, kommt es unvermeidlich zur Selektion von resistenten Bakterienstämmen. Deswegen ist die Forschung gezwungen, neue therapeutische Konzepte zu entwickeln. Das Quorum Sensing (QS) Kommunikationssystem reguliert die Pathogenität der Bakterien ohne ihre Lebensfähigkeit zu beeinflussen. Deshalb wird QS als ein ideales Target angesehen, um neue anti-infektive Wirkstoffe (QS Inhibitoren, QSIs) zu entwickeln, die eine deutlich geringere Resistenzbildungsrate besitzen sollten. Für *P. aeruginosa* haben wir begonnen QSIs gegen den wichtigen QS Rezeptor PqsR zu entwickeln. Die ersten PqsR Antagonisten (z.B. **I-20**/**II-1**) wurden durch Modifikation des natürlichen Agonisten HHQ erhalten. Der aktivste Antagonist war in *P. aeruginosa* wenig wirksam,was auf eine unerwartete Umkehr der Funktionalität der Substanz zurückgeführt werden konnte. Schutz vor der ungewollten Biotransformation durch chemische Modifikation führte zu dem aktivsten anti-infektiven Wirkstoff (**II-3**) innerhalb dieser Arbeit. Bei einer Konzentration von nur 22 nM konnte **II-3** *Galleria Mellonella* vollständig vor *P. aeruginosa* Infektion schützen. Somit haben wir das erste Proof-of-Concept für die Relevanz von PqsR als therapeutisches Target geliefert. Zur Verbesserung der Druglikeness wurden die Verbindungen weiter optimiert. Dabei wurde eine weitere vielversprechende Verbindung **III-16** mit verbesserter Löslichkeit identifiziert. Zusammenfassend beschreibt die vorliegende Arbeit die Identifizierung von Inhibitoren eines neuen anti-infektiven Targets, die Rettung inaktiver Substanzen durch eine rationale Strategie, sowie ein Verfahren zur Verbesserung der physicochemischen Wirkstoffeigenschaften. Sie zeigt einen möglichen Weg auf, um zukünftig Antibiotika-resistente Infektionen mit *P. aeruginosa* zu bekämpfen.

# Papers Composing this Dissertation

This doctoral dissertation comprises three publications, which are referred to in the text by their Roman numerals.

I. **Discovery of Antagonists of PqsR, a Key Player in 2-Alkyl-4-quinolone-Dependent Quorum Sensing in *Pseudomonas aeruginosa***

   Cenbin Lu, Benjamin Kirsch, Christina Zimmer, Johannes C. de Jong, Claudia Henn, Christine K. Maurer, Mathias Müsken, Susanne Häussler, Anke Steinbach, Rolf W. Hartmann

   *Chemistry & Biology* **2012**, *19*, 381–390.

II. **Overcoming the Unexpected Functional Inversion of a PqsR Antagonist in *Pseudomonas aeruginosa*: an *in vivo* Potent Antivirulence Agent Targeting *pqs* Quorum Sensing**

   Cenbin Lu, Christine K. Maurer, Benjamin Kirsch, Anke Steinbach, Rolf W. Hartmann

   *Angewandte Chemie International Edition* **2014**, *53*, 1109–1112.

III. **Optimization of Anti-virulence PqsR Antagonists Regarding Aqueous Solubility and Biological Properties Resulting in New Insights in Structure-activity Relationships**

   Cenbin Lu, Benjamin Kirsch, Christine K. Maurer, Johannes C. de Jong, Andrea Braunshausen, Anke Steinbach, Rolf W. Hartmann

   *European Journal of Medicinal Chemistry* **2014**, *79*, 173–183.

# Contribution Report

The author wishes to clarify his contributions to the papers **I**–**III** composing this dissertation.

**I.** Significant contribution to the antagonist design conception. Syntheses and characterization of the compounds (**1**–**21** and **29**–**42**), with the rest compounds synthesized by Dr. Johannes C. de Jong. Significant contribution to the interpretation of the results to SAR. Significant contribution to the composition of manuscript.

**II.** Significant contribution to the antagonist design conception. Syntheses and characterization of the compounds (**1**–**3**). Significant contribution to the evaluation of compound in nematode infection model. Significant contribution to the composition of manuscript.

**III.** Significant contribution to the antagonist design conception. Syntheses and characterization of the compounds (**1**–**31**). Significant contribution to the interpretation of the results to SAR and SPR. Significant contribution to the composition of manuscript.

# Further Publications of the Author

The author also contributes to the following papers by synthesizing compounds and by composing the manuscript. However, these works are marginal comparing to the main body of this dissertation and therefore are not included.

IV. **Antibiotic-free Nanotherapeutics: Ultra-small Mucus-penetrating Solid Lipid Nanoparticles Enhance the Pulmonary Delivery and Antivirulence of Novel Quorum Sensing Inhibitors**

Noha Nafeea, Ayman Husaria, Christine K. Maurer, Cenbin Lu, Anke Steinbach, Rolf W. Hartmann, Claus-Michael Lehr, Marc Schneider

To be submitted.

V. **Chapter 8.2: Synthetic QSIs Blocking Receptor Signaling or Signal Molecule Biosynthesis in *P. aeruginosa***

Christine K. Maurer, Cenbin Lu, Martin Empting, Rolf W. Hartmann

*Quorum Sensing VS Quorum Quenching: A Battle with no End in Sight.* ed. Vipin Chandra Kalia (Springer-Verlag GmbH Berlin Heidelberg) submitted.

# Acknowledgement

I hereby extend my heartfelt thanks to my doctoral advisor, Prof. Dr. Rolf W. Hartmann, for introducing me into the field of quorum sensing inhibition and giving me such an amazing topic for my PhD work. His innovative ideas, broad knowledge and enthusiasm for science always guided and encouraged me during my PhD studies. I treasure this experience of working with him very much.

I express my sincere gratitude to Prof. Dr. Claus-Michael Lehr for being the chairman of the promotion committee.

I gratefully acknowledge my Berichterstatter Prof. Dr. Rolf Müller for the review of this dissertation.

I would like to thank Dr. André Schäftlein for being the member of the promotion committee.

I appreciate Dr. Anke Steinbach, Dr. Johannes C. de Jong, Dr. Simon Lucas and Dr. Martin Empting as excellent group leaders. Thank you for your trust, instruction and encouragement.

The full support from Dr. Matthias Negri, Dr. Stefan Boettcher, Dr. Josef Zapp and Dr. Matthias Groh in structure study as well as LC-MS and NMR measurement and resolution, respectively, is effusive in my gratitude.

I would like to thank Dr. Christina Zimmer, Dr. Andrea Braunshausen, Dr. Jörg Haupenthal, Ms. Simone Amman, Ms. Jeannine Jung, Ms. Jannine Ludwig and Ms. Carina Scheid for their kind help in biological evaluation of synthesized compounds.

I convey my warmest thanks to all members of the PQS group. Special thanks to Christine K. Maurer and Benjamin Kirsch for the productive and wonderful teamwork.

I would thank the members of the team of Praktitum für Organische Chemie: Dr. Matthias Engel, Dr. Michael Ring, Dr. Cornelia M. Grombein, Juliette Emmerich, Michael P. Storz and Jan H. Sahner. I cherish the past good days we spent together.

I am grateful to Dr. Matthias Engel, Dr. Stefan Boettcher, Dr. Qingzhong Hu, Dr. Kuiying Xu, Dr. Martin Frotscher, Mr. Lothar Jager, Ms. Katrin Schmitt, Ms. Martina Schwarz and Ms. Barbara Boeffel for their help with my accommodation and in coping with all kinds of bureaucratic procedures as I came here for the first time.

Finally, I would like to express my deep love to my family. I thank my beloved parents, who are adamant in support of me to actualize my dream. I thank my devoted wife for sharing my joyance and solacing my fidgetiness during my PhD studies. Special thanks to my grandparents, two venerable chemists, who were the first teachers to initiate me into chemistry and biology. Thank you for being in my life.

# Abbreviations

| | |
|---|---|
| 3-oxo-C12-HSL | *N*-3-oxododecanoyl-L- homoserine lactone |
| AI | autoinducer |
| AMPs | antimicrobial peptides |
| C4-HSL | *N*-butanoyl-L-homoserine lactone |
| CBF | ciliary beat frequency |
| CF | cystic fibrosis |
| CLSM | confocal laser scanning microscopy |
| Duox/$SCN^-$/LPO | dual oxidase-thiocyanate-lactoperoxidase |
| EDG | electron-donating group |
| eDNA | extracellular DNA |
| EPS | extracellular polymeric substances |
| EWG | electron-withdrawing group |
| GCSF | granulocyte colony-stimulating factor |
| GM-CSF | granulocyte-macrophage colony-stimulating factor |
| GSH | glutathione |
| HAQ | 2-alkyl-4-hydroxyquinoline |
| HHQ | 2-heptyl-4-hydroxyquinoline |
| ISS | International Space Station |
| MOA | mechanism of action |
| MvfR | multiple virulence factor regulator |
| MVs | membrane vesicles |
| ORFs | open reading frames |
| *P. aeruginosa* | *Pseudomonas aeruginosa* |
| PE | *pseudomonas* elastase |
| PMNs | polymorphonuclear leukocytes |
| PQS | *Pseudomonas* quinolone signal |
| QS | quorum sensing |
| QSIs | quorum sensing inhibitors |
| ROS | reactive oxygen species |
| SEM | scanning electron micrograph |
| V-ATPase | vacuolar ATPase |

# Contents

# 1 Introduction

Nowadays, it is well recognized that bacteria do not live as a loose community but organize their behaviors via cell-to-cell communication systems and act as a multicellular organism. Such well coordinated group behaviors are usually associated with pathogenicity (e.g. production of virulence factors, formation of biofilm), however, normally not involved in bacterial viability. Along with the understanding of bacterial communication, a novel anti-infective strategy is brought to light, which selectively attenuates bacterial pathogenicity without affecting the growth by disrupting cell-to-cell communication. Such a strategy would in all probability bring us the dawn of overcoming the rising problem of antibiotic resistance during the long-lasting war between human beings and pathogenic bacteria.

## 1.1 *Pseudomonas aeruginosa*

*Pseudomonas aeruginosa* is a common important Gram-negative bacterium (**Figure 1**) first isolated in 1882 by the French pharmacist and bacteriologist Carle Gessard from wound of soldiers whose bandages had a blue and green color (Gessard, 1984). It possesses a notable large and diverse genome of 5–7 Mb encoding circa 6000 open reading frames (ORFs) (Stover et al., 2000). The high genetic and metabolic versatility enables *P. aeruginosa* to adapt most natural and artificial environments throughout the world from soil, water, tissues of plants and animals, medical equipments, even to International Space Station (ISS) (Kim et al., 2013).

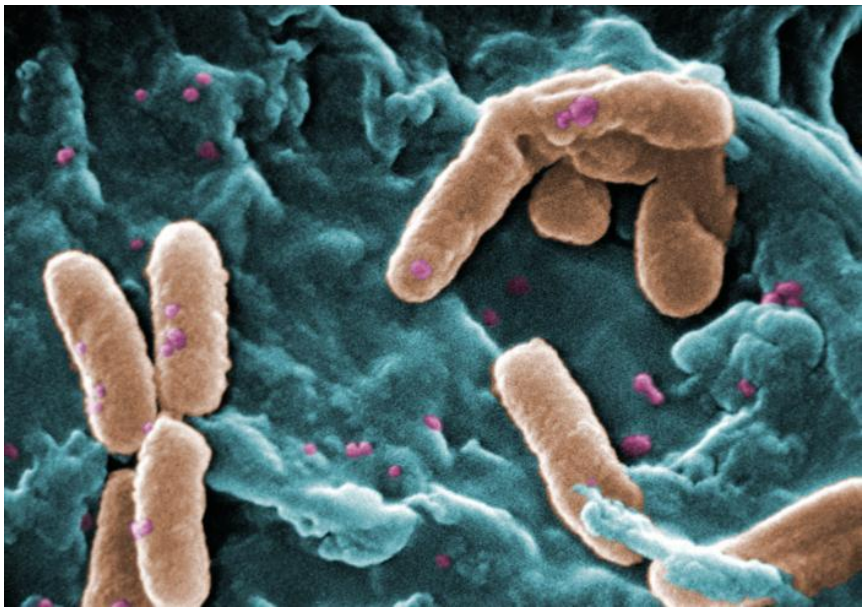

**Figure 1. Scanning electron micrograph (SEM) of *P. aeruginosa*.**
(adopted from http://phil.cdc.gov/phil/details.asp?pid=10043)

As an opportunistic human pathogen *P. aeruginosa* is able to colonize in burns, wound, blood,

gastrointestinal, pulmonary and urinary tracts, and is a leading cause of life-threatening nosocomial infections. It preferentially infects immuno-compromised individuals and cystic fibrosis (CF) patients, and is the main responsible factor for chronic lung infections (Koch and Hoiby, 1993) as well as the mortality of CF patients (Govan and Deretic, 1996).

The eradication of *P. aeruginosa* is a great medical challenge because it is intrinsically resistant to antibiotics or disinfectants (Strateva and Yordanov, 2009). Besides, this microorganism is able to produce an arsenal of virulence factors as well as establish microcolonies encased with exopolysaccharides forming a biofilm community. Virulence factors and biofilm help the bacterial cells to effectively counterwork the human immune response and dramatically decrease the susceptibility to antibiotics (Costerton et al., 1999).

## 1.2 Quorum Sensing (QS) and QS-regulated Pathogenicity/ Virulence of *P. aeruginosa*

### 1.2.1 Quorum Sensing

Quorum sensing (QS) is a cell-to-cell communication system first discovered in the bioluminescent bacterium *Vibrio fischeri* (Nealson et al., 1970). It allows bacteria to determine their local population, make cell density-dependent collective decisions thereby coordinating the whole bacterial community to behavior like a multicellular organism (**Figure 2**). Notably, such well coordinated group behaviors are normally not involved in bacterial viability (Galloway et al., 2012; LaSarre and Federle, 2013) but always connected to pathogenicity/virulence, including the expression of virulence factors, the formation of biofilm, swarming, swimming as well as twitching, which facilitate the invasion into the hosts, counteract host immune system as well as promote resistance/tolerance towards conventional antibiotics (Miller and Bassler, 2001).

A typical QS system consists of three components: a signal molecule (termed autoinducer or AI), a receptor/transcriptional regulator and a synthase producing AI. AI is able to specifically activate the receptor thereby initiating the transcription of certain genes including those for AI biosynthesis (gene encoding the synthase), which enables a positive autoinducing loop. However, at a low population the AI secreted into the surrounding medium is strongly diluted due to the diffusion, thus, the activation of the receptor is only at a basal level. As the cell density increases, the AI reaches a threshold concentration leading to a full activation of the receptor and up-regulation of target genes, most of which, as mentioned above, are related to the bacterial pathogenicity (**Figure 2**) (Miller and Bassler, 2001).

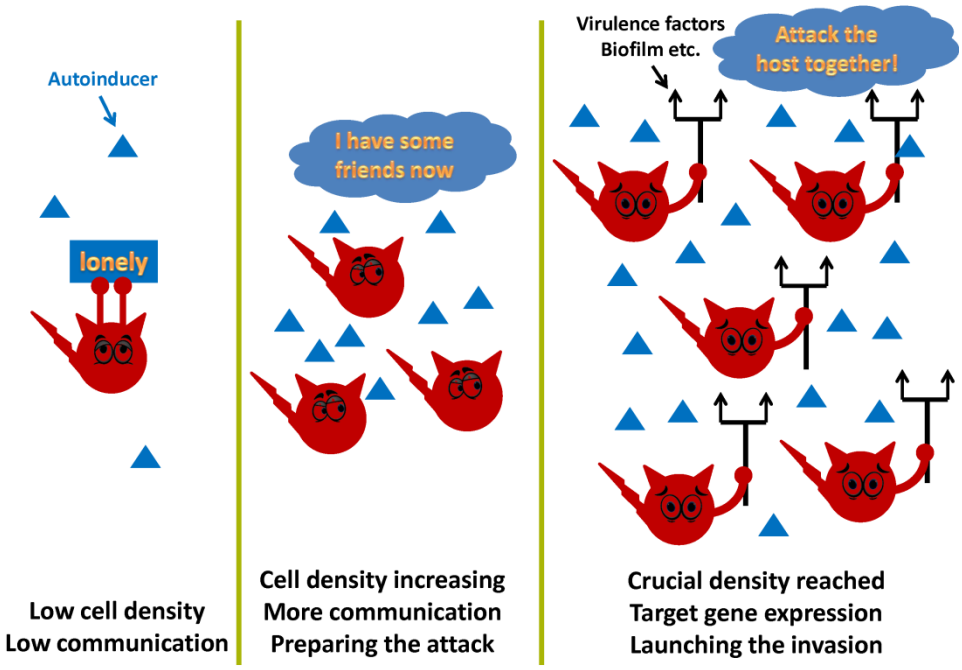


**Figure 2. Pathogen determines cell density and coordinates gene expression for infections via QS communication.**

*P. aeruginosa* employs three main QS systems, denoted *las* (Gambello and Iglewski, 1991; Passador et al., 1993), *rhl* (Ochsner et al., 1994; Ochsner and Reiser, 1995) and *pqs* (Pesci et al., 1999). All the networks are hierarchically interconnected: *las* controls the other two systems (Pesci et al., 1997; Wade et al., 2005), and is therefore regarded as the master regulator; *pqs* positively regulates the *rhl* signaling (McKnight et al., 2000), while *rhl* in turn puts a negative feedback upon *pqs* (**Figure 3**) (McGrath et al., 2004; Wade et al., 2005). Although *las* is generally to be considered to sit on the top of the QS hierarchy of *P. aeruginosa*, it is worth to note that the subordinate systems, *rhl* and *pqs*, can still be activated in the absence of *las* under certain conditions (Dekimpe and Deziel, 2009; Diggle et al., 2003; Lee et al., 2013).

For the *las* QS the synthase LasI produces the AI *N*-3-oxododecanoyl-L- homoserine lactone (3-oxo-C12-HSL), which activates the receptor LasR. Similarly, RhlI produces *N*-butanoyl-L-homoserine lactone (C4-HSL), which stimulates RhlR. While both homoserine-mediated QS systems are broadly applied by various bacteria, the recently discovered species-specific *pqs* QS only occurs in *Pseudomonas* (Pesci et al., 1999), and is receiving increasing attention. The *Pseudomonas* Quinolone Signal (PQS) and to a lesser extent its precursor 2-heptyl-4-hydroxyquinoline (HHQ), two most predominant members of the 2-alkyl-4-hydroxyquinoline (HAQ) family (Deziel et al., 2004) function as AIs of the *pqs* system, and activate their cognate receptor PqsR (Cao et al., 2001; Xiao et al., 2006), a LysR-type transcriptional regulator (Maddocks and Oyston, 2008) that drives the coordinated expression of

nearly 200 genes (**Figure 3**). Many of these genes are related to virulence factors, such as *phzA1-G1*, which is involved in the biosynthesis of pyocyanin, *hcnAB*, which is responsible for production of hydrogen cyanide, *lasB*, which encodes elastase B and *lecA*, which codes for Lectin A (Cao et al., 2001; Deziel et al., 2005). The *pqs* QS also indirectly promotes the production of rhamnolipids via activating the *rhl* system as mentioned before. Besides virulence factors, biofilm formation is also regulated by the *pqs* system (Diggle et al., 2003). Moreover, other QS regulated activities, for instance membrane vesicles formation (Mashburn-Warren et al., 2009; Mashburn-Warren et al., 2008), are under the control of *pqs* signaling. Furthermore, PqsR activates *pqsABCD* located in the *pqs* operon to express the synthases, which conduct the biosynthesis of the AI HHQ, which is further converted to PQS by the LasR-regulated monooxygenase PqsH (Deziel et al., 2004; Gallagher et al., 2002; Schertzer et al., 2010). Thus, a positive feedback is triggered by activation of PqsR by either PQS or HHQ (McGrath et al., 2004), which allows an initial rapid increase of extracellular PQS levels during an exponential growth phase.

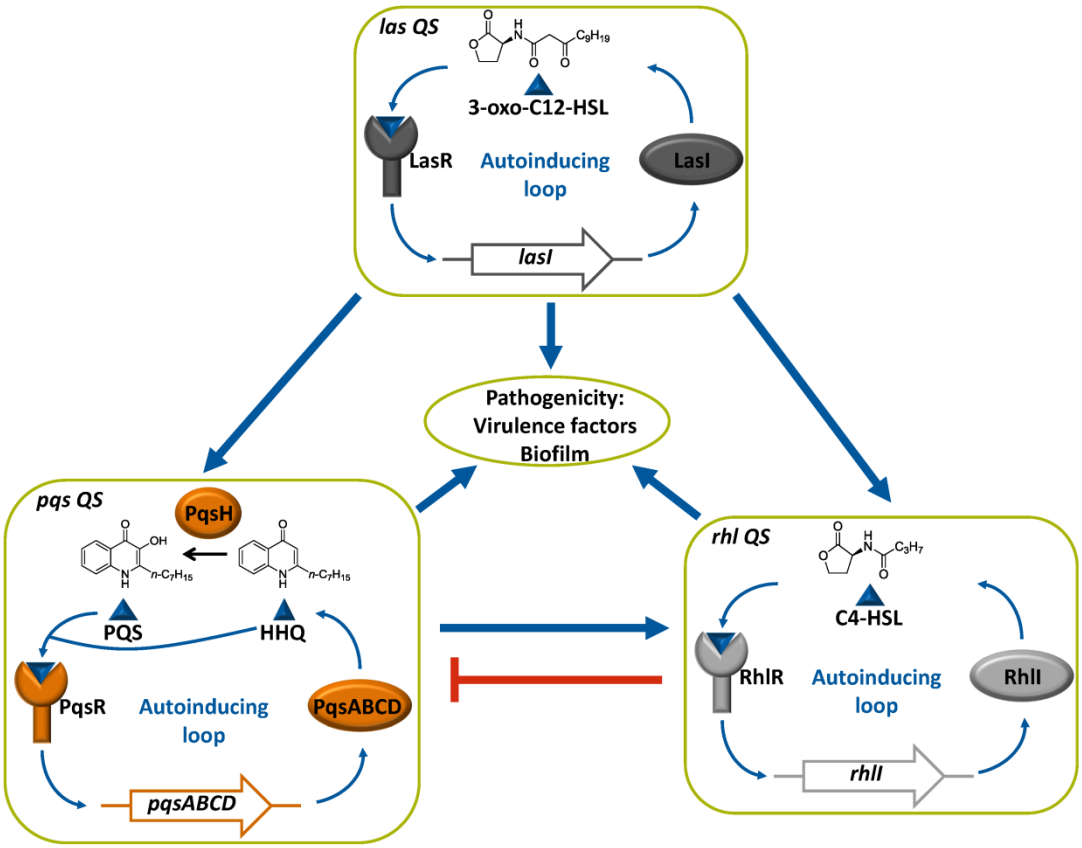


**Figure 3. Three intertwined QS systems in *P. aeruginosa*.**

### 1.2.2 Virulence Factors

Virulence factors are molecules or cell structures expressed by pathogenic bacteria contributing to the virulence/pathogenicity such as destructive enzymes, toxins, siderophores, pili and flagella.

The virulence factors empower the bacteria to invade the host, escape from host immune surveillance, repress the host immune response, as well as decrease the susceptibility towards antibiotics (Lyczak et al., 2000). The virulence factors play undoubtedly a critical role for the infections, however, they are normally not involved in bacterial growth (Galloway et al., 2012; LaSarre and Federle, 2013). In this section elastase B, rhamnolipids and pyocyanin are chosen as representative virulence factors of *P. aeruginosa*, which are directly or indirectly controlled by *pqs* QS.

#### 1.2.2.1 Elastase B

Elastase B, also termed LasB protease, *pseudomonas* elastase (PE) or pseudolysin, is a 33 kDa elastolystic metalloprotease from the thermolysin family (Kessler et al., 1998; Morihara, 1995) encoded by the *lasB* gene of *P. aeruginosa*. The activation of *lasB* is positively controlled by *pqs* QS, and exogenous PQS strongly induces expression of elastase B even in the *las* mutant (McKnight et al., 2000). This destructive enzyme is able to destroy host tissues via specific cleavage of the structural proteins such as type III and IV collagens (Heck et al., 1986), which are common components of the extracellular matrix widely existing in dermis, lung, blood vessel walls, liver and spleen (Miller and Gay, 1982). Elastase B damages tight junction-associated proteins ZO-1 and ZO-2 thereby breaking down the epithelial barriers (Azghani, 1996; Azghani et al., 1990; Azghani et al., 1993). Moreover, this protease also functions as a powerful weapon towards host innate and adaptive immune systems, since it degrades a battery of cytokines (e.g. INF-γ, IL-2 and IL-8), chemokines, immunoglobulins (e.g. IgA and IgG), human airway lysozymes (Jacquot et al., 1985), antimicrobial peptides (AMPs) as well as phagocytosis-related surfactant proteins e.g. SP-A Kuang (Kuang et al., 2011). Overall, Elastase B supports the *P. aeruginosa* infections in a variety of ways, and therefore is regarded as an important contributor to pathogenicity.

#### 1.2.2.2 Rhamnolipids

Rhamnolipids are a class of glycolipids produced by *P. aeruginosa* including monorhamnolipid and dirhamnolipid (**Chart 1**). Three enzymes RhlA, RhlB and RhlC, all of which are under control of *pqs* and *rhl* QS (Deziel et al., 2005; Ochsner et al., 1994; Ochsner and Reiser, 1995; Rahim et al., 2001), are required for the biosynthesis of rhamnolipids.

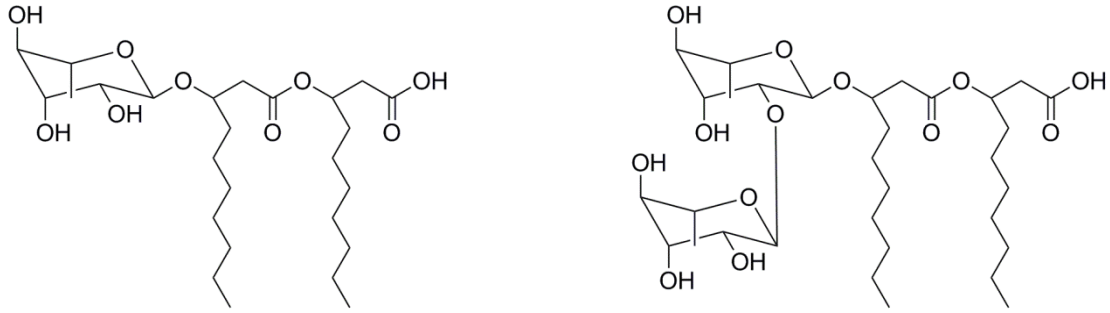


**Chart 1. Structures of rhamnolipids.**

Although these heat-stable glycolipids are well known for their properties as biosurfactants, multiple biological functions have been discovered. First, rhamnolipids guarantee a trouble-free QS communication. The AI of *pqs* QS, PQS, shows a poor solubility due to the high lipophilicity making a great problem for signal transmission for *P. aeruginosa*. Besides packing PQS into membrane vesicles (MVs) to assist the delivery (Mashburn and Whiteley, 2005), the bacteria also use rhamnolipids to enhance the solubility of PQS likely via forming micelles (Calfee et al., 2005). Second, rhamnolipids act as wetting agents to reduce surface tension and correspondingly enhance bacterial translocation abilities in the medium e.g. swarming and twitching (Glick et al., 2010). Due to the massive influence on bacterial motility the surfactants play a crucial role for determining and maintaining biofilm architecture. Rhamnolipids are responsible for keeping the fluid channels around the biofilm open possibly by preventing planktonic cells from attaching to the formed biofilm. This is supported by the result that *rhlA* mutant, which is not able to produce rhamnolipids, is unable to sustain the water channels around the biofilm and forms a thick and flat biofilm (Davey et al., 2003). Third, rhamnolipids function as toxins to host cells. In addition to rupturing erythrocytes (hemolysis) (Johnson and Boese-Marrazzo, 1980), this virulence determinant is detrimental to immunocytes, particularly, the polymorphonuclear leukocytes (PMNs), which are directly induced to necrosis (Jensen et al., 2007). Usually, rhamnolipids form an anti-PMNs shield outside of the biofilm *in vivo* and collapse the attack of PMNs besieging the *P. aeruginosa* aggregate. The subsequent necrotic lysis of the immunological cells not only elevates the inflammation levels to recruit more PMNs to be victims of rhamnolipids killing but also supplies more extracellular DNA (eDNA, a component of biofilm, also see below, "**1.2.3 biofilm**") to strengthen the biofilm (Alhede et al., 2014). All the evidences underline the crucial role of rhamnolipids in the infectious process.

#### 1.2.2.3 Pyocyanin

Pyocyanin is a redox-active pigment possessing a phenazine core (**Chart 2**). Its biosynthesis is

conducted by synthases PhzA1-G1, PhzM and PhzS. There is an intimate connexion with *pqs* QS. On one hand, HHQ/PQS-deficient mutants (*pqsA* and *pqsR* mutants) are unable to produce pyocyanin (Cao et al., 2001; Deziel et al., 2004); on the other hand, pyocyanin formation is also controlled in a HHQ/PQS-independent manner by the action of PqsE, which is co-regulated in the *pqs* operon (*pqsABCDE*), and is able to restore pyocyanin levels in *pqsA* or *pqsR* mutants (Farrow et al., 2008; Rampioni et al., 2010).

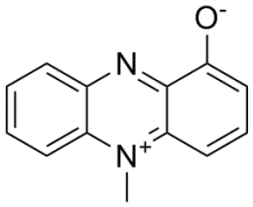


Pyocyanin

**Chart 2. Structures of pyocyanin.**

As a multifunctional virulence factor pyocyanin is of great significance for *P. aeruginosa*. First, due to its redox properties pyocyanin functions as an electron transporter that accepts and transfers electrons generated from bacterial respiration chain to electron acceptors distant from the colonies (e.g. an air-water interface), thus, enable the aerobic respiration of *P. aeruginosa* even under oxygen-limited conditions (Rada and Leto, 2013). Second, this compound displays antibiotic activities towards protozoa, fungi and bacteria, especially Gram-positive bacteria, therefore helping its producer organism to gain advantages over other competitors in the environment (Baron and Rowe, 1981). Third, the interaction between pyocyanin and molecular oxygen affords reactive oxygen species (ROS) e.g. $H_2O_2$, which induces a cell lysis of *P. aeruginosa* and subsequently promotes the release of eDNA (Das and Manefield, 2012). This result implies that the virulence determinant may indirectly contribute to biofilm formation (Das et al., 2013). Fourth, pyocyanin causes massive cell dysfunction, injury and death of hosts. Most of these activities are attributed to the disruption of redox homeostasis, in other words, exposure of host cells to oxidative stress, by means of depleting intracellular pools of NAD(P)H and glutathione (GSH), generating superoxide as well as downstream ROS (Muller, 2002; O'Malley et al., 2004). Particularly for mammalian cells pyocyanin has a variety of biological effects: it elicits mucin overproduction, and diminishes the ciliary beat frequency (CBF) of nasal ciliated epithelium cells preventing the host from wiping out the pathogens (Wilson et al., 1988); it decreases mitochondrial aconitase activity and membrane potential, represses the cellular respiration and depletes intracellular ATP levels (O'Malley et al., 2003a); it inactivates vacuolar ATPase (V-ATPase), and interrupts non-mitochondrial ATP consumption and generation as well as V-ATPase-regulated physiological processes e.g.

receptor-mediated endocytosis and altered localization of cystic fibrosis transmembrane conductance regulator (Lau et al., 2004); it also impairs the cellular catalase activity via both transcriptional regulation and direct inactivation of the enzyme depriving the ability of the cells to break down the tissue-damaging $H_2O_2$ (O'Malley et al., 2003b). Besides, pyocyanin is able to block the dual oxidase-thiocyanate-lactoperoxidase (Duox/$SCN^-$/LPO) system hampering the production of microbicidal oxidant hypothiocyanite (Rada et al., 2008). Moreover, pyocyanin modulates host immune response by induction of a series of cytokines, such as TNF-a, IL-1β, granulocyte colony-stimulating factor (GCSF), granulocyte-macrophage colony-stimulating factor (GM-CSF), IL-6, IL-11, IL-19, IL-20, IL-23 and IL-24, many of which are involved in the inflammatory process (Rada et al., 2011). The multiple biological functions, especially the ability to interact with hosts emphasize pyocyanin as a key virulence factor of *P. aeruginosa*.

### 1.2.3 Biofilm

Under appropriate conditions, planktonically grown *P .aeruginosa* can switch from the nomadic existence to a biofilm lifestyle. A biofilm is defined as a structured community of aggregated bacterial cells embedded into self-produced extracellular polymeric substances (EPS) composed of polysaccharides, eDNA and proteins (Costerton et al., 1999; Costerton et al., 2003).

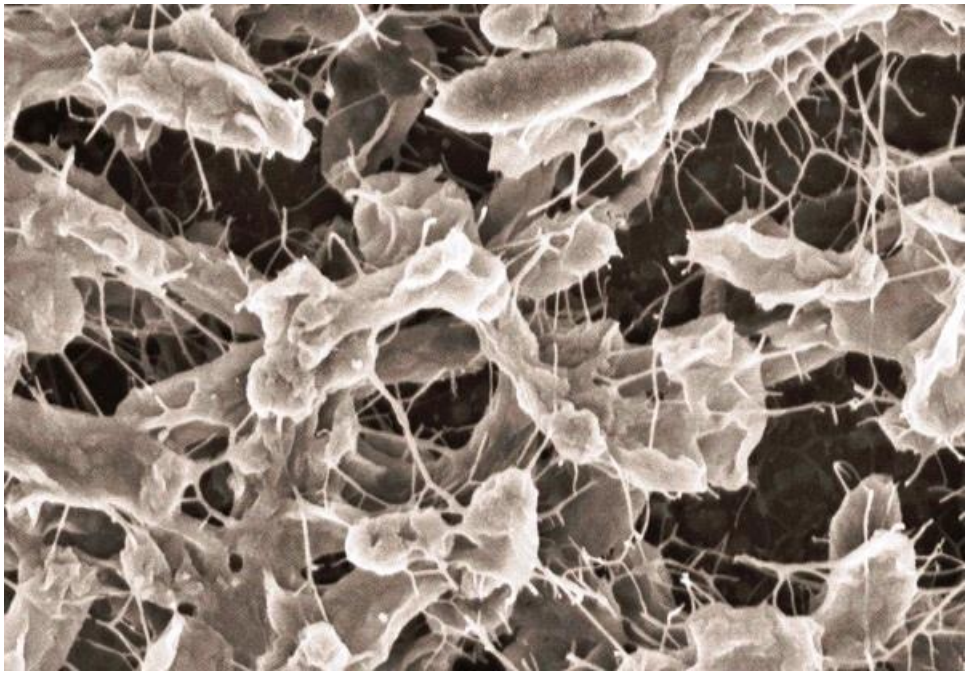

**Figure 3. SEM image of *P. aeruginosa* biofilm.**
(modified from http://eyemicrobiology.upmc.com/PhotoGallery.htm. The author expresses his thanks to the Charles T. Campbell Laboratory and Dr. R. M. Q. Shanks for this figure)

QS is closely connected with such a process (Irie and Parsek, 2008), as the communication

systems control an array of factors that structure biofilm formation, such as rhamnolipids, as mentioned before, which actively maintain open channels that allow the distribution of nutrients and oxygen in the community (Davey et al., 2003), lectins A and B (Winzer et al., 2000), which may contribute to the adhesion of bacteria to the corresponding host tissue, and eDNA resulted from bacterial autolysis provoked either by pyocyanin (Das and Manefield, 2012) or directly by *pqs* QS (D'Argenio et al., 2002), which is a main component of the extracellular matrix. Biofilm not only provides the bacteria a shelter for hiding but also, more importantly, protect the pathogen from a broad spectrum of environmental challenges, particularly antibiotics and host immune system (Hall-Stoodley et al., 2004). Biofilm dramatically increases bacterial tolerance towards traditional antimicrobial agents via diverse mechanisms: first, it serves as a physical diffusion barrier hindering certain antibiotics to penetrate into the full depth of the biofilm; second, special constituents of EPS are able to actively neutralize antibiotics, e.g. the negatively charged eDNA can either directly bind drugs with opposite charges like aminoglycosides, thus impeding the access to the sites of action (Purdy Drew et al., 2009; Ramphal et al., 1988), or indirectly induce *pmr* genes to counteract AMPs (Mulcahy et al., 2008); third, due to nutrient limitation inside the biofilm, the regular bacterial cells exist in a low-growing or starve state having a reduced metabolism rate, and this physiological status leads to diminished sensitivity towards antibiotics targeting active cell process (Costerton et al., 1999); fourth, in addition to the regular cells, there is a small subpopulation of spontaneously dormant and non-dividing variants termed persister cells living in the community, which are much more tolerant towards antimicrobials than other cells (Lewis, 2010). The protective effects of biofilm against host immune system are generally based on physical shielding, induction of necrosis of immunological cells as well as cleavage of immune-related proteins as mentioned above.

## 1.3 PqsR Antagonists as QS Inhibitors (QSIs) for Anti- virulence Therapy against *P. aeruginosa* Infections

### 1.3.1 Anti-virulence Therapy via Quorum Sensing Inhibition

Nowadays, human beings are confronted with an alarming situation in view of the lack of effective therapies against antibiotic-resistant bacterial infections (Arias and Murray, 2009). The predicament is attributed to the mode of action of marketed antibiotics, which is based on interference with bacterial growth (via e.g. targeting cell-wall biosynthesis, inhibiting protein production, or disrupting DNA replication), which results in an inevitable selection of resistant strains (Levy and Marshall, 2004). The emergence of bacterial resistance urgently requires the development of novel anti-infective strategies, however, unfortunately, the discovery of novel anti-infectives that are less prone to resistance is challenging, and the interest of the pharmaceutical

industry to develop new antibiotics is decreasing (Lewis, 2012).

The anti-virulence therapy is a promising strategy to overcome the growing and challenging resistance problem by means of targeting non-vital cell functions that are associated with the bacterial pathogenicity. This novel therapeutic concept has decided advantages over conventional antibiotics-treatment, because the selective intervention into the pathogenic mechanisms without affecting on bacterial viability reduces natural election pressure and therefore delays or avoids the development of resistance (Cegelski et al., 2008; Galloway et al., 2012; Rasko et al., 2008).

Since QS regulates the expression of a large set of pathogenicity-associated genes, corruption of the cell-to-cell communication system by QS inhibitors (QSIs) is an ideal approach for an anti-virulence therapy to disarm rather than kill the pathogens. Basically, three key nodes of the network can be targeted by QSIs: 1) blockade of signal molecule production, e.g. via inhibiting AI synthases; 2) inactivation of signal molecules, via chemical or enzymatic destruction of AIs; 3) interference with signal receptors via antagonizing endogenous agonists or destructing the receptor (Rasmussen and Givskov, 2006a, b).

### 1.3.2 PqsR as an Eligible Target for QSIs

*P. aeruginosa* causes severe and fatal infections and possesses significant intrinsic resistance towards a wide range of conventional antimicrobials including β-lactams, fluoroquinolones, tetracycline, and chloramphenicol (Strateva and Yordanov, 2009). Search for a novel and effective approach to cure the obstinate *P. aeruginosa* infections, anti-virulence therapy via QSIs has been absorbing great attention of researchers worldwide.

QSIs interfering with HSL-based signal pathways (*las* and *rhl* systems) have been investigated. The majority of these anti-*las* or anti-*rhl* QSIs are natural product-derived halogenated furanone compounds (Hentzer et al., 2003) and HSL analogs (Galloway et al., 2011). However, such QSIs suffered from either cytotoxicity towards mammalian cells (Yang et al., 2014) or low activity of repressing the production of virulence factors, and none of them has reached clinical studies to date.

While other research groups are concentrating on compounds targeting *las* or *rhl* QS, we focus on the *P. aeruginosa* specific *pqs* QS, and regard the receptor PqsR as a highly attractive target to develop QSIs (PqsR antagonists) for the following reasons: 1) as mentioned above, *pqs* QS plays a critical role for the pathogenicity, thus, we believe that the blockage of PqsR should attenuate the *pqs*-dependent virulence. This concept has been supported by the fact that the *pqsR* mutant strain displays a reduced mortality rate in mice (Xiao et al., 2006). Additionally, the mutation of *pqs*-controlled virulence genes results in decreased pathogenicity in plants, nematodes and insects (Jander et al., 2000; Mahajan-Miklos et al., 1999). Moreover, based on the fact that PQS is produced in high amounts in the sputum of the CF patients (Collier et al., 2002), it is assumed that

blocking the *pqs* QS system should make the *P. aeruginosa* lung infection in CF patients better treatable. 2) Whereas HSL-mediated QS is widespread among Gram-negative bacteria, we speculate that species-selective targeting of specific regulatory *pqs* QS might help to minimize adverse effects on beneficial bacterial consortia present in the host that are observed with broad-spectrum antibiotics. 3) Considering that the results obtained with inhibitors of AI synthases are less than satisfactory (PqsA and PqsD inhibitors require high concentrations to achieve desirable effects) (Lesic et al., 2007; Storz et al., 2012), we suspect that antagonizing endogenous ligands at the signal receptor should more directly and efficiently impact the QS circuit than blocking of the signal synthases. To the best of our knowledge, there were no such antagonists reported until we started this project. During the cause of the project we discovered the first QSIs targeting PqsR in 2012.

# 2 Work Strategy

## 2.1 Design of PqsR Antagonists

To the best of our knowledge, there is no appropriate crystal structure of PqsR with satisfactory resolution available for protein structure-based drug design to date, and no antagonist of this receptor had been reported before we started this project. The natural ligands, PQS and HHQ are all agonists. Nevertheless, we used them for the design of potential antagonists (ligand-based approach), since it has been known for a long time that antagonists can be obtained by structural modification of agonists (Hartmann et al., 1980).

Although PQS is the most potent natural ligand, we used the less potent HHQ (Xiao et al., 2006) as a starting point for the following reasons: 1) the 3-hydroxy group of PQS has been proven to be responsible for interaction with lipid A of outer membrane lipopolysaccharides (Mashburn-Warren et al., 2008). Thus, HHQ lacking this group should exhibit a lower tendency to membrane association. 2) HHQ does not display iron chelating (Bredenbruch et al., 2006; Diggle et al., 2007) or pro-oxidant properties in contrast to PQS (Haussler and Becker, 2008). Therefore modification of HHQ should avoid these unwanted interactions. Initially, we modified the stereo-electronic configuration of HHQ by changing the length of the alkyl side chain and by introducing electron-donating (EDG) and withdrawing groups (EWG) into the benzene moiety of the quinolone structure. In the next step, to further optimize the active compounds regarding stability and water solubility, the 3-position of HHQ was substituted by diverse functional groups, and an oxygen atom was inserted into the alkyl side chain.

## 2.2 Biological Evaluation of Synthesized Compounds

The functionality of the prepared compounds towards PqsR was initially determined in a β-galactosidase reporter gene assay established in *E. coli*. Strong antagonists were then investigated in a second reporter gene assay constructed in *P. aeruginosa*. Next, the potent compounds were assayed using *P. aeruginosa* wild type PA14 for their biological effects on the production of AIs as well as the virulence factor pyocyanin. Finally, the *in vivo* anti-virulence potency of the most promising compound was evaluated in nematode and insect infection models. Besides, water solubility and iron-chelating properties were detected using standard HPLC and CAS methods, respectively.

# 3 Results and Discussions

## 3.1 Paper I: Discovery of Antagonists of PqsR, a Key Player in 2-Alkyl-4-quinolone-Dependent Quorum Sensing in *Pseudomonas aeruginosa*

This paper has been published in *Chemistry & Biology* **2012**, *19*, 381–390.
Reprinted with permission from *Elsevier*.

Chemistry & Biology
Article

# Discovery of Antagonists of PqsR, a Key Player in 2-Alkyl-4-quinolone-Dependent *Quorum Sensing* in *Pseudomonas aeruginosa*

Cenbin Lu,[1] Benjamin Kirsch,[1] Christina Zimmer,[1] Johannes C. de Jong,[1] Claudia Henn,[1] Christine K. Maurer,[1] Mathias Müsken,[2] Susanne Häussler,[2,3] Anke Steinbach,[1,*] and Rolf W. Hartmann[1,4,*]
[1]Helmholtz Institute for Pharmaceutical Research Saarland, Campus C2.3, 66123 Saarbrücken, Germany
[2]Twincore, Department of Pathophysiology of Bacterial Biofilms, Feodor-Lynen-Strasse 7, 30625 Hannover, Germany
[3]Helmholtz Centre for Infection Research, Chronic Pseudomonas Infection Research Group, Inhoffenstrasse 7, 38124 Braunschweig, Germany
[4]Pharmaceutical and Medicinal Chemistry, Saarland University, Campus C2.3, 66123 Saarbrücken, Germany
*Correspondence: anke.steinbach@helmholtz-hzi.de (A.S.), rolf.hartmann@helmholtz-hzi.de (R.W.H.)
DOI 10.1016/j.chembiol.2012.01.015

## SUMMARY

The *pqs quorum sensing* communication system of *Pseudomonas aeruginosa* controls virulence factor production and is involved in biofilm formation, therefore playing an important role for pathogenicity. In order to attenuate *P. aeruginosa* pathogenicity, we followed a ligand-based drug design approach and synthesized a series of compounds targeting PqsR, the receptor of the *pqs* system. In vitro evaluation using a reporter gene assay in *Escherichia coli* led to the discovery of the first competitive PqsR antagonists, which are highly potent ($K_{d,app}$ of compound 20: 7 nM). These antagonists are able to reduce the production of the virulence factor pyocyanin in *P. aeruginosa*. Our finding offers insights into the ligand-receptor interaction of PqsR and provides a promising starting point for further drug design.

## INTRODUCTION

*Pseudomonas aeruginosa* is an opportunistic pathogen that causes life-threatening nosocomial infections and is a major problem for cystic fibrosis (CF) patients that leads to inflammation and chronic persistent lung infections.

It is responsible for 90% of chronic lung infections of CF patients (Koch and Høiby, 1993) and is considered as the major cause of mortality (Govan and Deretic, 1996). Its eradication is very difficult because it forms microcolonies encased with exopolysaccharides forming a biofilm community that defends the bacterial cells against adverse conditions, counterworks the human immune response, and decreases the susceptibility to antibiotics dramatically (Costerton et al., 1999).

Moreover, this microorganism possesses an exceptional adaptability to the fluctuating environments and expresses an arsenal of virulence factors, including exotoxins, hemolysins, and exoproteases. The coordinated production and secretion of these virulence factors, as well as the biofilm formation, are controlled by a cell-density-dependent cell-to-cell communication system known as quorum sensing (QS; Swift et al., 2001). QS functions by secreting and sensing of signaling molecules called autoinducers (AIs). Once at a high cell density, the AIs reach a threshold concentration in the culture and interact with specific receptors to regulate their target gene expression. *P. aeruginosa* uses two *lux*-type QS systems known as *las* (Gambello and Iglewski, 1991; Passador et al., 1993) and *rhl* (Ochsner et al., 1994; Ochsner and Reiser, 1995). The synthase LasI produces the molecule 3-oxo-$C_{12}$-HSL (*N*-3-oxododecanoyl-L-homoserine lactone), which activates the receptor LasR. Similarly, RhlI produces $C_4$-HSL (*N*-butanoyl-L-homoserine lactone), which stimulates RhlR. While both homoserine-mediated QS systems are broadly applied by various bacteria, 2-alkyl-4-quinolone-dependent QS occurs in *Pseudomonas* (Pesci et al., 1999) and in *Burkholderia* species (Diggle et al., 2006), whereas only *P. aeruginosa* produces *Pseudomonas* quinolone signal (PQS). PQS and, to a lesser extent, its precursor 2-heptyl-4-hydroxyquinoline (HHQ; Figure 1)—the two most predominant members of the 2-alkyl-4-hydroxyquinoline (HAQ) family (Déziel et al., 2004)—activate PqsR (synonym MvfR: multiple virulence factor regulator; Cao et al., 2001; Xiao et al., 2006), a LysR-type transcriptional regulator (Maddocks and Oyston, 2008) that drives the coordinated expression of nearly 200 genes. Many of these genes are related to virulence factors, such as *phzA1-G1*, which are involved in the biosynthesis of pyocyanin; *hcnAB*, which is responsible for production of hydrogen cyanide; *lasB,* which encodes elastase B; *rhlAB,* which is involved in biosynthesis of rhamnolipids; and *lecA*, which codes for Lectin A (Cao et al., 2001; Déziel et al., 2005). Besides virulence factors, the biofilm formation is also controlled by the *pqs* system (Diggle et al., 2003). Moreover, other QS-regulated activities, for instance, membrane vesicle formation (Mashburn-Warren et al., 2008, 2009), are under the control of *pqs* signaling. Furthermore, PqsR drives the biosynthesis of the PQS precursor HHQ through activation of *pqsABCD* and *phnAB* operons, which is further converted to PQS by the LasR-dependent monooxygenase PqsH (Gallagher et al., 2002; Déziel et al., 2004; Schertzer et al., 2010). Thus, a positive autoinducing loop is triggered by activation of PqsR by either PQS or HHQ (McGrath et al., 2004), which allows an initial rapid increase of extracellular PQS levels during an exponential growth phase.

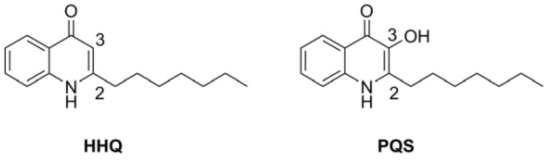


**Figure 1. Structures of HHQ and PQS**
PQS and, to a lesser extent, its precursor HHQ activate PqsR to drive target gene transcription.

QS inhibitors (QSIs) that specifically interfere with the bacterial cell-to-cell communication are discussed as an alternative approach to conventional antibacterial therapy (Rasmussen and Givskov, 2006; Bjarnsholt and Givskov, 2007). The selective intervention in pathogenicity without effect on bacterial growth may reduce natural selection pressure and therefore delay or avoid the development of resistance.

Since the *pqs* system plays a critical role for the pathogenicity, we consider its receptor PqsR as an attractive target protein for the development of QSIs to disrupt the *pqs*-dependent gene expression. This concept has been supported by the fact that *P. aeruginosa pqsR*$^{-}$ mutant strains display a reduced mortality rate in mice (Xiao et al., 2006). The mutation of *pqs*-controlled virulence genes results in decreased pathogenicity in plants, nematodes, and insects (Mahajan-Miklos et al., 1999; Jander et al., 2000). Moreover, based on the fact that PQS is produced in high amounts in the sputum of CF patients (Collier et al., 2002), it can be assumed that blocking the *pqs* QS system should make the *P. aeruginosa* lung infection in CF patients better treatable.

Our primary goal is to develop PqsR antagonists as QSIs of the *pqs* system. Although, to our knowledge, no PqsR antagonist has been published to date, initial investigations of ligand-receptor interaction of this target have been conducted by other research groups. In a recent study, Hodgkinson and co-workers presented structure-activity relationships (SARs) of PQS analogs. It was found that various substituents in the quinolone core, like hydroxy and methoxy, influence the agonistic activity (Hodgkinson et al., 2010) and that the alkyl side chain plays an important role for activation of PqsR (Fletcher et al., 2007; Hodgkinson et al., 2010).

In this article, we present the first PqsR antagonists to our knowledge. Following a ligand-based drug design approach, a set of HHQ and PQS analogs were synthesized, the side chain was varied and substituents were introduced into the carbocyclic moiety of the quinolone molecule. The biological evaluation was performed in vitro with a β-galactosidase reporter gene assay in *Escherichia coli*. Agonistic and antagonistic properties were determined, and competition experiments were conducted to investigate the binding site of the antagonists. For examination of the effect in *P. aeruginosa* PA14 cells, we determined the extracellular levels of the virulence factor pyocyanin and PQS. The antibacterial effect of the compounds on an *E. coli tolC* strain was tested.

## RESULTS

### Design of PqsR Antagonists

To our knowledge, the protein structure of PqsR has not been published and antagonists of this receptor are not known. The natural ligands are all agonists. Nevertheless, we used them for the design of potential antagonists (ligand-based approach) since it has been known for a long time that antagonists can be obtained by structural modification of agonists (Hartmann et al., 1980; Klebe, 2009).

Although PQS is the most potent natural ligand, we used the less potent HHQ (Xiao et al., 2006) for the following reasons: (1) The 3-hydroxy group of PQS has been proved to be responsible for interaction with lipid A of outer membrane lipopolysaccharides (Mashburn-Warren et al., 2008). Thus, HHQ lacking this group should exhibit a lower tendency to membrane association. (2) HHQ does not display iron chelating (Bredenbruch et al., 2006; Diggle et al., 2007) or pro-oxidant properties in contrast to PQS (Häussler and Becker, 2008). Therefore, modification of HHQ should avoid these unwanted interactions. In this work, we modified the stereo-electronic configuration of HHQ by changing the length of the alkyl side chain and by the introduction of electron-donating groups (EDGs) and -withdrawing groups (EWGs) into the benzene moiety of the quinolone structure. Besides, several corresponding PQS analogs were prepared for comparison.

### Synthesis

HHQ and its analogs were prepared in 2-3 steps according to a literature procedure (Woschek et al., 2007, Figure 2). The condensation of β-ketoesters with aniline or substituted anilines followed by cyclization of the resulting enamine in refluxing diphenyl ether yielded HHQ and its derivatives **1-7**, **9-12**, **14-21**, **24**, and **26-30**. Compounds **22**, **23**, and **25** were commercially available. Hydroxy-substituted products **8** and **13** were obtained by demethylation of the methoxy-substituted intermediates **9** and **14** (Konieczny et al., 2005).

Compounds **7**, **8**, **10-21**, and **26-30** are described for the first time, to our knowledge. The synthesis of PQS and its congeners (**31-42**) is provided in the Supplemental Information available online.

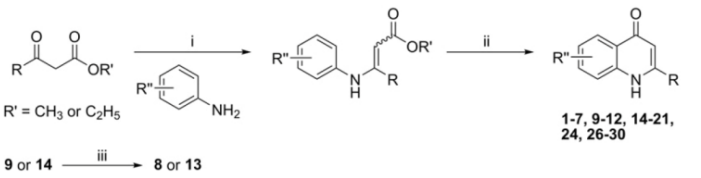


**Figure 2. Synthesis Route of HHQ and PQS Analogs**
Reagents and conditions: (i) *p*-TsOH, *n*-hexane, reflux; (ii) $Ph_2O$, reflux; (iii) $BF_3$● $SMe_2$, dichlormethane, room temperature, then $CH_3OH$.
See also Figure S3.

**Table 1. Agonistic and Antagonistic Activities of HHQ Analogs**

| Compd | R | R″ | PqsR Stimulation Induced by 10 μM Test Compd Compared to 50 nM PQS (= 1.00) | Inhibition of PqsR Stimulation Induced by 1 μM HHQ in the Presence of 10 μM Test Compd (Full Inhibition = 1.00) |
|---|---|---|---|---|
| Variation of Side Chain | | | | |
| 1 | $CH_3$ | H | 0.03 | 0.18 |
| 2 | *n*-$C_5H_{11}$ | H | 0.03 | 0.33 |
| 3 | *n*-$C_6H_{13}$ | H | 0.49* | 0.19 |
| 4 | *n*-$C_7H_{15}$ | H | 0.67[a],* | – |
| 5 | *n*-$C_8H_{17}$ | H | 0.69[a],* | 0.09 |
| 6 | *n*-$C_9H_{19}$ | H | 0.35* | 0.26* |
| 7 | *n*-$C_3H_6Ph$ | H | 0.29* | 0.32* |
| Introduction of Substituents in the Carbocyclic Ring | | | | |
| 8 | *n*-$C_7H_{15}$ | 7-OH | 0.46* | 0.02 |
| 9 | *n*-$C_7H_{15}$ | 7-$OCH_3$ | 0.74* | −0.24 |
| 10 | *n*-$C_7H_{15}$ | 8-$OCH_3$ | 0.02 | 0.21* |
| 11 | *n*-$C_7H_{15}$ | 8-$C_2H_5$ | 0.05 | 0.17 |
| 12 | *n*-$C_7H_{15}$ | 8-F | 0.67* | −0.04 |
| 13 | *n*-$C_7H_{15}$ | 6-OH | 0.66* | −0.09 |
| 14 | *n*-$C_7H_{15}$ | 6-$OCH_3$ | 0.18 | 0.23* |
| 15 | *n*-$C_7H_{15}$ | 6-$CH_3$ | 0.54* | 0.12 |
| 16 | *n*-$C_7H_{15}$ | 6-F | 0.65* | 0.21* |
| 17 | *n*-$C_7H_{15}$ | 6-Cl | 0.29* | 0.49* |
| 18 | *n*-$C_7H_{15}$ | 6-CN | 0.05 | 1.00* |
| 19 | *n*-$C_7H_{15}$ | 6-$CF_3$ | 0.00 | 0.95* |
| 20 | *n*-$C_7H_{15}$ | 6-$NO_2$ | 0.00 | 1.00* |
| 21 | *n*-$C_7H_{15}$ | 6-$CF_3$, 8-$OCH_3$ | 0.00 | 0.61* |
| Variation of Side Chain[b] and $CF_3$ Position of Compd **19** | | | | |
| 22 | H | 6-$CF_3$ | 0.00 | 0.05 |
| 23 | $CH_3$ | 6-$CF_3$ | 0.02 | 0.12 |
| 24 | $C_2H_5$ | 6-$CF_3$ | 0.00 | 0.12 |
| 25 | *n*-$C_3H_7$ | 6-$CF_3$ | 0.00 | 0.38 |
| 26 | *n*-$C_4H_9$ | 6-$CF_3$ | 0.02 | 0.64* |
| 27 | *n*-$C_5H_{11}$ | 6-$CF_3$ | 0.02 | 0.93* |
| 28 | *n*-$C_6H_{13}$ | 6-$CF_3$ | 0.01 | 0.97* |
| 19[b] | *n*-$C_7H_{15}$ | 6-$CF_3$ | 0.00 | 1.00* |
| 29 | *n*-$C_7H_{15}$ | 7-$CF_3$ | 0.50* | 0.00 |
| 30 | *n*-$C_7H_{15}$ | 8-$CF_3$ | 0.10 | 0.25 |

β-Galactosidase reporter gene assay was performed in *E. coli* transformed with the plasmid pEAL08-2 encoding PqsR and the reporter gene *lacZ* controlled by the *pqsA* promoter. For the agonist test, the compounds were measured at 10 μM and 1μM (data not shown); for the antagonist test, the compounds were measured at 10 μM and 1 μM (data not shown) in the presence of 1 μM HHQ. Mean value of at least two independent experiments with n = 4, SD < 25%. Significance: For the agonist test, induction compared to the basal value; for the antagonist test, decrease of the HHQ or PQS-induced induction. Cmpd, compound. *$p < 0.05$.

[a]The stimulations induced by **4** and **5** at 1 μM were 0.75 ($p < 0.05$) and 0.62 ($p < 0.05$), respectively.

[b]Compounds **22-28** and **19** here were tested at 5 μM, for antagonist test, in the presence of 50 nM PQS.

See also Tables S1 and S2.

## Biological Evaluation

### *Evaluation of the Agonistic and Antagonistic Activities in Reporter Gene Assay*

The PqsR-mediated transcriptional effect of the compounds was evaluated as previously described in a HTS β-galactosidase reporter gene assay in *E. coli* containing the plasmid pEAL08-2, which encodes PqsR under the control of the *tac* promoter and the β-galactosidase reporter gene *lacZ* controlled by the *pqsA* promoter (Cugini et al., 2007).

For the variation of the side chain, we found that, in the agonist test, HHQ with *n*-heptyl revealed a very high activity (compound **4,** Table 1). Compound **3** with an *n*-hexyl side chain still showed moderate activity, but further shortening of the chain length (compound **1** and **2**) resulted in complete loss of potency.

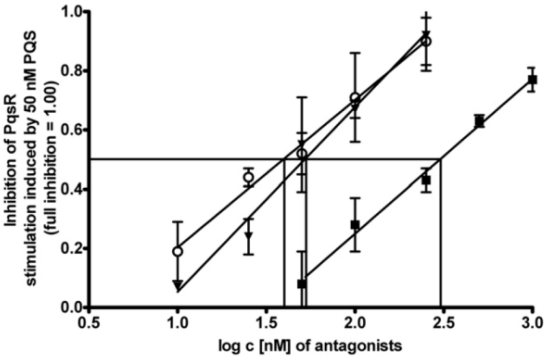


**Figure 3. Determination of $IC_{50}$ Values**

$IC_{50}$ values were determined in the reporter gene assay. Compounds **18** (■), **19** (○) and **20** (▼) were tested at five concentrations in competition with 50 nM PQS. $IC_{50}$ values: compound **18**, 259 ± 114 nM; **19**, 54 ± 23 nM; and **20**, 51 ± 19 nM. Mean value of two experiments with n = 4.

Elongation of the side chain by one carbon (compound **5**) did not reduce the PqsR stimulation at 10 μM (whereas, at 1 μM, a slight decrease was observed). The HHQ analog with *n*-nonyl (compound **6**) showed a diminished activity. Introduction of a 3-phenylpropyl side chain (compound **7**) also led to a decrease in activity. These results indicate that the ability of HHQs to activate PqsR is dependent on the side chain with *n*-heptyl being the optimal. This phenomenon was also found for PQS side-chain analogs in this study (compounds **31-35**; Table S1), which is in agreement with previous observations (Fletcher et al., 2007; Hodgkinson et al., 2010). However, PQS analog **35** with a longer side chain (*n*-nonyl) was better tolerated by PqsR than the corresponding HHQ analog (compound **6**). In the antagonist test, none of the HHQ side-chain analogs at 10 μM was able to strongly inhibit the PqsR stimulation.

To continue our search for PqsR antagonists, we then focused on the introduction of EDGs and EWGs into the benzene part of HHQ. Introduction of an EDG such as hydroxy or methoxy into 7-position resulted only in agonists (compounds **8** and **9**), and the agonistic potency of compound **8** was significantly reduced compared to HHQ ($p < 0.05$). Contrariwise, their congeners with methoxy or ethyl group in 8-position (compounds **10** and **11**) showed no agonistic activity, while compound **12** with an electron-withdrawing fluoro substituent in the same position revealed agonistic effect. Regarding the 6-position, the introduction of hydroxy, methyl, or fluoro led to agonists (compounds **13**, **15**, and **16**). Substitution with methoxy or chloro (compounds **14** and **17**) led to a drop of agonistic activity. The agonistic potency of three HHQ analogs with strong EWGs in 6-position, nitrile, trifluoromethyl, or nitro (compounds **18-20**), was completely eliminated. What was most interesting was that these compounds exhibited strong antagonistic properties by completely or almost completely inhibiting the PqsR stimulation. The antagonistic potency of two position isomers of **19**, compounds **29** and **30** with trifluoromethyl in 7- or 8-position, was strongly reduced compared to the 6-position analog.

We assumed that the alkyl side chain of HHQ contributes to the poor water solubility as reported for the PQS analogs (Hodgkinson et al., 2010). In order to improve this physicochemical property of compound **19** and to clarify the effect of the side chain on the antagonistic activity, short chain compounds **22-28** were synthesized. Indeed, shortening of the side chain improved the aqueous solubility (Table S2) but also resulted in a decrease of activity. At 5 μM, compounds **27** and **28** were as potent as compound **19**. However, at a lower concentration of 50 nM (data not shown), only compound **19** revealed antagonistic activity. This result shows that the antagonistic activity of the analogs of compound **19** also strongly depends on the alkyl side chain as described for the agonistic activity of HHQ (Table 1) and PQS (Table S1).

For the purpose of obtaining a more active antagonist, we combined the structures of the very potent compound **19** with the antagonist **10** to prepare compound **21**. It showed higher antagonistic potency than **10** but was not as effective as **19**.

The corresponding PQS analogs of compounds **9**, **12**, **14**, **15**, and **16** either displayed high agonistic activity (compounds **37** and **39**; Table S1) or showed no antagonistic potency (compound **36**, **38**, and **40**).

To further characterize the potency of the antagonists, we determined $IC_{50}$ values using the same reporter gene assay (Figure 3).

HHQ analogs with trifluoromethyl and nitro functional groups in 6-position were found to be equipotent (compound **19**: $IC_{50}$ = 54 ± 23 nM; compound **20**, $IC_{50}$ = 51 ± 19 nM) and were more active than compound **18** with a nitrile group ($IC_{50}$ = 259 ± 114 nM).

The fitting of dose-response curves of PQS with increasing concentrations of the antagonists **18-20** (0-200 nM) by nonlinear Schild regression analysis allowed the calculation of the apparent dissociation constant $K_{d,app}$ (Figure 4).

For compounds **18-20**, $K_{d,app}$ values were determined and high affinities were observed ($K_{d,app}$ = 556 nM, 17 nM, and 7 nM, respectively).

Furthermore, direct evidence for binding of a selected antagonist (compound **18**) to PqsR was provided by surface plasmon resonance (SPR) biosensor experiments. For this purpose, a truncated soluble form of PqsR, $PqsR^{C87}$ (Xiao et al., 2006), was cloned, heterologeously expressed in *E. coli*, purified as SUMO-tagged fusion protein ($His_6SUMO\text{-}PqsR^{C87}$), biotinylated (Klein et al., 2011), and immobilized on a streptavidin-coated sensorchip. A high affinity to the truncated target was determined ($K_d$ = 57 nM; Figure S1).

To gain further information about the binding site of the three antagonists **18-20** to PqsR, we performed competitive experiments in the presence of PQS.

As depicted in Figure 5, compounds **18-20** were displaced in a dose-dependent manner by the native ligand PQS. This result indicates that these compounds are efficient competitors to the receptor. For compound **18**, a higher concentration (250 nM) is needed to reach the similar antagonistic effect in comparison with the other two compounds.

### Effect on Virulence Factors Production in *P. aeruginosa* PA14

To examine the biological effect of the intervention in the *pqs* system, we investigated the impact of the PqsR antagonists **18** and **19** on the production of the PQS-regulated virulence factor

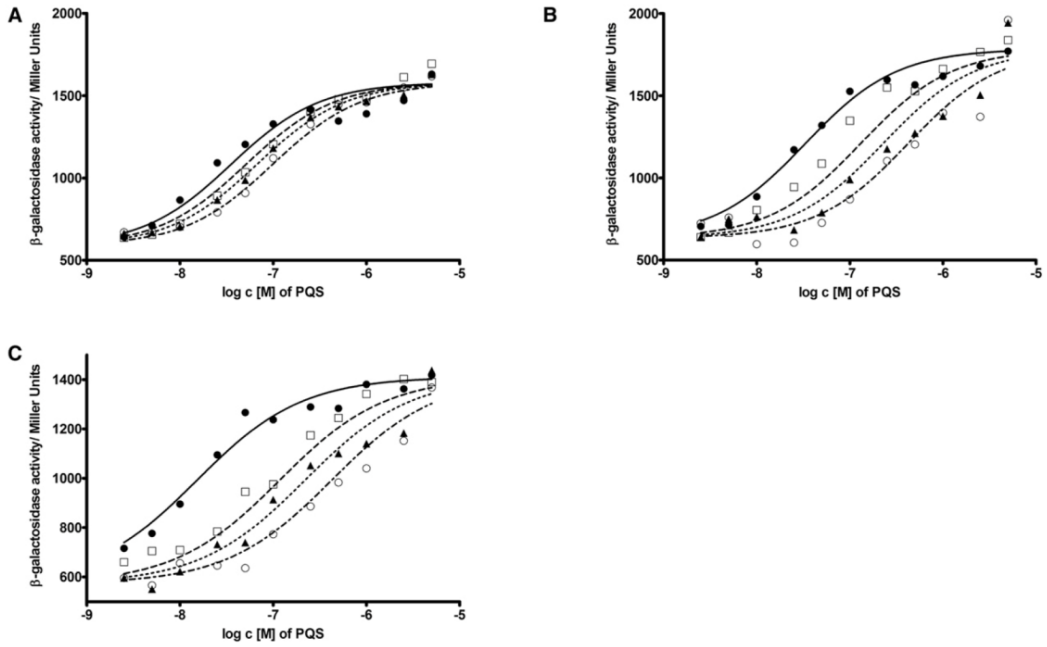


**Figure 4. Determination of the Apparent $K_d$ Values**

Compounds **18** (A), **19** (B) and **20** (C) at four concentrations, 0 nM (●), 50 nM (□), 100 nM (▲) and 200 nM (○) were competed with PQS (2.5-5,000 nM) in the reporter gene assay. The Schild slope was constrained equal to 1.0. Apparent $K_d$ values: compound **18**, 556 nM; **19**, 17 nM; and **20**, 7 nM.
See also Figure S1.

pyocyanin in *P. aeruginosa* PA14 with agonists **15** and **17** for comparison.

As shown in Figure 6, the antagonist compound **19** is able to reduce the pyocyanin production in *P. aeruginosa* PA14 supernatants by 74% at a concentration of 3 μM. In a comparison of the effects of both antagonists, compound **19** is more active than **18**. This observation is consistent with the higher activity of compound **19** observed in the reporter gene assay. As expected, the agonists **15** and **17** did not display significant reduction of pyocyanin production at the concentrations of 0.5–5 μM.

The production of elastase as well as rhamnolipids, in which *pqs* system is involved, was also examined in *P. aeruginosa* PA14. Unlike the result from the pyocyanin assay, the production of elastase and rhamnolipids was unaffected in the presence of compound **18** or **19** at 5 μM (data not shown).

### *Effect on Extracellular PQS Levels*

In a further experiment in *P. aeruginosa* PA14, we examined whether the extracellular PQS levels were also affected by the PqsR antagonists. Therefore, PQS in PA14 culture supernatants was quantified using liquid chromatography with tandem mass spectrometry (LC-MS/MS). The *pqsA*$^-$ mutant, deficient in PQS and pyocyanin production, was used as the reference strain. However, first results indicate that the extracellular PQS levels were not significantly reduced in the presence of the PqsR antagonist, compound **19** at concentrations up to 5 μM.

### *Determination of Antibacterial Effect*

We evaluated the antibacterial effect of all compounds using a filter disc diffusion technique on *E. coli tolC* strain (Table S3). It was found that the PqsR antagonists **18**, **19**, and **20** did not exhibit any antibacterial properties against *E. coli tolC* (25 μg in filter disc). Furthermore, growth kinetics of *P. aeruginosa* PA14 in the presence of two antagonists **18** and **19** were determined and are shown to be unaffected at a concentration of 5 μM (Figure S2). These results are in line with our approach of selectively targeting bacterial QS-controlled virulence without any impact on bacterial viability.

## DISCUSSION

The usage and misusage of antibiotics in the traditional treatment of infections result in natural selection pressure that leads to the widespread emergence of antibiotic resistance, which is a serious and urgent medical problem. QSIs are compounds that are able to interfere with bacterial QS signaling pathways thereby impairing QS-mediated group behaviors such as virulence factor production and biofilm formation without inhibition of the bacterial growth. We regard PqsR, the receptor of the *P. aeruginosa*-specific *pqs* QS system, as an attractive target to develop QSIs and expect that PqsR antagonists should limit *pqs*-related pathogenicity.

Following a ligand-based approach, we modified the structure of HHQ. Considering that some variation of the side chain of PQS

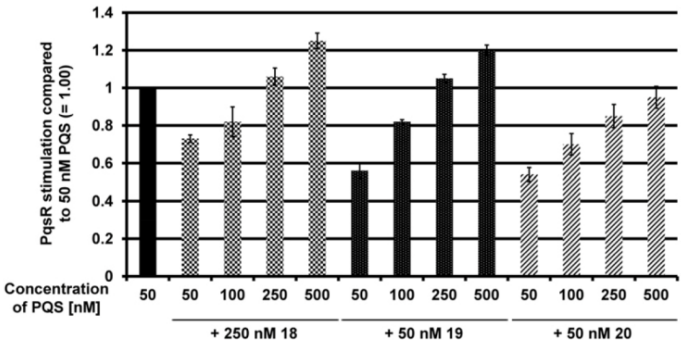


**Figure 5. Dose-Dependent Displacement of Antagonists by PQS**

Competitive binding studies of compounds **18**-**20** were performed in the reporter gene assay using increasing concentrations of PQS (50-500 nM). Mean value of one experiment with n = 4, SD < 10%. Black bars, control; black and white mosaic bars, compound 18; black and white dotted bars, compound 19; hatched bars, compound 20.

or introduction of certain functional groups into the benzene part of the quinolone moiety resulted in decrease of agonistic activity of PQS (Fletcher et al., 2007; Hodgkinson et al., 2010), we assumed that such modifications on HHQ may also remove the agonistic potency and provide a starting point to discover PqsR antagonists. Indeed, three highly potent PqsR antagonists were identified from HHQ core-substituted analogs.

## SARs and Biological Implications

The data from the reporter gene assay reveal that the HHQ side chain plays an important role for the activities of the compounds, whereas the substituents at the benzene core are decisive for agonistic and antagonistic properties. It is interesting that agonists, compounds with agonistic and antagonistic properties as well as pure antagonists, were obtained.

The side chain must consist of at least six C atoms to result in biologically active compounds. It can be longer than the one of the natural ligands HHQ and PQS (7 C atoms). In this regard, it is worth noting that HHQ and PQS analogs with a *n*-nonyl side chain (compound **6**, Table 1; compound **35**, Table S1), which are natural occurring HAQs, obviously also function as PqsR ligands in *P. aeruginosa* (Hodgkinson et al., 2010; Heeb et al., 2011).

It is most interesting that all HHQ analogs with strong EWGs in 6-position revealed antagonistic potency. The introduction of nitrile, trifluoromethyl, and nitro led to the discovery of the first PqsR antagonists (compounds **18**, **19**, and **20**). Investigation of the binding mode of these compounds identified them as competitive antagonists. From analysis of the $IC_{50}$ and $K_{d,\ app}$ values, the following correlation between activity and electronegativity can be drawn: The increase of the electronegativity (nitro ≈ trifluoromethyl > nitrile; Sanderson, 1983; Bratsch, 1985) of the substituent in 6-position results in a rise in potency. In order to examine whether the antagonistic effects are singly attributable to the nature of the substituents, their position was varied in compound **19**. It is interesting that the position isomers with trifluoromethyl in 7- or 8-position (compounds **29** and **30**) were unable to antagonize the PqsR stimulation induced by HHQ. This implies that not only the electron-withdrawing effects but also the position of the EWG at the benzene core are responsible.

Combining the substituents of a weak antagonist (compound **10**) and a strong antagonist (compound **19**), bisubstituted HHQ compound **21** was identified as a moderate antagonist. We suppose that, for compound **21**, the electronic effects of the electron-donating methoxy group in 8-position and the electron-withdrawing trifluoromethyl group in 6-position may counteract each other (for example, their effect on the NH group of the quinolone core).

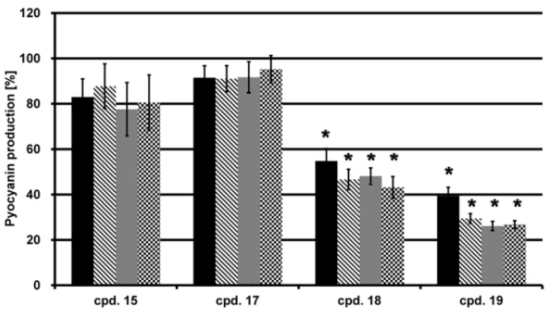


**Figure 6. Effect on Pyocyanin Production in *P. aeruginosa* PA14**

The pyocyanin levels in *P. aeruginosa* PA14 were spectrophotometrically determined at $A_{520\ nm}$ in the presence of compounds (cmpds.) **15**, **17**, **18**, and **19** at 0.5 μM (black bars), 1.5 μM (hatched bars), 3 μM (small-checkered bars), 5 μM (large-checkered bars). Mean value of one experiment with n = 4, SD < 15%. Significance: reduction of pyocyanin production compared to the control. *p < 0.003. For antibacterial activity, see also Table S3 and Figure S2.

## Intricate Interplay between Pyocyanin and the *pqs* System

Pyocyanin is an important virulence factor in *P. aeruginosa* that is required for full pathogenicity and is associated with morbidity and mortality in CF patients (Courtney et al., 2007). Its production has been described to be controlled by PqsR, which activates the transcription of the *pqsABCDE* operon (Cao et al., 2001; Déziel et al., 2004) in which *pqsABCD* is responsible for HHQ biosynthesis (Bredenbruch et al., 2005; Pistorius et al., 2011). HAQ-deficient mutants (*pqsA*$^-$ and *pqsR*$^-$) are unable to produce pyocyanin (Cao et al., 2001; Déziel et al., 2004), while PQS-deficient mutant *pqsH*$^-$ still produces 25% pyocyanin compared with wild-type (Xiao et al., 2006). Moreover, pyocyanin formation is also controlled in a HAQ-independent manner by the action of PqsE, which is coregulated in the *pqsABCDE* operon; it is able to restore pyocyanin levels in HAQ-deficient *pqsA*$^-$ or *pqsR*$^-$ mutants (Farrow et al., 2008; Rampioni et al., 2010). Therefore, PqsR antagonists that block the transcription

of the *pqsABCDE* operon—and, therefore, the production of HAQs and PqsE—should disrupt pyocyanin formation. Treatment of *P. aeruginosa* PA14 with compounds **18** and **19** revealed that PqsR ligands with antagonistic activity are capable of diminishing extracellular pyocyanin levels relative to control in the low micromolar range while PqsR ligands with agonistic activity (compounds **15** and **17**) did not exhibit a significant effect. What is most interesting is that the extracellular PQS levels that are abolished in a *pqsR*$^{-}$ mutant were not affected in the presence of compounds **18** or **19** at 5 μM. Differences in genetic backgrounds of *E. coli* and *P. aeruginosa* like efflux pumps (e.g., Lamarche and Déziel, 2011) might play a role, as discussed by Hodgkinson and co-workers, where PQS is about 1,000 times more sensitive to transcriptional activation of the *pqsA-lacZ* fusion in the heterologous *E. coli* than in *P. aeruginosa* (Fletcher et al., 2007; Hodgkinson et al., 2010). Besides, we speculate that there may be some unknown effects (e.g., inhibition of enzymes involved in biosynthesis of pyocyanin by PqsR antagonists. Mavrodi et al., 2001) in QS circuitry. Further studies to investigate these unexpected phenomena are currently underway. Anyway, we have clearly demonstrated that the tight binding to PqsR (compound **18** by SPR) leads to strong antagonistic effects (reporter gene assay). However, only pyocyanin production is reduced; no effects are observed regarding PQS and rhamnolipid formation and elastase activity.

In conclusion, the PqsR antagonists provide an interesting starting point for further drug design efforts on this target protein to develop effective antivirulence drugs. In a next step, the discovered antagonists will be further optimized concerning their aqueous solubility.

## SIGNIFICANCE

**PqsR is the receptor of *pqs quorum sensing* cell-to-cell communication system of the human pathogen *P. aeruginosa*, which controls the expression of various virulence factors and is involved in biofilm formation. This receptor plays an important role for pathogenicity and therefore appears to be an attractive target for antivirulence drugs. This work describes, to our knowledge, the discovery of the first antagonists of PqsR with $IC_{50}$ and $K_{d,app}$ values in the low nanomolar range that have been determined in heterologous *E. coli* reporter gene system. An activity in vivo is demonstrated by the antagonist 19, which reduces virulence factor pyocyanin production by 74% in *P. aeruginosa* PA14 at a concentration of 3 μM. We examined the binding of these active compounds in competition experiments and identified them as competitive antagonists. As expected, the PqsR antagonists do not reduce viability of *P. aeruginosa*; therefore, they should not induce natural selection pressure. This property makes these compounds important as they could overcome the shortcomings of traditional antibiotics. These PqsR antagonists are highly valuable scientific tools for in-depth study of the ligand-receptor interaction of PqsR and the function of the *pqs* system. Our finding provides an important step toward further drug design targeting PqsR and may open new avenues for the combat against *P. aeruginosa* infection.**

## EXPERIMENTAL PROCEDURES

### Synthesis of the Title Compounds 18–20

#### *Chemical and Analytical Methods*

$^{1}H$ and $^{13}C$ NMR spectra were recorded on a Bruker DRX-500 instrument. Chemical shifts are given in parts per million (ppm), and tetramethylsilane was used as internal standard for spectra obtained in $CDCl_3$, MeOH-$d_4$, and DMSO-$d_6$. All coupling constants (*J*) are given in hertz. LC/MS was performed on an MSQ electro spray mass spectrometer (Thermo Fisher). The system was operated by the standard software Xcalibur. An RP C18 NUCLEODUR 100-5 (125 × 3 mm) column (Macherey-Nagel GmbH) was used as stationary phase with water/acetonitrile mixtures as eluents. All solvents were high-pressure liquid chromatography grade. Reagents were used as obtained from commercial suppliers without further purification. Flash chromatography was performed on silica gel 60, 70-230 mesh (Fluka), and the reaction progress was determined by thin-layer chromatography analyses on silica gel 60, $F_{254}$ (Merck). Visualization was accomplished with UV light. All microwave irradiation experiments were carried out in a multiSYNTH all-in-one microwave (MLS GmbH). We measured the melting points using melting point apparatus SMP3 (Stuart Scientific). The apparatus is uncorrected.

#### *General Procedure*

A solution of β-ketoester (9.24 mmol, 1 equiv), aniline (9.24 mmol, 1 equiv), and *p*-TsOH · $H_2O$ (50 mg, 0.29 mmol) in *n*-hexane (20 ml) was heated at reflux using a Dean-Stark separator for 5 hr. After cooling, the solution was concentrated in vacuo, and the residue was added dropwise to refluxing (260°C) diphenyl ether (5 ml). Refluxing was continued for 30 min. After cooling to room temperature, $Et_2O$ (15 ml) and 2 M HCl (20 ml) were added and the mixture was left overnight at 5°C. If a crystalline solid had formed, it was collected and washed with $Et_2O$. If no solid had formed, ammonia was added to basify the mixture. HHQ analogs were purified by crystallization from ethyl acetate or column chromatography on silica gel (Woschek et al., 2007).

*2-Heptyl-4-oxo-1,4-dihydroquinoline-6-carbonitrile; 18*. Compound **18** was obtained from 4-aminobenzonitrile (441 mg, 3.73 mmol) and ethyl 3-oxodecanoate (800 mg, 3.74 mmol) after crystallization as a white solid (164 mg, 0.61 mmol, 16%), melting point (mp) 196-199°C. $^{1}H$-NMR (500 MHz, DMSO-$d_6$): δ = 0.74 (t, *J* = 7.0 Hz, 3H), 1.13-1.21 (m, 8H), 1.56 (quint, *J* = 7.0 Hz, 2H), 2.50 (t, *J* = 7.5 Hz, 2H), 5.94 (s, 1H), 7.55 (d, *J* = 8.5 Hz, 1H), 7.84 (dd, *J* = 2.0 Hz, 8.5 Hz, 1H), 8.27 (d, *J* = 2.0 Hz, 1H) 11.69 (brs, 1H). $^{13}C$-NMR (125 MHz, DMSO-$d_6$): δ = 13.8, 21.9, 28.0, 28.3, 28.3, 31.0, 33.2, 104.9, 109.9, 118.7, 119.5, 124.1, 130.6, 133.4, 142.5, 154.9, 175.6. LC/MS: *m/z* 269.28 ($MH^+$), 99.4%.

*2-Heptyl-6-(trifluoromethyl)quinolin-4(1H)-one; 19*. Compound **19** was obtained from 4-(trifluoromethyl)aniline (602 mg, 3.74 mmol) and ethyl 3-oxodecanoate (800 mg, 3.74 mmol) after acidification with concentrated HCl and crystallization as a white solid (94 mg, 0.30 mmol, 8%), mp 233-237°C. $^{1}H$-NMR (500 MHz, DMSO-$d_6$): δ = 0.83 (t, *J* = 6.5 Hz, 3H), 1.25-1.34 (m, 8H), 1.70 (quint, *J* = 7.5 Hz, 2H), 2.73 (t, *J* = 7.5 Hz, 2H), 6.34 (s, 1H), 7.92-7.97 (m, 2H), 8.36 (d, *J* = 0.5 Hz, 1H). $^{13}C$-NMR (125 MHz, DMSO-$d_6$): δ = 14.2, 22.4, 28.7, 28.9, 31.5, 33.8, 108.5, 120.6, 122.6 (q, $J_{CF}$ = 3.7 Hz), 123.1, 124.6 (q, $J_{CF}$ = 270.0 Hz), 124.7 (q, $J_{CF}$ = 32.0 Hz), 128.3 (q, $J_{CF}$ = 3.0 Hz), 142.5, 157.6, 174.9. LC/MS: *m/z* 312.31 ($MH^+$), 97.0%.

*2-Heptyl-6-nitroquinolin-4(1H)-one; 20*. Compound **20** was obtained from 4-nitroaniline (515 mg, 3.73 mmol) and ethyl 3-oxodecanoate (800 mg, 3.74 mmol) after crystallization as a brown solid (12 mg, 0.04 mmol, 1%), mp 185-186°C. $^{1}H$-NMR (500 MHz, MeOH-$d_4$): δ = 0.91 (t, *J* = 7.0 Hz, 3H), 1.33-1.50 (m, 8H), 1.88 (quint, *J* = 7.5 Hz, 2H), 3.08 (t, *J* = 7.5 Hz, 2H), 7.08 (s, 1H), 8.15 (d, *J* = 9.5 Hz, 1H), 8.73 (dd, *J* = 2.0 Hz, 9.5 Hz, 1H), 9.18 (d, *J* = 2.0 Hz, 1H). $^{13}C$-NMR (125 MHz, MeOH-$d_4$): δ = 11.6, 20.9, 27.3, 27.5, 27.6, 30.0, 32.8, 105.1, 118.3, 118.9, 119.6, 126.2, 140.7, 144.3, 162.4, 170.6. LC/MS: *m/z* 289.29 ($MH^+$), 98.6%.

Synthesis of other HHQ analogs, PQS analogs, and β-ketoesters are provided in the Supplemental Information.

### Reporter Gene Assay

The ability of the compounds to either stimulate or antagonize the PqsR-dependent transcription was evaluated as previously described using a β-galactosidase reporter gene assay (Cugini et al., 2007) in *E. coli* expressing PqsR, with some modifications to enable a higher throughput (Griffith and

Wolf, 2002). PQS, HHQ, and its analogs were diluted in ethyl acetate and added to the wells of a 96-deep-well plate, and the solvent was evaporated. Overnight cultures of *E. coli* DH5α cells containing the plasmid pEAL08-2, which encodes PqsR under the control of the *tac* promoter and the β-galactosidase reporter gene *lacZ* controlled by the *pqsA* promoter, were diluted 1:100 in Luria-Bertani (LB) medium with ampicillin (50 μg/ml). The culture was incubated at 37°C with shaking until it reached an $OD_{600}$ of 0.2. For the determination of agonistic activities, 1 ml aliquots were supplemented with either PQS (50 nM) or the test compound: for HHQ analogs, 10 μM; for 6-trifluoromethyl HHQs **22**-**28**, 5 μM; PQS analogs **31**-**42**, 50 nM. Ethyl acetate was used as a control. Antagonistic effects of the compounds were evaluated in the presence of either 1 μM HHQ or 50 nM PQS. The β-galactosidase activity was determined after a 2.5 hr incubation period at 37°C with shaking (150 rpm). $OD_{600}$, $OD_{420}$, and $OD_{550}$ were measured, and the activity is expressed as ratio of the ethyl acetate control relative to the cultures that received either PQS, a test compound, or both. $IC_{50}$ values of antagonists **18**-**20** were determined by variation of the concentration of the test compounds in competition with 50 nM PQS. Binding affinities of antagonists **18**-**20** were determined by mutual variations of concentrations of the test compounds and of PQS (50-500 nM). The Gaddum/Schild $IC_{50}$ shift model (GraphPad Prism, trial version 5.0) was applied for nonlinear regression and determination of $K_d$ values; the Schild slope was constrained equal to 1.0 (Arunlakshana and Schild, 1959).

### Protein Expression and Purification

$His_6$SUMO-$PqsR^{C87}$ was expressed in *E. coli* and purified with a single affinity chromatography step. Briefly, *E. coli* BL21 (DE3) cells containing the pSUMO3_ck4_$pqsR^{C87}$ plasmid were grown in LB medium (50 μg/ml kanamycin) at 37°C to an $OD_{600}$ of approximately 0.8 units and induced with 0.2 mM IPTG for 16 hr at 16°C. The cells were harvested by centrifugation (5,000 rpm, 10 min, 4°C), and the cell pellet was resuspended in 100 ml binding buffer (50 mM Tris-HCl, pH 7.8, 150 mM NaCl, 20 mM imidazole, 10% glycerol (v/v)) and lysed by sonication for a total process time of 2.5 min. Cell debris was removed by centrifugation (13,000 rpm, 30 min), and the supernatant was filtered through a syringe filter (0.2 μm). The clarified lysate was immediately applied to a Ni-NTA column (GE Healthcare), washed with 50 mM Tris HCl, pH 7.8, 150 mM NaCl, 20 mM imidazole, 10% glycerol (v/v), and eluted with 500 mM imidazole containing buffer. The protein-containing fractions were buffer exchanged into 20 mM Tris, pH 7.4, 150 mM NaCl, and 10% glycerol (v/v) using a PD10 column (GE Healthcare) and were judged pure by SDS-PAGE. The $His_6$SUMO-tagged proteins were used for biotinylation.

### Minimal Biotinylation of $His_6$SUMO-$PqsR^{C87}$

Minimal biotinylation of the $His_6$SUMO-$PqsR^{C87}$ was achieved by mixing 56 nmol of $His_6$SUMO-$PqsR^{C87}$ with 28 nmol of EZ-link sulfoNHS LC-LC-biotin (Thermofisher Scientific) that was freshly dissolved in water. Biotinylation reaction mixture was incubated on ice for 2 hr. To remove unreacted biotin reagent, we subjected the entire biotinylation mixture to size exclusion chromatography on a Superdex200 HR (16/600) column equilibrated in storage buffer (1× PBS, pH 7.4, 10% glycerol (v/v)). A protein peak containing biotinylated $His_6$SUMO-$PqsR^{C87}$ protein was collected (0.3 mg/ml), stored at −80°C, and used for SPR studies.

### SPR Studies

We performed SPR binding studies using a Reichert SR7500DC instrument optical biosensor (Reichert Technologie, Depew, NY, USA). SAD500 sensor chips from Xantec (Xantec Analytics, Düsseldorf) were used.

### Immobilization of Biotinylated $His_6$Sumo-$PqsR^{C87}$

Biotinylated $His_6$SUMO-$PqsR^{C87}$ was immobilized on a SAD500 (Streptavidin-coated) sensor chip at 25°C. HEPES (50 mM HEPES, pH 7.4, 150 mM NaCl, 3 mM EDTA) was used as the immobilization buffer. The streptavidin carboxymethyl dextran surface was preconditioned for 30 min with running buffer until the baseline was stable. Biotinylated $His_6$SUMO-$PqsR^{C87}$ was diluted into running buffer to a concentration of 100 μg/ml and coupled to the surface with a 4 min injection. Biotinylated $His_6$SUMO-$PqsR^{C87}$ (39494 Da) was immobilized at densities of 2,556 RU (Chip (I)) and 4,463 RU (Chip (II)) for the binding experiments of compound **18**.

### Binding Affinity for Compound 18

The binding experiment was performed at 12°C at a constant flow rate of 50 μl/min in instrument running buffer (50 mM HEPES, pH 7.4, 150 mM NaCl, 3 mM EDTA, 5% DMSO (v/v), 0.05% P20 (v/v). A 180 μM solution of compound **18** in DMSO was directly diluted to a concentration of 9 μM (50 mM HEPES, pH 7.4, 150 mM NaCl, 3 mM EDTA, 0.05% P20 (v/v)) and then diluted threefold from 9 μM down to 4.1 nM in the running buffer. Before starting the experiments, 12 warm-up blank injections were performed. Zero-buffer blank injections and DMSO calibrations were included for double referencing. Individual concentrations were injected from lowest to highest concentrations for 100 s association and 15 min dissociation time. Experiments were performed twice with two independently immobilized SAD500 chips. Scrubber software was used for processing and analyzing data.

### Pyocyanin Assay

*P. aeruginosa* PA14 cultures and a corresponding *pqsA*$^-$ knockout strain as a reference were grown at 37°C under shaking conditions (180 rpm) in LB medium in the absence and presence of test compounds (0.5 μM, 1.5 μM, 3 μM, and 5μM) overnight. After centrifugation (10 min, 2,600 × g), culture supernatants were extracted with equal volumes of chloroform. A total of 0.75 ml of the lower organic phase was supplemented with 0.25 ml of 0.2 N HCl solution and shaken for 30 s. The upper reddish phase was collected, and $OD_{520}$ was measured.

### Elastase Assay

Elastase activity of *P. aeruginosa* PA14 cultures was measured with Elastine Congo Red (ECR), which is cleaved upon elastolytic activity releasing the soluble red pigment CR. In brief, 1 ml culture supernatants of overnight cultures (180 rpm at 37°C) were mixed with 1 ml of ECR buffer (0.1 M Tris-HCl pH 7.2, 1 mM $CaCl_2$,) containing 20 mg of ECR (Sigma-Aldrich) and incubated for 3 hr at 37°C with constant shaking. After incubation, insoluble ECR was spinned down by centrifugation at 13,000 × g for 5 min, and the absorbance of the supernatant was measured at 495 nm (measurement was performed immediately after incubation since no stop reactant was added).

### Rhamnolipid Assay

To determine rhamnolipid production of *P. aeruginosa* PA14 cultures, we performed a modified orcinol assay for the detection of glycolipids. For that, 300 μl aliquots of the supernatants of 24-hr-old cultures were extracted with 1,700 μl diethylether. One milliliter of the ether phases was mixed with 600 μl 20 mM HCl, and 500 μl of the resulting organic phases were transferred and dried under the hood. After evaporation, 100 μl 1.6% orcinol and 900 μl 60% $H_2SO_4$ were added, and the samples were incubated for 30 min at 80°C. After incubation, the absorbance was measured at 421 nm.

### Determination of Extracellular PQS Levels

Extracellular PQS produced by *P. aeruginosa* PA14 was determined in 250 ml Erlenmeyer flasks containing 25 ml cultures in LB medium. Flasks were incubated at 37°C in an orbital shaker at 200 rpm. Cultures were inoculated with an overnight culture to obtain a starting $OD_{600}$ = 0.025. DMSO solutions of inhibitors were added to the cultures to a final DMSO concentration of 0.5%. For PQS analysis, 500 μl of each culture ($OD_{600}$ = 2.5) were mixed with 1 ml methanol containing the internal standard. After centrifugation (9,000 × g, 10 min), 160 μl of the supernatant were transferred to glass vials for LC-MS/MS analysis. For each sample, cultivation and extraction were performed in duplicates.

### LC-MS/MS Analysis

We performed the analyses using a TSQ Quantum mass spectrometer equipped with an ESI source and a triple quadrupole mass detector (Thermo Finnigan, San Jose, CA). The MS detection was carried out at a spray voltage of 3.6 kV, a nitrogen sheath gas pressure of $4.0 \times 10^5$ Pa, an auxiliary gas pressure of $1.0 \times 10^5$ Pa, a capillary temperature of 360°C, a tube lens offset of 94 V, and source CID of 10 V.

Observed ions were as follows (values are given, respectively, for mother ion [m/z]; collision energy [V]; product ion [m/z]; scan time [s]; scan width [m/z]): PQS: 260.160; 34; 175.053; 0.2; 3.000, internal standard (Amitriptyline): 278.000; 22; 232.970; 0.1; 3.000.

Xcalibur software was used for data acquisition and quantification with the use of a calibration curve relative to the area of the internal standard. All samples were injected by autosampler (Surveyor, Thermo Finnigan) with a volume of 20 μl. A Hypersil Gold 3 μm (150 × 2.1 mm) column (ThermoScientific, Dreieich, Germany) was used as stationary phase under isocratic conditions, with 55% of 10 mM ammonium acetate containing 0.1% trifluoroacetic acid (TFA) (v/v) and 45% of acetonitrile containing 0.1% TFA (v/v) over 6.5 min at a flow rate of 4,500 μl/min.

### Determination of Antibacterial Activity

Filter disc diffusion tests were performed on LB agar that was supplemented with an overnight culture of *E. coli tolC* to a final $OD_{600}$ of 0.01. Agar plates were incubated at 30°C with filter paper discs that were prepared to contain 25 μg test compounds. Chloramphenicol discs were included as reference.

### Determination of the Growth Curves of *P. aeruginosa* PA14

Cultures of *P. aeruginosa* PA14 were inoculated with an overnight culture to obtain a starting $OD_{600}$ = 0.025 and grown in three replicates in 250 ml Erlenmeyer flasks containing 25 ml LB medium at 37°C and 200 rpm in an orbital shaker. DMSO solutions of compounds **18** and **19** were added to the cultures to a final DMSO concentration of 0.5%. We measured bacterial growth as a function of $OD_{600}$ using FLUOstar Omega (BMG LABTECH, Ortenberg, Germany). *P. aeruginosa* PA14 cultures containing 0.5% DMSO were used as a control.

## SUPPLEMENTAL INFORMATION

Supplemental Information includes three tables, three figures, and Supplemental Experimental Procedures and can be found with this article online at doi:10.1016/j.chembiol.2012.01.015.

## ACKNOWLEDGMENTS

We thank the DAAD (German Academic Exchange Service) for providing a fellowship to C.L. We are very grateful to Dr. Cugini and Dr. Hogan (Dartmouth Medical School, Hanover, NH, USA) for kindly supplying the plasmid pEAL08-2. We thank Professor Rolf Müller of the Helmholtz-Institute for Pharmaceutical Research Saarland, Saarbrücken, Germany, for providing the *E. coli tolC* strain and the pSUMO3_ck4_pqsR$^{C87}$ plasmid.

Received: September 30, 2011
Revised: January 10, 2012
Accepted: January 13, 2012
Published: March 22, 2012

## REFERENCES

Arunlakshana, O., and Schild, H.O. (1959). Some quantitative uses of drug antagonists. Br. J. Pharmacol. *14*, 48–58.

Bjarnsholt, T., and Givskov, M. (2007). Quorum-sensing blockade as a strategy for enhancing host defences against bacterial pathogens. Philos. Trans. R. Soc. B Biol. Sci. *362*, 1213–1222.

Bratsch, S.G. (1985). Group electronegative method with Pauling units. J. Chem. Educ. *62*, 101–103.

Bredenbruch, F., Nimtz, M., Wray, V., Morr, M., Müller, R., and Häussler, S. (2005). Biosynthetic pathway of *Pseudomonas aeruginosa* 4-hydroxy-2-alkylquinolines. J. Bacteriol. *187*, 3630–3635.

Bredenbruch, F., Geffers, R., Nimtz, M., Buer, J., and Häussler, S. (2006). The *Pseudomonas aeruginosa* quinolone signal (PQS) has an iron-chelating activity. Environ. Microbiol. *8*, 1318–1329.

Cao, H., Krishnan, G., Goumnerov, B., Tsongalis, J., Tompkins, R., and Rahme, L.G. (2001). A quorum sensing-associated virulence gene of *Pseudomonas aeruginosa* encodes a LysR-like transcription regulator with a unique self-regulatory mechanism. Proc. Natl. Acad. Sci. USA *98*, 14613–14618.

Collier, D.N., Anderson, L., McKnight, S.L., Noah, T.L., Knowles, M., Boucher, R., Schwab, U., Gilligan, P., and Pesci, E.C. (2002). A bacterial cell to cell signal in the lungs of cystic fibrosis patients. FEMS Microbiol. Lett. *215*, 41–46.

Costerton, J.W., Stewart, P.S., and Greenberg, E.P. (1999). Bacterial biofilms: a common cause of persistent infections. Science *284*, 1318–1322.

Courtney, J.M., Bradley, J., Mccaughan, J., O'Connor, T.M., Shortt, C., Bredin, C.P., Bradbury, I., and Elborn, J.S. (2007). Predictors of mortality in adults with cystic fibrosis. Pediatr. Pulmonol. *42*, 525–532.

Cugini, C., Calfee, M.W., Farrow, J.M., 3rd, Morales, D.K., Pesci, E.C., and Hogan, D.A. (2007). Farnesol, a common sesquiterpene, inhibits PQS production in *Pseudomonas aeruginosa*. Mol. Microbiol. *65*, 896–906.

Déziel, E., Lépine, F., Milot, S., He, J.X., Mindrinos, M.N., Tompkins, R.G., and Rahme, L.G. (2004). Analysis of *Pseudomonas aeruginosa* 4-hydroxy-2-alkylquinolines (HAQs) reveals a role for 4-hydroxy-2-heptylquinoline in cell-to-cell communication. Proc. Natl. Acad. Sci. USA *101*, 1339–1344.

Déziel, E., Gopalan, S., Tampakaki, A.P., Lépine, F., Padfield, K.E., Saucier, M., Xiao, G., and Rahme, L.G. (2005). The contribution of MvfR to *Pseudomonas aeruginosa* pathogenesis and quorum sensing circuitry regulation: multiple quorum sensing-regulated genes are modulated without affecting *lasRI*, *rhlRI* or the production of N-acyl-L-homoserine lactones. Mol. Microbiol. *55*, 998–1014.

Diggle, S.P., Lumjiaktase, P., Dipilato, F., Winzer, K., Kunakorn, M., Barrett, D.A., Chhabra, S.R., Cámara, M., and Williams, P. (2006). Functional genetic analysis reveals a 2-Alkyl-4-quinolone signaling system in the human pathogen *Burkholderia pseudomallei* and related bacteria. Chem. Biol. *13*, 701–710.

Diggle, S.P., Winzer, K., Chhabra, S.R., Worrall, K.E., Cámara, M., and Williams, P. (2003). The *Pseudomonas aeruginosa* quinolone signal molecule overcomes the cell density-dependency of the quorum sensing hierarchy, regulates *rhl*-dependent genes at the onset of stationary phase and can be produced in the absence of LasR. Mol. Microbiol. *50*, 29–43.

Diggle, S.P., Matthijs, S., Wright, V.J., Fletcher, M.P., Chhabra, S.R., Lamont, I.L., Kong, X., Hider, R.C., Cornelis, P., Cámara, M., and Williams, P. (2007). The *Pseudomonas aeruginosa* 4-quinolone signal molecules HHQ and PQS play multifunctional roles in quorum sensing and iron entrapment. Chem. Biol. *14*, 87–96.

Farrow, J.M., 3rd, Sund, Z.M., Ellison, M.L., Wade, D.S., Coleman, J.P., and Pesci, E.C. (2008). PqsE functions independently of PqsR-*Pseudomonas* quinolone signal and enhances the *rhl* quorum-sensing system. J. Bacteriol. *190*, 7043–7051.

Fletcher, M.P., Diggle, S.P., Crusz, S.A., Chhabra, S.R., Cámara, M., and Williams, P. (2007). A dual biosensor for 2-alkyl-4-quinolone quorum-sensing signal molecules. Environ. Microbiol. *9*, 2683–2693.

Gallagher, L.A., McKnight, S.L., Kuznetsova, M.S., Pesci, E.C., and Manoil, C. (2002). Functions required for extracellular quinolone signaling by Pseudomonas aeruginosa. J. Bacteriol. *184*, 6472–6480.

Gambello, M.J., and Iglewski, B.H. (1991). Cloning and characterization of the *Pseudomonas aeruginosa lasR* gene, a transcriptional activator of elastase expression. J. Bacteriol. *173*, 3000–3009.

Govan, J.R., and Deretic, V. (1996). Microbial pathogenesis in cystic fibrosis: mucoid *Pseudomonas aeruginosa* and *Burkholderia cepacia*. Microbiol. Rev. *60*, 539–574.

Griffith, K.L., and Wolf, R.E., Jr. (2002). Measuring beta-galactosidase activity in bacteria: cell growth, permeabilization, and enzyme assays in 96-well arrays. Biochem. Biophys. Res. Commun. *290*, 397–402.

Hartmann, R.W., Kranzfelder, G., von Angerer, E., and Schönenberger, H. (1980). Antiestrogens. Synthesis and evaluation of mammary tumor inhibiting activity of 1,1,2,2-tetraalkyl-1,2 -diphenylethanes. J. Med. Chem. *23*, 841–848.

Häussler, S., and Becker, T. (2008). The pseudomonas quinolone signal (PQS) balances life and death in Pseudomonas aeruginosa populations. PLoS Pathog. *4*, e1000166.

Heeb, S., Fletcher, M.P., Chhabra, S.R., Diggle, S.P., Williams, P., and Cámara, M. (2011). Quinolones: from antibiotics to autoinducers. FEMS Microbiol. Rev. *35*, 247–274.

Hodgkinson, J., Bowden, S.D., Galloway, W.R.J.D., Spring, D.R., and Welch, M. (2010). Structure-activity analysis of the *Pseudomonas* quinolone signal molecule. J. Bacteriol. *192*, 3833–3837.

Jander, G., Rahme, L.G., and Ausubel, F.M. (2000). Positive correlation between virulence of *Pseudomonas aeruginosa* mutants in mice and insects. J. Bacteriol. *182*, 3843–3845.

Klebe, G. (2009). Von Agonisten zu Antagonisten. In Wirkstoffdesign, Second Edition (Heidelberg, Germany: Spektrum Akademischer Verlag), pp. 118–119.

Klein, T., Henn, C., de Jong, C.J., Zimmer, C., Pistorius, D., Müller, R., Steinbach, A., and Hartmann, R.W. (2011). Identification of small-molecule antagonists of the *Pseudomonas aeruginosa* transcriptional regulator PqsR: biophysically guided hit discovery and optimization. ACS Chem. Biol., in press.

Koch, C., and Høiby, N. (1993). Pathogenesis of cystic fibrosis. Lancet *341*, 1065–1069.

Konieczny, M.T., Maciejewski, G., and Konieczny, W. (2005). Selectivity adjustment in the cleavage of allyl phenyl and methyl phenyl ethers with boron trifluoride–methyl sulfide complex. Synthesis *10*, 1575–1577.

Lamarche, M.G., and Déziel, E. (2011). MexEF-OprN efflux pump exports the Pseudomonas quinolone signal (PQS) precursor HHQ (4-hydroxy-2-heptylquinoline). PLoS ONE *6*, e24310.

Maddocks, S.E., and Oyston, P.C. (2008). Structure and function of the LysR-type transcriptional regulator (LTTR) family proteins. Microbiology *154*, 3609–3623.

Mahajan-Miklos, S., Tan, M.W., Rahme, L.G., and Ausubel, F.M. (1999). Molecular mechanisms of bacterial virulence elucidated using a *Pseudomonas aeruginosa-Caenorhabditis elegans* pathogenesis model. Cell *96*, 47–56.

Mashburn-Warren, L., Howe, J., Garidel, P., Richter, W., Steiniger, F., Roessle, M., Brandenburg, K., and Whiteley, M. (2008). Interaction of quorum signals with outer membrane lipids: insights into prokaryotic membrane vesicle formation. Mol. Microbiol. *69*, 491–502.

Mashburn-Warren, L., Howe, J., Brandenburg, K., and Whiteley, M. (2009). Structural requirements of the *Pseudomonas* quinolone signal for membrane vesicle stimulation. J. Bacteriol. *191*, 3411–3414.

Mavrodi, D.V., Bonsall, R.F., Delaney, S.M., Soule, M.J., Phillips, G., and Thomashow, L.S. (2001). Functional analysis of genes for biosynthesis of pyocyanin and phenazine-1-carboxamide from *Pseudomonas aeruginosa* PAO1. J. Bacteriol. *183*, 6454–6465.

McGrath, S., Wade, D.S., and Pesci, E.C. (2004). Dueling quorum sensing systems in *Pseudomonas aeruginosa* control the production of the *Pseudomonas* quinolone signal (PQS). FEMS Microbiol. Lett. *230*, 27–34.

Ochsner, U.A., and Reiser, J. (1995). Autoinducer-mediated regulation of rhamnolipid biosurfactant synthesis in *Pseudomonas aeruginosa*. Proc. Natl. Acad. Sci. USA *92*, 6424–6428.

Ochsner, U.A., Koch, A.K., Fiechter, A., and Reiser, J. (1994). Isolation and characterization of a regulatory gene affecting rhamnolipid biosurfactant synthesis in Pseudomonas aeruginosa. J. Bacteriol. *176*, 2044–2054.

Passador, L., Cook, J.M., Gambello, M.J., Rust, L., and Iglewski, B.H. (1993). Expression of *Pseudomonas aeruginosa* virulence genes requires cell-to-cell communication. Science *260*, 1127–1130.

Pesci, E.C., Milbank, J.B.J., Pearson, J.P., McKnight, S., Kende, A.S., Greenberg, E.P., and Iglewski, B.H. (1999). Quinolone signaling in the cell-to-cell communication system of *Pseudomonas aeruginosa*. Proc. Natl. Acad. Sci. USA *96*, 11229–11234.

Pistorius, D., Ullrich, A., Lucas, S., Hartmann, R.W., Kazmaier, U., and Müller, R. (2011). Biosynthesis of 2-Alkyl-4(1*H*)-quinolones in *Pseudomonas aeruginosa*: potential for therapeutic interference with pathogenicity. ChemBioChem *12*, 850–853.

Rampioni, G., Pustelny, C., Fletcher, M.P., Wright, V.J., Bruce, M., Rumbaugh, K.P., Heeb, S., Cámara, M., and Williams, P. (2010). Transcriptomic analysis reveals a global alkyl-quinolone-independent regulatory role for PqsE in facilitating the environmental adaptation of *Pseudomonas aeruginosa* to plant and animal hosts. Environ. Microbiol. *12*, 1659–1673.

Rasmussen, T.B., and Givskov, M. (2006). Quorum-sensing inhibitors as anti-pathogenic drugs. Int. J. Med. Microbiol. *296*, 149–161.

Sanderson, R.T. (1983). Polar covalence (New York: Academic Press).

Schertzer, J.W., Brown, S.A., and Whiteley, M. (2010). Oxygen levels rapidly modulate *Pseudomonas aeruginosa* social behaviours via substrate limitation of PqsH. Mol. Microbiol. *77*, 1527–1538.

Swift, S., Downie, J.A., Whitehead, N.A., Barnard, A.M.L., Salmond, G.P.C., and Williams, P. (2001). Quorum sensing as a population-density-dependent determinant of bacterial physiology. Adv. Microb. Physiol. *45*, 199–270.

Woschek, A., Mahout, M., Mereiter, K., and Hammerschmidt, F. (2007). Synthesis of 2-heptyl-1-hydroxy-4(1*H*)-quinolone unexpected rearrangement of 4-(alkoxycarbonyloxy)quinoline *N*-oxides to 1-(alkoxycarbonyloxy)-4(1*H*)-quinolones. Synthesis *10*, 1517–1522.

Xiao, G., Déziel, E., He, J., Lépine, F., Lesic, B., Castonguay, M.H., Milot, S., Tampakaki, A.P., Stachel, S.E., and Rahme, L.G. (2006). MvfR, a key *Pseudomonas aeruginosa* pathogenicity LTTR-class regulatory protein, has dual ligands. Mol. Microbiol. *62*, 1689–1699.

## 3.2 Paper II: Overcoming the Unexpected Functional Inversion of a PqsR Antagonist in *Pseudomonas aeruginosa*: an *in vivo* Potent Antivirulence Agent Targeting *pqs* Quorum Sensing

This paper has been published in *Angewandte Chemie International Edition* **2014**, *53*, 1109–1112. Reprinted with permission from *John Wiley and Sons*.

Angewandte International Edition Chemie

DOI: 10.1002/anie.201307547

Drug Discovery

# Overcoming the Unexpected Functional Inversion of a PqsR Antagonist in *Pseudomonas aeruginosa*: An In Vivo Potent Antivirulence Agent Targeting *pqs* Quorum Sensing**

*Cenbin Lu, Christine K. Maurer, Benjamin Kirsch, Anke Steinbach,* and Rolf W. Hartmann**

***Abstract:*** *The virulence regulator PqsR of Pseudomonas aeruginosa is considered as an attractive target for attenuating the bacterial pathogenicity without eliciting resistance. However, despite efforts and desires, no promising PqsR antagonist has been discovered thus far. Now, a surprising functionality change of a highly affine PqsR antagonist in P. aeruginosa is revealed, which is mediated by a bacterial signal molecule synthase and responsible for low cellular potency. Blockade of the susceptible position led to the discovery of the first antivirulence compound that is potent in vivo and targets PqsR, thus providing a proof of concept for this novel antivirulence therapy.*

Nowadays, human beings are confronted with an alarming situation in view of the lack of effective therapies against antibiotic-resistant bacterial infections.[1] The predicament is attributed to the mode of action of marketed antibiotics, which is based on interference with bacterial growth, which results in an inevitable selection of resistant strains.[2] Consequently, the discovery of novel anti-infectives that are less prone to resistance is challenging. However, the interest of the pharmaceutical industry to develop new antibiotics is decreasing.[3] Furthermore, progress is hampered by a high attrition rate of compounds that are active in cell-free assays, but inefficient in bacteria.[4] A promising strategy to overcome the growing and challenging resistance problem is to selectively target non-vital functions that are associated with the pathogenicity of a bug, such as the production of virulence factors.[5–8] The human opportunistic pathogen *P. aeruginosa* causes severe and fatal infections in cystic fibrosis patients. Aside from an extensive inflammatory response that is dominated by polymorphonuclear neutrophils,[9] virulence factors play a critical role in progressive lung deterioration during infection. Their production is controlled by a cell-density-dependent extraordinary cell-to-cell communication system, which is known as quorum sensing (QS) and uses signal molecules.[10,11] With a focus on developing anti-infectives with novel modes of action, recent contributions from academia[12–14] highlight quorum sensing inhibitors (QSIs) as potential powerful agents for antivirulence therapy. The quorum sensing of the *Pseudomonas* quinolone signal (*pqs*) is a potential target in *P. aeruginosa*. A first attempt to interfere with this system resulted in compounds with low efficiency in an animal model.[15] Herein, we describe an unexpected functional inversion of a QS receptor antagonist (a QSI) into an agonist by *P. aeruginosa* and report the first in vivo potent antivirulence agent targeting *pqs* QS.

PqsR is a key DNA-binding receptor of this *pqs* QS system that is specific to *P. aeruginosa* and a critical regulator that fine-tunes a large set of genes that encode for virulence factors, such as pyocyanin, elastase B, and hydrogen cyanide.[16,17] PQS and 2-heptyl-4-hydroxyquinoline (HHQ) are the natural ligands and agonists of the receptor (Figure 1a), and function as the signal molecules of *pqs* QS.[18,19] The biosynthesis of HHQ is conducted by the enzymes PqsABCD, which are encoded by genes located in the *pqs* operon. The transcription of this operon is in turn positively regulated by PqsR. The synthase PqsH finally hydroxylates HHQ to form PQS (Figure 1a).[20–22] A *pqsR* knock-out mutant of *P. aeruginosa* that is deficient in *pqs* QS does not produce any pyocyanin, and displays reduced pathogenicity.[19,21] Thus, we considered PqsR as an attractive target for the development of QSIs. Based on the scaffold of HHQ, we recently reported compound **1** (Figure 1a), which is, to the best of our knowledge, the only PqsR antagonist described to date. It showed an $IC_{50}$ of 51 nM in an *E. coli* reporter gene assay.[23] Considering its high activity towards PqsR, **1** only moderately reduced the production of pyocyanin (Table 1). Therefore, we decided to further characterize the behavior of the antagonist in *P. aeruginosa*. Most interestingly, **1**, which showed a purely antagonistic activity in *E. coli* reporter gene assays (Figure 1b and c), displayed a dose-dependent agonistic activity in *P. aeruginosa* (Figure 1c), which could be the reason for the marked loss of antagonistic activity of **1** ($IC_{50}$ = 51 nM in *E. coli*, 60% inhibition at 10 μM in *P. aeruginosa*; Table 1). The opposite nature of the functional properties in the two bacterial species suggests that a biotransformation of the compound may have occurred in *P. aeruginosa*. We turned our attention to the enzymes that are involved in the *pqs* QS signaling pathway and speculated that a biochemical modification of **1** into **2** by PqsH occurs (Figure 1a) for the following reasons: 1) Compound **1** is structurally very similar

[*] C. Lu,[+] C. K. Maurer,[+] B. Kirsch, Dr. A. Steinbach, Prof. Dr. R. W. Hartmann
Helmholtz-Institute for Pharmaceutical Research Saarland & Pharmaceutical and Medicinal Chemistry, Saarland University
Campus C2.3, 66123 Saarbrücken (Germany)
E-mail: anke.steinbach@helmholtz-hzi.de
rolf.hartmann@helmholtz-hzi.de

[+] These authors contributed equally to this work.

[**] We thank Drs. Daniele Bano and Kostoula Troullinaki (German Center for Neurodegenerative Diseases, Bonn, Germany) for providing *C. elegans*, Dr. Matthew Wand (Health Protection Agency, Salisbury, UK) for valuable advice regarding the *G. mellonella* infection model, and Dr. Andrea Braunshausen for helpful discussions. *pqs* = *Pseudomonas* quinolone signal.

Supporting information for this article is available on the WWW under http://dx.doi.org/10.1002/anie.201307547.

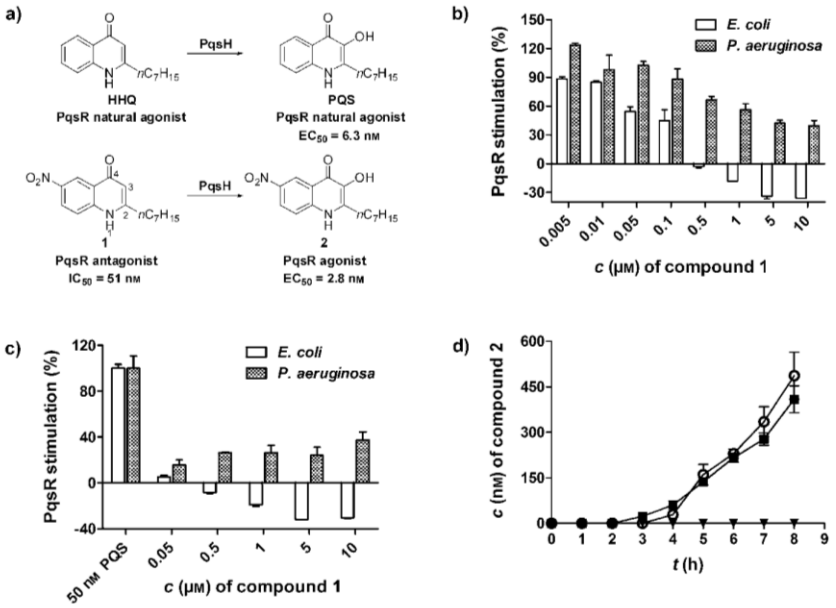


***Figure 1.*** Characterization of the PqsR antagonist **1** in *E. coli* and *P. aeruginosa* and time-dependent formation of **2**. a) Chemical structures of HHQ, PQS, **1**, and **2**. b) Antagonist test of **1** in β-galactosidase reporter gene assays based on *E. coli* or *P. aeruginosa*. The assays were performed in the presence of PQS (50 nM). For the *y* axis, 0% is defined as the basal PqsR stimulation without ligands, and 100% is defined as the PqsR stimulation by PQS (50 nM). Mean values of two independent experiments with $n=4$ are given, error bars represent standard deviation. c) Agonist test of **1** in β-galactosidase reporter gene assays based on *E. coli* or *P. aeruginosa*. For the *y* axis, 0% and 100% stimulation are defined as above. Mean values of two independent experiments with $n=4$ are given, error bars represent standard deviation. Significance of agonistic activity for **1** in *P. aeruginosa* compared to basal level: $p<0.05$. d) Time-course studies of the production of **2** in PA14 (○), *pqsH* (▼), and *pqsA* (■) mutants. Strains were incubated with **1** (5 μM). Mean values of one experiment with $n=3$ are given, error bars represent standard deviation.

***Table 1:*** Determination of antagonistic activity and effects on PQS, HHQ, and the virulence factor pyocyanin.

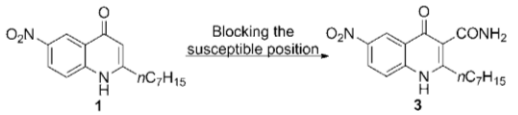


| Parameter | **1** | **3** |
|---|---|---|
| $IC_{50}$ in *E. coli* [nM] | 51 | 35 |
| $IC_{50}$ in *P. aeruginosa* [nM] | 60% inhibition[a] | 404 |
| Reduction of PQS levels[b] | 14%* | 37%* |
| Reduction of HHQ levels[b] | 1% | 54%* |
| Reduction of pyocyanin levels[b] | 44%* | 81%* ($IC_{50}$: 2 μM) |

PQS, HHQ, and pyocyanin assays were performed in PA14. Mean values of at least two independent experiments with $n=3$ are given, standard deviation less than 25%. Significance: * $p<0.05$. [a] Tested at 10 μM. [b] Tested at 15 μM.

to the natural ligand HHQ, which is converted into PQS by PqsH; 2) Many PQS analogues show agonistic activity towards PqsR;[23,24] 3) **1** revealed an agonistic activity in *P. aeruginosa* as mentioned above. To prove this hypothesis, ultrahigh-performance liquid chromatography (UHPLC) tandem mass spectrometry was applied to observe the supposed product of biotransformation **2** in *P. aeruginosa* (wild type; PA14). Interestingly, after incubation of PA14 with **1**, the chromatogram of selected reaction monitoring (SRM) transition $m/z$ 303 > 218 revealed a signal peak with identical retention times for the proposed product and the chemically synthesized compound **2** (Supporting Information, Figure S1). To further validate bacterial-cell-mediated conversion of **1** into **2**, and to examine the involvement of PqsH in this process, a time-course study was conducted. The production of **2** in PA14 and in the native-ligand-free mutant *pqsA*[21] with functional PqsH was time-dependent, whereas the *pqsH* mutant failed to synthesize **2** (Figure 1d; for the results after 16 h, see Figure S2). This result clearly identifies PqsH as the enzyme responsible for the biotransformation. Subsequently, we examined the activity of product **2**. In a competition experiment performed in *E. coli*, **2** efficiently restored the PqsR stimulation that was repressed by antagonist **1** (in the antagonist test, **2** restored almost 50% of the PqsR stimulation, even in competition with **1** at ten times higher concentrations; Figure S3). Compound **2** ($EC_{50}$ = 2.8 nM; $EC_{50}$: ligand concentration to achieve a half-maximal degree of PqsR receptor stimulation) is even more active than the strongest natural PqsR agonist PQS ($EC_{50}$ = 6.3 nM). Taken together, these findings explain that the unexpected agonistic activity that was observed for **1** in *P. aeruginosa* is due to PqsH-mediated functional inversion (Figure 1a).

For a rational development of potent and stable PqsR antagonists, the susceptible 3-position had to be blocked by substitution of the hydrogen atom with an appropriate functional group. A small library of 3-substituted compounds ($CONH_2$, COOH, COOEt, and CONHOH) were synthesized (data not shown). In terms of their agonistic/antagonistic profiles, the carboxamide **3** (for its synthesis, see Figure S4) turned out to be the most promising derivative. Accordingly, **3** was used for further biological evaluation. Most interestingly, **3** showed high potency in the *E. coli* reporter gene assay, but retained its antagonistic activity in *P. aeruginosa* without displaying any agonistic activity up to 15 μM (Table 1).

Next, the effects of the antagonists on the production of the signal molecules were examined in PA14.[25] Compared with **1**, the improved antagonist **3** was able to strongly reduce the HHQ and PQS levels by over 50% and 30%, respectively, at a concentration of 15 μM (Table 1). We then investigated the production of pyocyanin, an important virulence factor

and a major contributor to the pathogenicity of *P. aeruginosa*.[26] Strikingly, **3** efficiently decreased the pyocyanin levels with an $IC_{50}$ of 2 μM, whereas **1** revealed a strongly reduced potency (44% at 15 μM). A growth-inhibition effect could be excluded based on growth curves of PA14 that were measured in the presence of antagonist (15 μM) in minimal medium (Figure S5). Overall, optimization of the antagonist led to enhanced effects on the reduction of signal-molecule and pyocyanin levels, which is in agreement with the improved antagonistic activity that was observed in the *P. aeruginosa* reporter gene assay. To the best of our knowledge, **3** is the compound that most effectively interferes with the *pqs* QS system in *P. aeruginosa*.

Encouraged by these results, we validated the PqsR antagonistic properties of **3** in appropriate animal experiments.[27] As *Caenorhabditis elegans* is sensitive towards a *P. aeruginosa* infection and its virulence factor pyocyanin,[28] **3** was evaluated in a *C. elegans* fast killing assay. The survival rate of *C. elegans* that were incubated on agar plates containing PA14 and **3** (15 μM) remained at 94%; in the absence of the antagonist, however, the survival rate continuously decreased to 47% (control) within six hours (Figure 2a). These results highlight a protective effect of **3** against *P. aeruginosa* infection in the nematode assay.

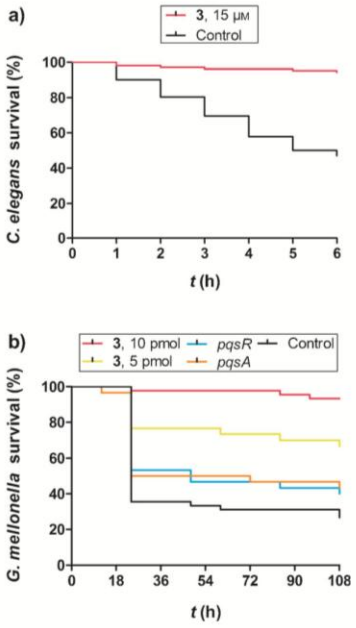


***Figure 2.*** Evaluation of the PqsR antagonist **3** in animal infection models. a) Kaplan–Meier survival curves of *C. elegans* incubated on agar plates containing PA14 and DMSO (control) or **3** (15 μM). Results represent cumulative data from three independent experiments. The survival rate was significantly larger for treated nematodes than for those in the control experiment ($p < 0.0001$; log-rank test). b) Survival curves of *G. mellonella* larvae infected with PA14 receiving no treatment (control) or receiving treatment with compound **3** (5 pmol or 10 pmol), and of larvae infected with the PA14 *pqsR* or *pqsA* mutants. Results represent combined data from at least two independent experiments. The survival rate was significantly larger for treated larvae than for larvae in the control experiment (5 pmol of **3**: $p < 0.001$, 10 pmol of **3**: $p < 0.0001$; log-rank test).

We further challenged a more complex animal infection model with *Galleria mellonella*. This insect model displays a significant positive correlation with a mouse model and is therefore considered as a powerful tool to investigate pathogenicity causing mammalian infections. The larvae of the greater wax moth are susceptible to PA14, with a 50% lethal dose of one bacterium.[29] *G. mellonella* larvae were infected with PA14 in the absence and presence of antagonist **3**. Most interestingly, the treatment of the PA14-infected larvae with antagonist **3** (10 pmol) led to a survival rate of 93% (Figure 2b), whereas only 36% of the infected larvae survived the first 24 h in the absence of **3** (control). Treatment with only 5 pmol of antagonist provided partial protection with a survival rate of 67%. It should be noted that **3** is intensively diluted by the hemolymph after injection. Given an average weight of 450 mg and assuming a total hemolymph volume of 450 μL for each larva, the antagonist exerted its therapeutic effect at a final concentration of 22 nM (corresponding to 7.3 $ng\,g^{-1}$ body weight) in the larva. Most interestingly, PA14-infected larvae receiving treatment with antagonist **3** showed much higher survival rates than those infected with the mutants *pqsA* and *pqsR*, which are deficient in *pqs* QS (Figure 2b). This implies that disruption of QS with small molecules, rather than genetic deletion, can be advantageous. Overall, the results from the two animal studies clearly show that **3** is a strong antivirulence agent.

In summary, we have revealed that the synthase PqsH converts the potent PqsR antagonist into a strong agonist; this process is responsible for the low efficacy of compound **1**. Surprisingly, such a slight structural modification (hydroxylation) leads to complete loss of the antagonistic activity of compound **1** and dramatically imparts the opposite functionality (agonism) to the ligand. A high percentage of anti-infectives suffer from ineffectiveness in cell-based assays or under in vivo conditions, which is generally considered to be due to penetration problems or efflux-pump-mediated excretion. As an optimization addressing these drawbacks is regarded as highly challenging, these compounds are usually discarded. Herein, we suggested that a rational consideration of other potential factors that impair the activity is rewarding. As shown in this case study, ineffective compounds can be rescued by medicinal-chemistry strategies, which decreases the attrition rate during the drug development process. Moreover, our research identified the PqsR antagonist **3** as an antivirulence agent that is highly potent in vivo, which provides the first proof of concept that PqsR antagonists reduce the mortality caused by *P. aeruginosa* in two animal models. This finding provides a promising starting point for further in vivo investigations using mammalian organisms and may open new avenues for the development of anti-infectives that are less prone to resistance. Furthermore, species-selective targeting of specific regulatory pathways might help to minimize adverse effects that are observed with broad-spectrum antibiotics.

Received: August 27, 2013
Revised: October 10, 2013
Published online: December 11, 2013

**Keywords:** antivirulence · drug discovery · inhibitors · medicinal chemistry · resistance


[1] C. A. Arias, B. E. Murray, *N. Engl. J. Med.* **2010**, *362-363*, 439 – 443.
[2] S. B. Levy, B. Marshall, *Nat. Med.* **2004**, *10*, 122 – 129.
[3] K. Lewis, *Nature* **2012**, *485*, 439 – 440.
[4] A. R. M. Coates, G. Halls, Y. Hu, *Br. J. Pharmacol.* **2011**, *163*, 184 – 194.
[5] L. Cegelski, G. R. Marshall, G. R. Eldridge, S. J. Hultgren, *Nat. Rev. Microbiol.* **2008**, *6*, 17 – 27.
[6] D. A. Rasko, V. Sperandio, *Nat. Rev. Drug Discovery* **2010**, *9*, 117 – 128.
[7] W. R. Galloway, J. T. Hodgkinson, S. Bowden, M. Welch, D. R. Spring, *Trends Microbiol.* **2012**, *20*, 449 – 458.
[8] K. M. O'Connell, J. T. Hodgkinson, H. F. Sore, M. Welch, G. P. Salmond, D. R. Spring, *Angew. Chem.* **2013**, *125*, 10904 – 10932; *Angew. Chem. Int. Ed.* **2013**, *52*, 10706 – 10733.
[9] D. G. Downey, S. C. Bell, J. S. Elborn, *Thorax* **2009**, *64*, 81 – 88.
[10] S. Swift, J. A. Downie, N. A. Whitehead, A. M. L. Barnard, G. P. C. Salmond, P. Williams, *Adv. Microb. Physiol.* **2001**, *45*, 199 – 270.
[11] S. T. Rutherford, B. L. Bassler, *Cold Spring Harbor Perspect. Med.* **2012**, *2*, a012427.
[12] R. Frei, A. S. Breitbach, H. E. Blackwell, *Angew. Chem.* **2012**, *124*, 5316 – 5319; *Angew. Chem. Int. Ed.* **2012**, *51*, 5226 – 5229.
[13] G. Brackman, S. Celen, K. Baruah, P. Bossier, S. V. Calenbergh, H. J. Nelis, T. Coenye, *Microbiology* **2009**, *155*, 4114 – 4122.
[14] M. P. Storz, C. K. Maurer, C. Zimmer, N. Wagner, C. Brengel, J. C. de Jong, S. Lucas, M. Müsken, S. Häussler, A. Steinbach, R. W. Hartmann, *J. Am. Chem. Soc.* **2012**, *134*, 16143 – 16146.
[15] B. Lesic, F. Lepine, E. Deziel, J. Zhang, Q. Zhang, K. Padfield, M. Castonguay, S. Milot, S. Stachel, A. A. Tzika, R. G. Tompkins, L. G. Rahme, *PLoS Pathog.* **2007**, *3*, 1229 – 1239.
[16] H. Cao, G. Krishnan, B. Goumnerov, J. Tsongalis, R. Tompkins, L. G. Rahme, *Proc. Natl. Acad. Sci. USA* **2001**, *98*, 14613 – 14618.
[17] E. Déziel, S. Gopalan, A. P. Tampakaki, F. Lépine, K. E. Padfield, M. Saucier, G. Xiao, L. G. Rahme, *Mol. Microbiol.* **2005**, *55*, 998 – 1014.
[18] E. C. Pesci, J. B. J. Milbank, J. P. Pearson, S. McKnight, A. S. Kende, E. P. Greenberg, B. H. Iglewski, *Proc. Natl. Acad. Sci. USA* **1999**, *96*, 11229 – 11234.
[19] G. Xiao, E. Deziel, J. He, F. Lepine, B. Lesic, M. Castonguay, S. Milot, A. P. Tampakaki, S. E. Stachel, L. G. Rahme, *Mol. Microbiol.* **2006**, *62*, 1689 – 1699.
[20] L. A. Gallagher, S. L. McKnight, M. S. Kuznetsova, E. C. Pesci, C. Manoil, *J. Bacteriol.* **2002**, *184*, 6472 – 6480.
[21] E. Deziel, F. Lepine, S. Milot, J. X. He, M. N. Mindrinos, R. G. Tompkins, L. G. Rahme, *Proc. Natl. Acad. Sci. USA* **2004**, *101*, 1339 – 1344.
[22] J. W. Schertzer, S. A. Brown, M. Whiteley, *Mol. Microbiol.* **2010**, *77*, 1527 – 1538.
[23] C. Lu, B. Kirsch, C. Zimmer, J. C. de Jong, C. Henn, C. K. Maurer, M. Müsken, S. Häussler, A. Steinbach, R. W. Hartmann, *Chem. Biol.* **2012**, *19*, 381 – 390.
[24] J. Hodgkinson, S. D. Bowden, W. R. J. D. Galloway, D. R. Spring, M. Welch, *J. Bacteriol.* **2010**, *192*, 3833 – 3837.
[25] C. K. Maurer, A. Steinbach, R. W. Hartmann, *J. Pharm. Biomed. Anal.* **2013**, *86C*, 127 – 134.
[26] J. M. Courtney, J. Bradley, J. Mccaughan, T. M. O'Connor, C. Shortt, C. P. Bredin, I. Bradbury, J. S. Elborn, *Pediatr. Pulmonol.* **2007**, *42*, 525 – 532.
[27] E. Papaioannou, P. D. Utari, W. J. Quax, *Int. J. Mol. Sci.* **2013**, *14*, 19309 – 19340.
[28] S. Mahajan-Miklos, M. Tan, L. G. Rahme, F. M. Ausubel, *Cell* **1999**, *96*, 47 – 56.
[29] G. Jander, L. G. Rahme, F. M. Ausubel, *J. Bacteriol.* **2000**, *182*, 3843 – 3845.

## 3.3 Paper III: Optimization of Anti-virulence PqsR Antagonists Regarding Aqueous Solubility and Biological Properties Resulting in New Insights in Structure-activity Relationships

This paper has been published in *European Journal of Medicinal Chemistry* **2014**, *79*, 173–183. 

European Journal of Medicinal Chemistry 79 (2014) 173–183

Contents lists available at ScienceDirect

European Journal of Medicinal Chemistry

journal homepage: http://www.elsevier.com/locate/ejmech

Short communication

# Optimization of anti-virulence PqsR antagonists regarding aqueous solubility and biological properties resulting in new insights in structure–activity relationships

Cenbin Lu [a,1], Benjamin Kirsch [a,1], Christine K. Maurer [a], Johannes C. de Jong [a], Andrea Braunshausen [a], Anke Steinbach [a], Rolf W. Hartmann [a,b,*]

[a] Helmholtz-Institute for Pharmaceutical Research Saarland, Campus C2.3, 66123 Saarbrücken, Germany
[b] Pharmaceutical and Medicinal Chemistry, Saarland University, Campus C2.3, 66123 Saarbrücken, Germany

ARTICLE INFO

*Article history:*
Received 29 October 2013
Received in revised form
3 April 2014
Accepted 4 April 2014
Available online 5 April 2014

*Keywords:*
*Pseudomonas aeruginosa* infection
Bacterial communication
*Quorum sensing* inhibitor
PqsR antagonist
Structure–activity relationship
Structure–property relationship

ABSTRACT

Increasing antibiotic resistance urgently requires novel therapeutic options to combat bacterial infections. The anti-virulence therapy selectively intervening with pathogenicity without affecting bacterial viability is such a strategy to overcome resistance. We consider the virulence regulator PqsR as an attractive target in the human pathogen *Pseudomonas aeruginosa*, and recently discovered the first PqsR antagonists, which, however, suffered from poor aqueous solubility. In this work, the antagonists were structurally modified to become more soluble, and their structure–activity as well as structure–property relationships were studied. A novel promising compound with improved solubility and enhanced anti-virulence activity was discovered ($IC_{50}$: 3.8 μM, pyocyanin). Our findings emphasize the crucial role of substituents at the 3-position and the carbonyl group at the 4-position for ligand–receptor interactions, and illuminate the way for further optimization of PqsR antagonists as anti-virulence agents.



## 1. Introduction

The opportunistic human pathogen *Pseudomonas aeruginosa* is one of the most common causes of nosocomial infections and a major problem in cystic fibrosis (CF) patients leading to inflammation, chronic persistent lung infections and high mortality [1,2]. Like many other pathogenic bacteria, *P. aeruginosa* expresses a battery of tissue-damaging virulence factors to facilitate infection via a cell density dependent cell-to-cell communication system known as *quorum sensing* [3] by secreting and sensing of signal molecules termed autoinducers (AIs). *P. aeruginosa* utilizes a unique species-specific *pqs* QS system [4], which is composed of two AIs, PQS (*P*seudomonas Quinolone Signal, Chart 1) and HHQ (2-heptyl-4-hydroxyquinoline), as well as PqsR which functions as a receptor and a virulence regulator [5,6]. The *pqs* QS system regulates expression of multiple virulence genes, such as *phzA1-G1*, which are involved in the biosynthesis of pyocyanin, *hcnAB*, responsible for the production of hydrogen cyanide, and *lasB*, which encodes elastase B [5,7]. Besides, PqsR drives the biosynthesis of its AI HHQ through activation of the *pqs* operon *pqsABCD*. HHQ is further converted to the more potent PQS by PqsH [8–10]. Thus, a positive autoinducing loop is triggered via stimulation of PqsR by PQS and HHQ [11].

The anti-virulence therapy using QS inhibitors (QSIs) selectively intervening with pathogenicity, e.g. by repressing the production of virulence factors, without impairing bacterial viability is discussed as an alternative approach to conventional anti-bacterial therapy. It is supposed that in anti-virulence therapy the selection pressure is reduced. This treatment option is therefore regarded as a promising strategy to overcome the rising and challenging resistance problem [12–14].

The critical virulence regulator PqsR has attracted rising attention by researchers as a favorable target for QSIs [15,16]. Based on the scaffold of the natural agonist HHQ, we recently developed the first PqsR antagonists. The compounds showed $IC_{50}$ values in the low nanomolar range (Chart 1) and reduced the production of the virulence factor pyocyanin in *P. aeruginosa* [17]. However, a major

* Corresponding author. Helmholtz-Institute for Pharmaceutical Research Saarland, Pharmaceutical and Medicinal Chemistry, Saarland University, Campus C2.3, 66123 Saarbrücken, Germany.
*E-mail addresses:* rolf.hartmann@helmholtz-hzi.de, rwh@mx.uni-saarland.de (R.W. Hartmann).
[1] These authors contributed equally to this work.

http://dx.doi.org/10.1016/j.ejmech.2014.04.016
0223-5234/

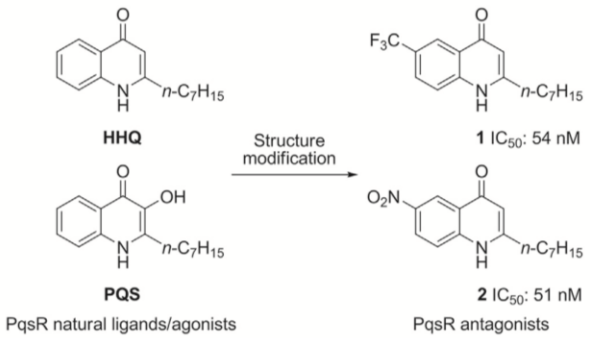


**Chart 1.** Discovery of the first PqsR antagonists by ligand-based approach.

drawback of these compounds is their poor aqueous solubility (<5 μM in 2% DMSO). This physicochemical property is essential for a compound to be considered as a drug candidate since a good solubility is important for pharmacokinetic properties [18]. Insufficient solubility is often the cause for failures in drug development [19]. Aiming at the improvement of the aqueous solubility we herein describe structure modifications of our PqsR antagonists and their impact on the biological properties of the new compounds, and discuss the obtained structure–activity (SAR) as well as structure–property relationships (SPR).

## 2. Results and discussion

### 2.1. Design

First, we suspected that the intermolecular stacking [20] or H-bond between the NH group at 1-position and the carbonyl group at 4-position may contribute to the poor solubility. Thus, a methyl group was introduced to block such interactions (compound class 1, Chart 2). Second, to increase the hydrophilicity, polar or ionisable groups were introduced into the molecule: oxygen was inserted into the alkyl side chain (compound class 2); the 3-position was substituted with e.g. amide, amino, carboxylic or hydroxamic acid groups (compound class 3); the benzene moiety substituted with electron withdrawing groups was replaced by pyridine (compound class 4). The structure modifications were performed based on antagonist **2** due to the good synthetic accessibility of the nitro compounds.

### 2.2. Chemistry

HHQ, **1**, **2**, **14**, **16**, **18**, **22**, **26** and **36** were synthesized as previously described [17]. Stirring of HHQ, **1** or **36** with methyl iodide under basic conditions yielded the class 1 compounds **3**–**5** (Scheme 1). Compounds **6**, **7**, **9** and **10** of class 2 were obtained by Conrad–Limpach cyclization: condensation of the β-ketoesters **33** and **34** with aniline or substituted anilines followed by cyclization of the resulting enamine in refluxing diphenyl ether yielded the desired products. Compound **11** was obtained via decarboxylation of **24** (Scheme 2). **6** was further converted to **8** by nitration. For preparation of class 3 and 4 compounds, the intermediates of the quinolone-3-carboxylic esters **17**–**20** and **29** were prepared by condensation of the isatoic anhydride derivatives with the β-ketoesters **32**–**34** under sodium hydride catalysis (Scheme 2). After hydrolysis of the quinolone-3-carboxylic esters the resulting acids **21**–**24** and **30** were further derivatized: **21** and **22** were condensed with ammonia or hydroxylamine to give the carboxamide **25** and the hydroxamic acids **27** and **28**, respectively. Decarboxylation of **30** at high temperature afforded **31**. Nitration of HHQ gave **12** (Scheme 1), which was further reduced to **13**. Reduction of the ester **17** with lithium aluminium hydride gave the hydroxymethyl compound **15** (Scheme 2).

### 2.3. Biological and physicochemical properties

The PqsR-mediated transcriptional effect of the compounds was evaluated as previously described in a β-galactosidase reporter gene assay in *Escherichia coli* containing the plasmid pEAL08-2. The latter encodes PqsR which is under control of the tac promoter and the β-galactosidase reporter gene *lacZ* controlled by the *pqsA* promoter. The solubility was initially determined based on observation of the solution clarity [17]. The eight best compounds were chosen for determination of PqsR antagonistic properties and calculation of logP values. Their aqueous solubility was determined using a standard HPLC protocol [21].

**Compound class 1**. The *O*-methylation of HHQ decreased the solubility of the molecule and led to neither agonistic nor antagonistic activity (**3**, Table 1), suggesting a critical role of the carbonyl group (but not NH group, see below) for the ligand–receptor interaction. As this modification led to a total loss of activity, we refrained from performing *O*-methylation with PqsR antagonists. The two *N*-methylated derivatives **4** and **5** revealed a moderate antagonistic activity with improved solubility compared with **1** (Tables 1 and 2). This result indicates the importance of the NH hydrogen for antagonistic activity. The better solubility might be due to the disruption of intermolecular interactions.

**Compound class 2**. Introduction of oxygen into the alkyl side chain of the antagonists **1** and **2** close to the quinolone core (**7** and **8**, Tables 1 and 2) resulted in a moderate antagonistic activity and an enhanced solubility (6–15 times). Interestingly, in case the oxygen was located far from the quinolone core (**10** and **11**), the potency was dramatically decreased (32–69 fold), whereas the solubility was strongly increased (15–66 fold). Similar as observed for the antagonists, the oxygen far from the core also made the agonists less potent (comparing **6** and **9**, Table 1). Overall, this data suggests that on one hand, the alkyl side chain-binding pocket of PqsR does not tolerate a deeply intruding oxygen (far from the core). On the other hand, such an oxygen imparts significant improvement of solubility possibly due to a better solvation without being shielded by the core.

**Compound class 3**. Most of the derivatives (**12**, **13**, **15**, **21**, **25** and **27**, Table 1) lacking the nitro group in 6-position displayed a moderate to strong agonistic activity regardless of the groups in 3-position. Particularly, removal of the nitro group in the antagonist **2** from the 6- into the 3-position resulted in agonist **12**, indicating that not only the electron-withdrawing property but also the position of the nitro group plays a crucial role for the antagonistic effect. Interestingly, the unique exception is the carboxylic acid ester **17**. Its weak antagonistic activity may be contributed to steric rather than electronic effects in contrast to **12**. However, a further introduction of a nitro group into the 6-positon of the ester (**18**, for **19** and **20**, combined with ether side chains) did not enhance the antagonistic activity. Substitution of the 3-position of antagonists **2**, **8** and **11** with a hydroxy (**14**), hydroxamic acid (**28**) or negatively ionizable group (carboxylic acids **22**–**24**) totally or partially reverses the functionality from antagonism to agonism, implying that the electron-donating property may favor PqsR stimulation. Most interestingly, a highly active antagonist **16** was regained from the pure agonist **14** through exchange of the hydroxy by a hydroxymethyl at the 3-position (Tables 1 and 2). Compound **26** with 3-carboxamide, as described in a previous work [22], is a potent antagonist. Overall, the result implies that substituents at the 3-

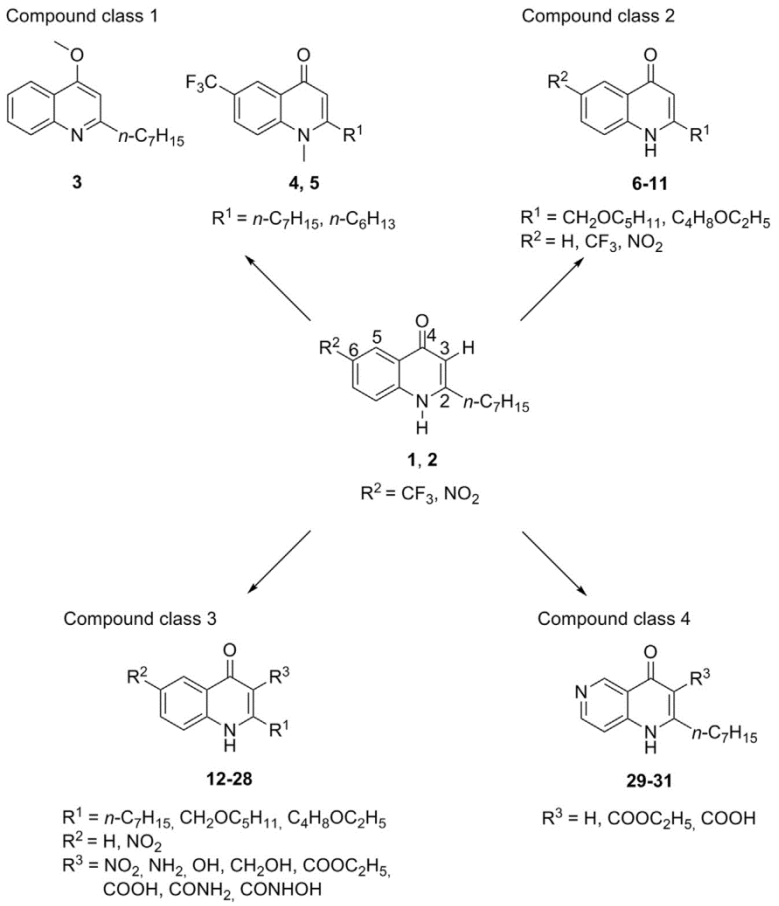


**Chart 2.** Structure modifications of PqsR antagonists **1** and **2** leading to compound classes 1–4.

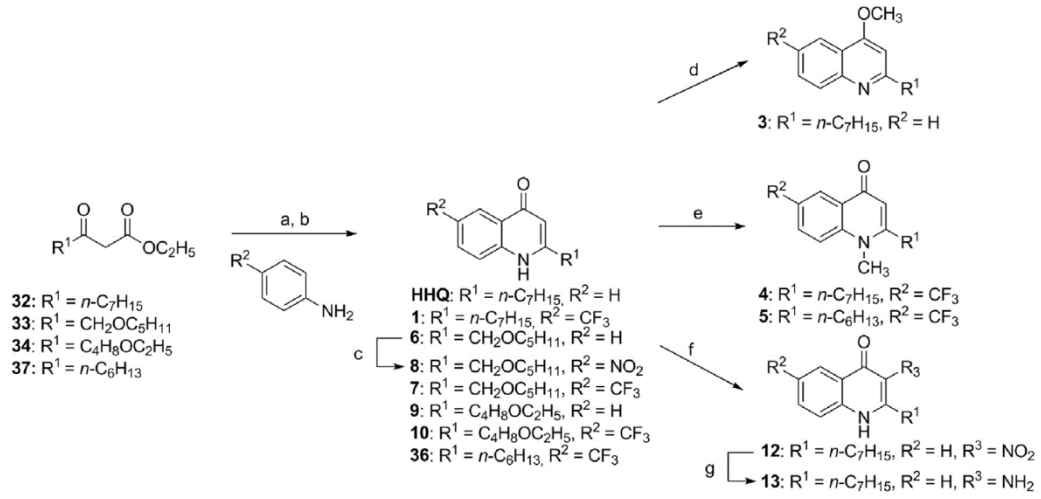


**Scheme 1.** Reagents and conditions: (a) *p*-TsOH·$H_2O$, *n*-hexane, reflux; (b) $Ph_2O$, reflux; (c) conc. $HNO_3$, conc. $H_2SO_4$, 0 °C – r.t.; (d) MeI, $Cs_2CO_3$, DMF, r.t.; (e) MeI, KOH, MeOH, r.t.; (f) conc. $HNO_3$, propionic acid, 110 °C; (g) $Fe^0$, $NH_4Cl$, EtOH, reflux.

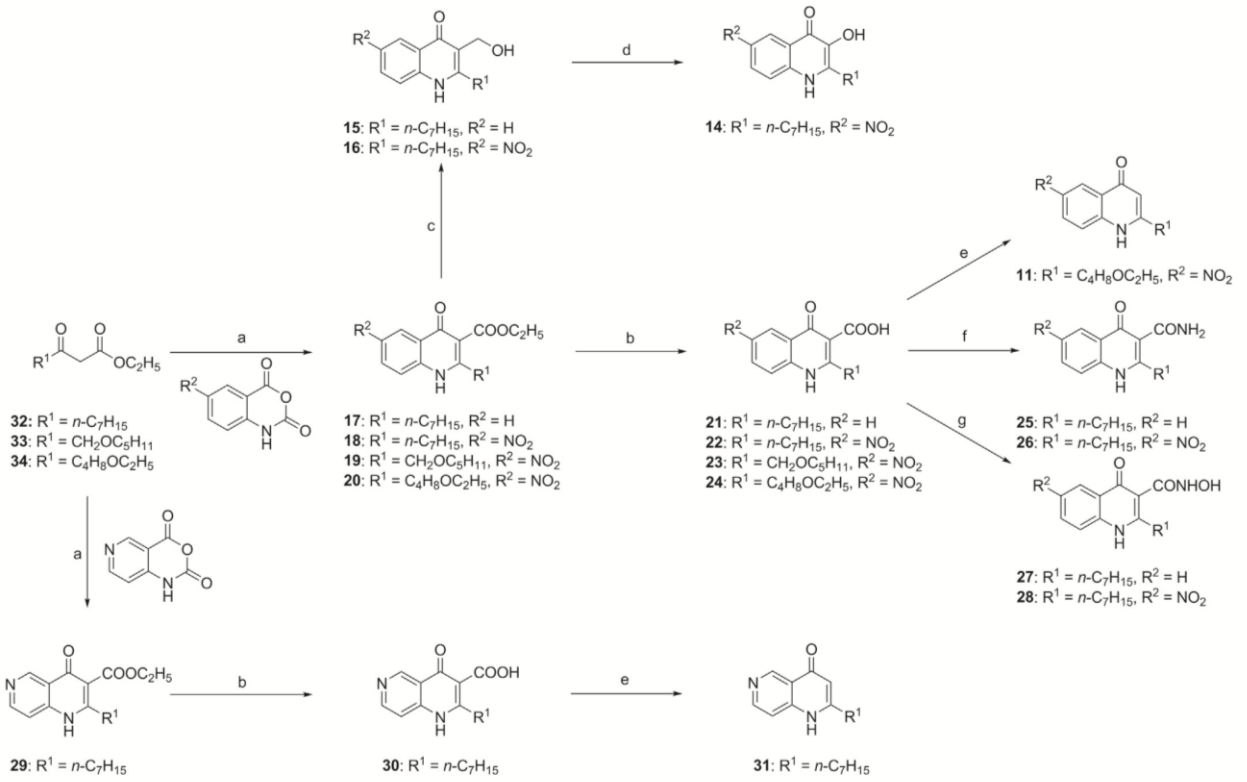


**Scheme 2.** Reagents and conditions: (a) NaH, dry DMF, r.t. then HCl; (b) NaOH, $H_2O$, reflux then HCl; (c) $LiAlH_4$, dry THF, 0 °C – r.t.; (d) $MnO_2$, dry THF, r.t. then $B(OH)_3$, conc. $H_2SO_4$, $H_2O_2$, THF, r.t.; (e) 310 °C; (f) *N,N'*-carbonyldiimidazole, $NH_3 \bullet H_2O$, dry DMF, 0 °C – r.t.; (g) *N,N'*-carbonyldiimidazole, *N*-methylmorpholine, $NH_2OH \cdot HCl$, dry DMF, 0 °C – r.t.

position are of decisive importance for the ligand functionality. Substitution in 3-position with amino or ionizable groups (**13**, **21**–**24**, **27** and **28**) resulted in a good solubility with the hydroxamic acids as the best compounds (>200 μM), while hydroxymethyl, ester and carboxamide groups led to either moderate enhancement (**15**, **16**, **18**, **19**, **25** and **26**) or slight reduction (**17** and **20**) of solubility compared with the corresponding unsubstituted compounds. The introduction of a nitro (**12**) or hydroxy group (**14**) did not make the compounds more soluble.

**Compound class 4**. Compound **31** shows agonistic properties (Table 1). Similar to the observation for the corresponding compounds from class 3 (**17** and **21**), the 3-ester **29** is an antagonist, whereas the 3-carboxylic acid **30** revealed agonistic activity. This result shows that the nitro group cannot be replaced by an aromatic ring nitrogen at same position without losing antagonism. As expected, all pyridine derivatives showed a good solubility.

According to the *in silico* prediction, the clogP values of the eight selected compounds are reduced except for compound **16** (Table 2, calculation with ACD Percepta Classic method). The decreased logP values are generally correlated to the enhanced water solubility.

In the next step the selected antagonists were evaluated for their effects on the production of the autoinducer PQS and the virulence factor pyocyanin in *P. aeruginosa*. Similar to the potent anti-virulence compound **26**, **16** with a hydroxymethyl group at the 3-position was able to efficiently repress the biosynthesis of PQS and pyocyanin, whereas all compounds unsubstituted in 3-position (**4**, **7**, **8**, **10** and **11**) were less active (Table 2). Beside this low antagonistic activity toward PqsR, the metabolic susceptibility in 3-position shall play a critical role for the low effectiveness of the unsubstituted compounds in *P. aeruginosa* as previously described for antagonist **2** [22].

Metal-chelating properties lead to growth inhibition of the bacteria via destabilization of the outer membrane [23,24] or reduction of iron availability [25], which is therefore unwanted for an anti-virulence strategy. The CAS iron chelation assay [26] showed that the most potent antagonists **16** and **26** do not have such undesirable properties (data not shown). As expected, no growth inhibition was observed for all tested antagonists in the PQS and pyocyanin assays (data not shown), indicating that their QS or virulence factor inhibitory effects are not caused via impairing bacterial viability.

## 3. Conclusion

Aiming at the development of more soluble and potent PqsR-targeting QSIs for an anti-virulence therapy, four classes of new quinolone compounds were designed and synthesized based on the scaffold of the first PqsR antagonists, and their SAR as well as SPR were systematically investigated. Particularly, a very promising compound **16** arose from this research with improvement on both aqueous solubility and virulence factor inhibition. Our findings give new insights into the ligand–receptor interactions for PqsR: the substituents at 3-position play a critical role for the ligand functionality, and the carbonyl group at 4-position is essential for the interactions between ligand and protein. These results provide a promising starting point for further optimization of PqsR antagonists to combat *P. aeruginosa* infections.

**Table 1**
Determination of solubility and evaluation of agonistic and antagonistic activities of compounds in reporter gene assay.

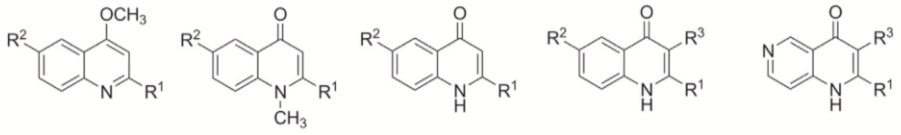

**3** **4,5** **HHQ, 1, 2, 6-11** **12-28** **29-31**

| Compd. | $R^1$ | $R^2$ | $R^3$ | Solubility in 2% DMSO[a], [μM] | PqsR stimulation induced by 5 μM test compd. compared to 50 nM PQS (=1.00)[b] | Inhibition of PqsR stimulation induced by 50 nM PQS in the presence of test compd. (full inhibition = 1.00)[b] | |
|---|---|---|---|---|---|---|---|
| | | | | | | 50 nM | 5 μM |
| *Reference compounds* | | | | | | | |
| **HHQ** | $n$-$C_7H_{15}$ | H | – | 15–50 | 0.75*[c] | – | – |
| **1** | $n$-$C_7H_{15}$ | $CF_3$ | – | <5 | 0.00 | 0.54* | 1.00* |
| **2** | $n$-$C_7H_{15}$ | $NO_2$ | – | <5 | 0.00[d] | 0.73* | 1.00* |
| *Compound class 1: N or O-methylation in 1- or 4-position* | | | | | | | |
| **3** | $n$-$C_7H_{15}$ | H | – | 5–15 | 0.03 | −0.23* | −0.06 |
| **4** | $n$-$C_7H_{15}$ | $CF_3$ | – | 5–15 | 0.00 | 0.31* | 1.00* |
| **5** | $n$-$C_6H_{13}$ | $CF_3$ | – | 15–50 | 0.00 | 0.45* | 1.00* |
| *Compound class 2: introduction of oxygen into 2-alkyl side chain* | | | | | | | |
| **6** | $CH_2OC_5H_{11}$ | H | – | >200 | 0.89* | 0.11 | 0.06 |
| **7** | $CH_2OC_5H_{11}$ | $CF_3$ | – | 15–50 | 0.00 | 0.29* | 1.00* |
| **8** | $CH_2OC_5H_{11}$ | $NO_2$ | – | 15–50 | 0.00 | 0.49* | 1.00* |
| **9** | $C_4H_8OC_2H_5$ | H | – | >200 | 0.31* | 0.54* | 0.42* |
| **10** | $C_4H_8OC_2H_5$ | $CF_3$ | – | >200 | 0.02 | 0.08 | 0.69* |
| **11** | $C_4H_8OC_2H_5$ | $NO_2$ | – | 50–100 | 0.13 | 0.06 | 0.72* |
| *Compound class 3: substitution in 3-position* | | | | | | | |
| **12** | $n$-$C_7H_{15}$ | H | $NO_2$ | <5 | 0.84* | 0.14 | 0.17 |
| **13** | $n$-$C_7H_{15}$ | H | $NH_2$ | 50–100 | 1.22* | −0.04 | −0.07 |
| **14** | $n$-$C_7H_{15}$ | $NO_2$ | OH | <5 | 1.25* | −0.31* | −0.29* |
| **15** | $n$-$C_7H_{15}$ | H | $CH_2OH$ | 50–100 | 0.49* | 0.05 | 0.28* |
| **16** | $n$-$C_7H_{15}$ | $NO_2$ | $CH_2OH$ | 5–15 | 0.00 | 0.45* | 1.00* |
| **17** | $n$-$C_7H_{15}$ | H | $COOC_2H_5$ | 5–15 | 0.00 | 0.18 | 0.32* |
| **18** | $n$-$C_7H_{15}$ | $NO_2$ | $COOC_2H_5$ | 5–15 | 0.00 | −0.08 | 0.20* |
| **19** | $CH_2OC_5H_{11}$ | $NO_2$ | $COOC_2H_5$ | 15–50 | 0.00 | 0.02 | 0.13 |
| **20** | $C_4H_8OC_2H_5$ | $NO_2$ | $COOC_2H_5$ | 5–15 | 0.09 | 0.02 | 0.27* |
| **21** | $n$-$C_7H_{15}$ | H | COOH | 15–50 | 0.73* | 0.12 | 0.41* |
| **22** | $n$-$C_7H_{15}$ | $NO_2$ | COOH | 15–50 | 0.78* | 0.11 | 0.34* |
| **23** | $CH_2OC_5H_{11}$ | $NO_2$ | COOH | 50–100 | 0.48* | 0.07 | 0.06 |
| **24** | $C_4H_8OC_2H_5$ | $NO_2$ | COOH | 50–100 | 0.42* | 0.01 | 0.33* |
| **25** | $n$-$C_7H_{15}$ | H | $CONH_2$ | 5–15 | 0.65* | 0.08 | 0.27* |
| **26** | $n$-$C_7H_{15}$ | $NO_2$ | $CONH_2$ | 15–50 | 0.00 | 0.60* | 1.00* |
| **27** | $n$-$C_7H_{15}$ | H | CONHOH | >200 | 0.83* | 0.15 | 0.29 |
| **28** | $n$-$C_7H_{15}$ | $NO_2$ | CONHOH | >200 | 0.30* | 0.30* | 0.78* |
| *Compound class 4: replacement of the benzene moiety by pyridine* | | | | | | | |
| **29** | $n$-$C_7H_{15}$ | – | $COOC_2H_5$ | 50–100 | 0.02 | 0.24* | 0.76* |
| **30** | $n$-$C_7H_{15}$ | – | COOH | 50–100 | 0.66* | 0.06 | 0.20 |
| **31** | $n$-$C_7H_{15}$ | – | H | 50–100 | 0.82* | 0.08 | 0.02 |

[a] Aqueous solutions containing 2% DMSO of the test compounds were prepared with final concentrations of 5, 15, 50, 100 and 200 μM. The solution clarity was examined.
[b] β-Galactosidase reporter gene assay was performed in *E. coli* transformed with plasmid pEAL08-2 encoding PqsR and reporter gene *lacZ* controlled by *pqsA* promoter. Mean value of at least two independent experiments with $n = 4$, standard deviation less than 25%. Significance: For the agonist test, induction compared to the basal value; for the antagonist test, reduction of the PQS-induced stimulation. *$p < 0.05$.
[c] Determined at 1 μM.
[d] Determined at 10 μM.

## 4. Experimental

### 4.1. Chemistry

Chemical and Analytical Methods.$^1$H and $^{13}$C NMR spectra were recorded on a Bruker DRX-500 instrument. Chemical shifts are given in parts per million (ppm) with the solvent resonance as internal standard for spectra obtained in $CDCl_3$, MeOH-$d_4$ and DMSO-$d_6$. All coupling constants ($J$) are given in hertz. Mass spectrometry (LC/MS) was performed on a MSQ® electro spray mass spectrometer (Thermo Fisher). The system was operated by the standard software Xcalibur®. A RP C18 NUCLEODUR® 100-5 (125 × 3 mm) column (Macherey–Nagel GmbH) was used as stationary phase with water/acetonitrile mixtures as eluent. All solvents were HPLC grade. Reagents were used as obtained from commercial suppliers without further purification. Flash chromatography was performed on silica gel 60, 70–230 mesh (Fluka) and the reaction progress was determined by thin-layer chromatography (TLC) analyses on silica gel 60, $F_{254}$ (Merck). Visualization was accomplished with UV light and staining with basic potassium permanganate ($KMnO_4$). The melting points were measured using melting point apparatus SMP3 (Stuart Scientific). The apparatus is uncorrected.

The following compounds were prepared according to previously described procedures: 1*H*-pyrido[4,3-*d*][1,3]oxazine-2,4-dione [27], HHQ, PQS, **1**, **2**, **14**, **16**, **18**, **22**, **26**, **32**, **36** and **37** [17].

**Table 2**
Physicochemical properties, PqsR antagonistic effects as well as reduction of PQS and pyocyanin levels in *P. aeruginosa* for selected antagonists.

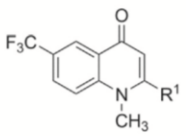

**4**: $R^1$ = *n*-$C_7H_{13}$
**5**: $R^1$ = *n*-$C_6H_{15}$

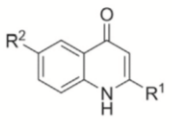

**1**: $R^1$ = *n*-$C_7H_{15}$, $R^2$ = $CF_3$
**2**: $R^1$ = *n*-$C_7H_{15}$, $R^2$ = $NO_2$
**7**: $R^1$ = $CH_2OC_5H_{11}$, $R^2$ = $CF_3$
**8**: $R^1$ = $CH_2OC_5H_{11}$, $R^2$ = $NO_2$
**10**: $R^1$ = $C_4H_8OC_2H_5$, $R^2$ = $CF_3$
**11**: $R^1$ = $C_4H_8OC_2H_5$, $R^2$ = $NO_2$

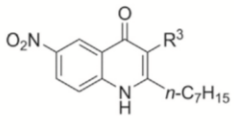

**16**: $R^3$ = $CH_2OH$
**26**: $R^3$ = $CONH_2$

| Compd. | clogP[a] | Solubility in 2% DMSO[b], [μM] | PqsR antagonistic activity $IC_{50}$, [nM] | Reduction with compd. at 15 μM, [%] | |
|---|---|---|---|---|---|
| | | | | PQS[c] | Pyocyanin[c] |
| *Reference compounds/starting point* | | | | | |
| **1** | 7.29/6.83 | 1.2 | 54 | −2.4[e] | 27*[e] |
| **2** | 6.73/5.31 | 5.6 | 51 | 14* | 44* |
| *Selected antagonists* | | | | | |
| **4** | 5.60/6.59 | 9.3 | 270 | 8.9 | 58* |
| **5** | 5.07/5.32 | n.d.[d] | 229 | n.d.[d] | n.d.[d] |
| **7** | 5.90/4.90 | 18 | 172 | 21 | 29* |
| **8** | 5.35/3.59 | 34 | 253 | 23* | 27* |
| **10** | 4.93/3.91 | 80 | 1712 | 8.6[e] | 39*[e] |
| **11** | 4.37/3.12 | 85 | 3511 | 13[e] | 23*[e] |
| **16** | 6.94/4.67 | 9.4 | 72 | 33* | 83* ($IC_{50}$: 3.8 μM) |
| **26** | 5.45/3.67 | 7.8 | 35 | 37* | 81* ($IC_{50}$: 2.0 μM) |

[a] The clogP values were calculated with ACD Percepta logP Classic/GALAS.
[b] Solubility was measured with HPLC method.
[c] PQS and pyocyanin assays were performed in *P. aeruginosa* PA14. All compounds were dissolved in LB medium. Mean value of at least two independent experiments with $n = 3$, standard deviation less than 25%. Significance: decrease of PQS levels or pyocyanin production compared to basal value, $^*p < 0.05$.
[d] Not determined.
[e] Determined at 10 μM, 250 μM and 100 μM, respectively.

**Procedure A**. A solution of β-ketoester (9.24 mmol, 1.0 equiv), aniline (9.24 mmol, 1.0 equiv) and *p*-TsOH·$H_2O$ (50 mg, 0.29 mmol, 3 mol %) in *n*-hexane (20 mL) was heated at reflux using a Dean–Stark separator for 5 h. After cooling the solution was concentrated under reduced pressure and the residue was added dropwise to refluxing (260 °C) diphenyl ether (5 mL). Refluxing was continued for 30 min. After cooling to room temperature, diethyl ether (15 mL) was added and the mixture was left standing overnight at 5 °C. The crystalline solid was isolated by filtration and washed with diethyl ether. The product was further purified by recrystallization from ethyl acetate or column chromatography on silica gel [17].

**Procedure B**. Under nitrogen atmosphere β-ketoester (15 mmol, 1.0 equiv) was added to a suspension of sodium hydride (50–65% w/w, 0.72 g, 15 mmol, 1.0 equiv) in dry DMF (50 mL), causing the liberation of hydrogen gas. A solution of isatoic anhydride derivative (15 mmol, 1.0 equiv) in dry DMF (30 mL) was added dropwise and stirred overnight. Most of the solvent was removed under reduced pressure and the remaining solvent treated with 1 M HCl, yielding the crude product as a yellow solid [28]. The 4-oxo-1,4-dihydroquinoline-3-ester derivative was purified by recrystallization from ethyl acetate/methanol or column chromatography on silica gel. The ester was suspended in 10% NaOH solution and heated at reflux for 4 h. After cooling to 0 °C on an ice water bath and extraction with ethyl acetate, the water phase was acidified with conc. HCl to reach a pH of 4.0–6.0. The 4-oxo-1,4-dihydroquinoline-3-carboxylic acid was isolated by filtration, washed with water and dried under vacuum.

*4.1.1. 2-Heptyl-4-methoxyquinoline (**3**)*

A mixture of HHQ (200 mg, 0.82 mmol, 1.0 equiv), $Cs_2CO_3$ (410 mg, 1.26 mmol, 1.5 equiv) and dry DMF (5 mL) was stirred at room temperature for 1 h. Methyl iodide (0.61 g, 4.32 mmol, 5.0 equiv) was added dropwise and the mixture was stirred for further 48 h. The reaction was poured onto water (16 mL) and diluted with chloroform (25 mL). The organic layer was washed with water (16 mL), dried over sodium sulfate and concentrated under reduced pressure [29]. After column chromatography on silica gel (twice, dichloromethane/methanol, 130/1 and n-hexane/ethyl acetate, 15/1) the product was isolated as a white solid (40 mg, 0.16 mmol, 20%), mp 40.5–41.3 °C. $^1$H NMR (500 MHz, $CDCl_3$): $\delta = 0.86$ (t, $J = 7.0$ Hz, 3H), 1.24–1.42 (m, 8H), 1.79 (quint, $J = 7.5$ Hz, 2H), 2.89 (t, $J = 7.5$ Hz, 2H), 4.01 (s, 3H), 6.61 (s, 1H), 7.41 (td, $J = 1.5$, 7.5 Hz, 1H), 7.63 (td, $J = 1.5$, 7.5 Hz, 1H), 7.45 (d, $J = 7.5$ Hz, 1H), 8.11 (dd, $J = 1.0$, 8.0 Hz, 1H). $^{13}$C NMR (125 MHz, $CDCl_3$): $\delta$ = 14.1, 22.6, 29.2, 29.6, 30.2, 31.8, 40.0, 55.5, 99.8, 120.0, 121.5, 124.7, 128.3, 129.6, 148.8, 162.3, 164.3. LC/MS: *m/z* 257.91 $[M+H]^+$, 95.8%.

*4.1.2. 2-Heptyl-1-methyl-6-(trifluoromethyl)quinolin-4(1H)-one (**4**)*

Methyl iodide (0.46 g, 3.24 mmol, 10.1 equiv) was added to a solution of **1** (100 mg, 0.32 mmol, 1.0 equiv), KOH (56 mg, 1.00 mmol, 3.1 equiv) in methanol (1 mL) and the mixture was stirred overnight at room temperature. After the precipitate was removed by filtration, the solvent was evaporated under reduced pressure [30]. After column chromatography on silica gel (dichloromethane/methanol, 100/1) the product was isolated as a white solid (25 mg, 0.08 mmol, 25%), mp 125.1–126.3 °C. $^1$H NMR (500 MHz, MeOH-$d_4$): $\delta = 0.92$ (t, $J = 7.0$ Hz, 3H), 1.31–1.53 (m, 8H), 1.74 (quint, $J = 7.5$ Hz, 2H), 2.90 (t, $J = 7.5$ Hz, 2H), 3.92 (s, 3H), 6.35 (s, 1H), 7.99–8.04 (m, 2H), 8.59–8.60 (m, 1H). $^{13}$C NMR (125 MHz, MeOH-$d_4$): $\delta$ = 14.4, 23.7, 29.6, 30.1, 30.3, 32.9, 35.6, 35.7, 112.1, 119.4, 124.4 (q, $J_{CF} = 4$ Hz), 125.5 (q, $J_{CF} = 270$ Hz), 126.6, 126.7 (q,

$J_{CF}$ = 33 Hz), 129.5 (q, $J_{CF}$ = 3 Hz), 145.3, 160.0, 178.9. LC/MS: *m/z* 325.79 $[M+H]^+$, 99.9%.

*4.1.3. 2-Hexyl-1-methyl-6-(trifluoromethyl)quinolin-4(1H)-one (**5**)*

The title compound was prepared using the same method as for the synthesis of **4** from **36** (100 mg, 0.34 mmol). After column chromatography on silica gel (dichloromethane/methanol, 100/1) the product was isolated as a white solid (30 mg, 0.10 mmol, 28%), mp 101.2–103.9 °C. $^1$H NMR (500 MHz, MeOH-$d_4$): $\delta$ = 0.94 (t, $J$ = 7.0 Hz, 3H), 1.35–1.52 (m, 6H), 1.74 (quint, $J$ = 7.5 Hz, 2H), 2.90 (t, $J$ = 8.0 Hz, 2H), 3.92 (s, 3H), 6.36 (s, 1H), 8.00–8.04 (m, 2H), 8.59–8.60 (m, 1H). $^{13}$C NMR (125 MHz, MeOH-$d_4$): $\delta$ = 14.4, 23.6, 29.6, 30.0, 32.6, 35.6, 35.7, 112.1, 119.4, 124.4 (q, $J_{CF}$ = 4 Hz), 129.5 (q, $J_{CF}$ = 3 Hz), 126.6, 126.8 (q, $J_{CF}$ = 33 Hz), 125.5 (q, $J_{CF}$ = 270 Hz), 145.3, 160.0, 178.9. LC/MS: *m/z* 311.94 $[M+H]^+$, 95.0%.

*4.1.4. 2-(Pentyloxymethyl)quinolin-4(1H)-one (**6**)*

The title compound was prepared according to procedure A from **33** (2.16 g, 10 mmol) and aniline (0.93 g, 10 mmol). After removal of solvent under reduced pressure and column chromatography on silica gel (dichloromethane/methanol, 60/1) the product was isolated as a brown solid (200 mg, 0.82 mmol, 8%), mp 107.9–110.2 °C. $^1$H NMR (500 MHz, DMSO-$d_6$): $\delta$ = 0.86 (t, $J$ = 7.0 Hz, 3H), 1.28–1.32 (m, 4H), 1.57 (quint, $J$ = 7.5 Hz, 2H), 3.48 (t, $J$ = 6.5 Hz, 2H), 4.45 (s, 2H), 6.05 (s, 1H), 7.27–7.30 (m, 1H), 7.60–7.65 (m, 2H), 8.05 (dt, $J$ = 1.0, 7.5 Hz, 1H), 11.58 (br, 1H). $^{13}$C NMR (125 MHz, DMSO-$d_6$): $\delta$ = 13.9, 21.9, 27.7, 28.7, 68.7, 70.2, 107.1, 118.2, 122.9, 124.8, 125.0, 131.7, 140.1, 149.5, 176.9. LC/MS: *m/z* 245.94 $[M+H]^+$, 99.9%.

*4.1.5. 2-(Pentyloxymethyl)-6-(trifluoromethyl)quinolin-4(1H)-one (**7**)*

The title compound was prepared according to procedure A from **33** (2.16 g, 10 mmol) and 4-(trifluoromethyl)aniline (1.61 g, 10 mmol). After recrystallization from ethanol the product was isolated as a white solid (1.51 g, 4.82 mmol, 48%), mp 215.8–216.5 °C. $^1$H NMR (500 MHz, DMSO-$d_6$): $\delta$ = 0.85 (t, $J$ = 7.1 Hz, 3H), 1.24–1.33 (m, 4H), 1.57 (quint, $J$ = 6.9 Hz, 2H), 3.49 (t, $J$ = 6.6 Hz, 2H), 4.48 (s, 2H), 6.18 (s, 1H), 7.82 (d, $J$ = 8.8 Hz, 1H), 7.93 (dd, $J$ = 8.8, 2.2 Hz, 1H), 8.32 (d, $J$ = 1.6 Hz, 1H), 11.93 (br, 1H). $^{13}$C NMR (125 MHz, DMSO-$d_6$): $\delta$ = 13.8, 21.9, 27.7, 28.7, 68.5, 70.3, 108.0, 119.9, 122.4 (q, $J_{CF}$ = 4 Hz), 123.2 (q, $J_{CF}$ = 32 Hz), 124.1, 124.2 (q, $J_{CF}$ = 272 Hz), 127.6 (q, $J_{CF}$ = 3 Hz), 142.3, 150.8, 176.3. LC/MS: *m/z* 313.97 $[M+H]^+$, 96.1%.

*4.1.6. 6-Nitro-2-(pentyloxymethyl)quinolin-4(1H)-one (**8**)*

A solution of **6** (80 mg, 0.33 mmol) in conc. $H_2SO_4$ (1 mL) was cooled to 0 °C, and a mixture of conc. $H_2SO_4$ (32 μL) and conc. $HNO_3$ (32 μL) was added slowly, maintaining the temperature at 0 °C. After the addition was complete, the mixture was allowed to reach room temperature with stirring for additional 2 h. The solution was poured onto ice, and the resulting precipitate was filtered and washed with water to give crude product [31]. After preparative thin layer chromatography on silica gel (dichloromethane/methanol, 20/1) the product was isolated as a yellow solid (25 mg, 0.09 mmol, 27%). mp 187.3–189.6 °C. $^1$H NMR (500 MHz, MeOH-$d_4$): $\delta$ = 0.93 (t, $J$ = 7.0 Hz, 3H), 1.33–1.43 (m, 4H), 1.69 (quint, $J$ = 7.5 Hz, 2H), 3.60 (t, $J$ = 6.5 Hz, 2H), 4.56 (s, 2H), 6.38 (s, 1H), 7.76 (d, $J$ = 9.5 Hz, 1H), 8.44 (dd, $J$ = 2.5, 9.0 Hz, 1H), 9.01 (d, $J$ = 2.5 Hz, 1H). $^{13}$C NMR (125 MHz, MeOH-$d_4$): $\delta$ = 14.4, 23.6, 29.4, 30.3, 69.9, 72.6, 109.2, 121.0, 122.9, 125.3, 127.3, 145.0, 154.2, 180.1. LC/MS: *m/z* 290.98 $[M+H]^+$, 99.0%.

*4.1.7. 2-(4-Ethoxybutyl)quinolin-4(1H)-one (**9**)*

The title compound was prepared according to procedure A from **34** (0.65 g, 3.0 mmol) and aniline (280 mg, 3.0 mmol). After removal of solvent under reduced pressure, column chromatography on silica gel (dichloromethane/methanol, 60/1–40/1) and preparative thin layer chromatography on silica gel (dichloromethane/methanol, 20/1) the product was isolated as a white solid (60 mg, 0.24 mmol, 8%), mp 98.3–100.5 °C. $^1$H NMR (500 MHz, MeOH-$d_4$): $\delta$ = 1.18 (t, $J$ = 7.0 Hz, 3H), 1.65–1.71 (m, 2H), 1.82–1.88 (m, 2H), 2.76 (t, $J$ = 7.5 Hz, 2H), 3.47–3.51 (m, 4H), 6.25 (s, 1H), 7.40 (td, $J$ = 1.0, 7.5 Hz, 1H), 7.59 (d, $J$ = 9.0 Hz, 1H), 7.70 (td, $J$ = 1.5, 7.5 Hz, 1H), 8.22 (d, $J$ = 8.0 Hz, 1H). $^{13}$C NMR (125 MHz, MeOH-$d_4$): $\delta$ = 15.5, 27.0, 30.2, 34.7, 67.2, 71.1, 108.9, 119.1, 125.1, 125.5, 126.0, 133.4, 141.6, 156.9, 180.7. LC/MS: *m/z* 245.85 $[M+H]^+$, 95.4%.

*4.1.8. 2-(4-Ethoxybutyl)-6-(trifluoromethyl)quinolin-4(1H)-one (**10**)*

The title compound was prepared according to procedure A from **34** (1.08 g, 5.00 mmol) and 4-(trifluoromethyl)aniline (0.81 g, 5.00 mmol). After recrystallization from ethanol the product was isolated as a white solid (280 mg, 0.89 mmol, 18%), mp 149.6–151.1 °C. $^1$H NMR (500 MHz, DMSO-$d_6$): $\delta$ = 1.17 (t, $J$ = 7.1 Hz, 3H), 1.62 (quint, $J$ = 6.6 Hz, 2H), 1.86 (quint, $J$ = 7.3 Hz, 2H), 2.78 (t, $J$ = 7.4 Hz, 2H), 3.44 (t, $J$ = 6.0 Hz, 2H), 3.45 (q, $J$ = 6.9 Hz, 2H), 6.25 (d, $J$ = 1.3 Hz, 1H), 7.72 (d, $J$ = 8.8 Hz, 1H), 7.76 (dd, $J$ = 8.8, 1.9 Hz, 1H), 8.64 (s, 1H), 12.26 (bs, 1H). $^{13}$C NMR (125 MHz, DMSO-$d_6$): $\delta$ = 15.2, 26.5, 28.4, 33.6, 66.4, 70.5, 109.4, 119.1, 123.6 (q, $J_{CF}$ = 4 Hz), 124.1 (q, $J_{CF}$ = 272 Hz), 124.3, 125.6, 127.9 (q, $J_{CF}$ = 3 Hz), 142.1, 155.8, 178.4. LC/MS: *m/z* 313.99 $[M+H]^+$, 95.7%.

*4.1.9. 2-(4-Ethoxybutyl)-6-nitroquinolin-4(1H)-one (**11**)*

Compound **24** (150 mg, 0.45 mmol) was carefully purged with nitrogen under stirring, then slowly heated past its melting point to 310 °C under inert atmosphere with continued stirring for 8 min. The reaction was cooled to room temperature after the evident evolution of carbon dioxide ceased. The resulting solid was dissolved in a dichloromethane/methanol (15/1) solution. Insoluble material was removed by filtration and the solvents were removed under reduced pressure [32]. The residue was purified by column chromatography on silica gel (dichloromethane/methanol, 60/1) to give the product as a yellow solid (103 mg, 0.36 mmol, 80%), mp 232.9–233.8 °C. $^1$H NMR (500 MHz, MeOH-$d_4$): $\delta$ = 1.11 (t, $J$ = 7.0 Hz, 3H), 1.61 (quint, $J$ = 7.0 Hz, 2H), 1.78 (quint, $J$ = 7.0 Hz, 2H), 2.69 (d, $J$ = 7.5 Hz, 2H), 3.42 (q, $J$ = 7.0 Hz, 4H), 6.20 (s, 1H), 7.62 (d, $J$ = 9.0 Hz, 1H), 8.37 (dd, $J$ = 2.5, 9.0 Hz, 1H), 8.96 (d, $J$ = 2.5 Hz, 1H). $^{13}$C NMR (125 MHz, MeOH-$d_4$): $\delta$ = 13.9, 25.2, 28.7, 33.2, 65.7, 69.5, 108.8, 119.1, 121.4, 123.4, 125.7, 143.5, 156.7, 178.5. LC/MS: *m/z* 290.70 $[M+H]^+$, 96.8%.

*4.1.10. 2-Heptyl-3-nitroquinolin-4(1H)-one (**12**)*

At 110 °C conc. $HNO_3$ (65% w/w, 15 μL, 0.30 mmol, 2.5 equiv) was added to a stirred suspension of HHQ (30 mg, 0.12 mmol, 1.0 equiv) in propionic acid (3 mL). The reaction mixture was heated for further 2 h with vigorous stirring. The resulting suspension was poured into ice. The solids were isolated by filtration washed with cold water and dried under vacuum to yield the product as a yellow solid (12 mg, 0.04 mmol, 33%) [33], mp 258.0–259.1 °C. $^1$H NMR (500 MHz, DMSO-$d_6$): $\delta$ = 0.85 (t, $J$ = 6.5 Hz, 3H), 1.25–1.34 (m, 8H), 1.70 (quint, $J$ = 7.5 Hz, 2H), 2.73 (t, $J$ = 7.5 Hz, 2H), 7.45 (t, $J$ = 7.5 Hz, 1H), 7.66 (d, $J$ = 7.5 Hz, 1H), 7.78 (t, $J$ = 7.5 Hz, 1H), 8.15 (d, $J$ = 8.0 Hz, 1H), 12.32 (br, 1H). $^{13}$C NMR (125 MHz, DMSO-$d_6$): $\delta$ = 13.9, 22.0, 28.1, 28.4, 28.6, 30.3, 31.0, 118.7, 124.8, 125.2, 125.3, 133.2, 135.6, 138.6, 149.4, 167.5. LC/MS: *m/z* 289.00 $[M+H]^+$, 96.7%.

*4.1.11. 3-Amino-2-heptylquinolin-4(1H)-one (**13**)*

A suspension of **12** (40 mg, 0.14 mmol, 1.0 equiv) in ethanol (2 mL) was heated at reflux. $Fe^0$ (80 mg, 1.40 mmol, 10 equiv) and an aqueous solution of $NH_4Cl$ (74 mg dissolved in 0.56 mL of water)

were added. The reaction was stirred at reflux to completeness. The warm mixture was filtered through a Celite patch and the remaining solids were washed several times with warm EtOH. The filtrates were combined and concentrated [33]. The residue was purified by preparative thin layer chromatography on silica gel (dichloromethane/methanol, 10/1) to give the product as a brown solid (13 mg, 0.05 mmol, 36%), mp 190.3–192.0 °C. $^1$H NMR (500 MHz, MeOH-$d_4$): $\delta$ = 0.89 (t, $J$ = 7.0 Hz, 3H), 1.28–1.48 (m, 8H), 1.76 (quint, $J$ = 7.5 Hz, 2H), 2.83 (t, $J$ = 8.0 Hz, 2H), 7.27–7.30 (m, 1H), 7.54 (d, $J$ = 3.5 Hz, 2H), 8.21 (d, $J$ = 8.5 Hz, 1H). $^{13}$C NMR (125 MHz, MeOH-$d_4$): $\delta$ = 14.4, 23.7, 28.8, 30.2, 30.7, 31.3, 32.9, 118.8, 123.8, 125.6, 128.6, 131.3, 138.6, 139.5, 171.2. LC/MS: $m/z$ 258.99 $[M+H]^+$, 99.9%.

#### 4.1.12. 2-Heptyl-3-(hydroxymethyl)quinolin-4(1H)-one (**15**)

At 0 °C $LiAlH_4$ (120 mg, 3.16 mmol, 2.0 equiv) was added to a stirred solution of **17** (500 mg, 1.59 mmol, 1.0 equiv) in dry THF (30 mL). After stirring at room temperature for 2 h ethyl acetate (10 mL) was added at 0 °C and after filtration the solvent was removed under reduced pressure [34]. The residue was purified by column chromatography (dichloromethane/methanol, 40/1) to give the product as a white solid (128 mg, 0.47 mmol, 30%), mp 297.2–298.6 °C. $^1$H NMR (500 MHz, DMSO-$d_6$): $\delta$ = 0.86 (t, $J$ = 7.0 Hz, 3H), 1.25–1.40 (m, 8H), 1.67 (quint, $J$ = 7.5 Hz, 2H), 2.73 (t, $J$ = 8.0 Hz, 2H), 4.48 (d, $J$ = 5.5 Hz, 2H), 4.58 (t, $J$ = 5.5 Hz, 1H), 7.26 (td, $J$ = 1.0, 7.5 Hz, 1H), 7.52 (d, $J$ = 8.0 Hz, 1H), 7.60 (td, $J$ = 1.0, 8.0 Hz, 1H), 8.07 (dd, $J$ = 1.5, 8.0 Hz, 1H), 11.39 (s, 1H). $^{13}$C NMR (125 MHz, DMSO-$d_6$): $\delta$ = 13.9, 22.0, 28.4, 29.0, 29.3, 31.1, 31.2, 54.1, 117.7, 118.0, 122.6, 123.9, 125.1, 131.3, 139.4, 152.3, 176.1. LC/MS: $m/z$ 315.86 $[M+H]^+$, 98.9%.

#### 4.1.13. Ethyl 2-heptyl-4-oxo-1,4-dihydroquinoline-3-carboxylate (**17**)

The title compound was obtained according to procedure B from **32** (3.40 g, 16 mmol), sodium hydride (50–65% w/w, 0.72 g, 15 mmol) and isatoic anhydride (2.45 g, 15 mmol). After recrystallization from ethyl acetate/methanol the product was isolated as a white solid (2.68 g, 8.51 mmol, 57%), mp 151.1–153.0 °C. $^1$H NMR (500 MHz, DMSO-$d_6$): $\delta$ = 0.85 (t, $J$ = 7.0 Hz, 3H), 1.25–1.34 (m, 11H), 1.66 (quint, $J$ = 7.5 Hz, 2H), 2.63 (t, $J$ = 8.0 Hz, 2H), 4.23 (q, $J$ = 7.0 Hz, 2H), 7.34 (td, $J$ = 1.5, 7.5 Hz, 1H), 7.56 (d, $J$ = 8.0 Hz, 1H), 7.67 (td, $J$ = 1.5, 7.5 Hz, 1H), 8.05 (dd, $J$ = 1.5, 7.5 Hz, 1H), 11.77 (br, 1H). $^{13}$C NMR (125 MHz, DMSO-$d_6$): $\delta$ = 13.9, 14,1, 22.0, 28.3, 28.7, 28.9, 31.0, 31.9, 60.3, 114.8, 118.1, 123.6, 124.4, 124.9, 132.2, 139.3, 152.1, 166.8, 173.6. LC/MS: $m/z$ 315.86 $[M+H]^+$, 98.9%.

#### 4.1.14. Ethyl 6-nitro-4-oxo-2-(pentyloxymethyl)-1,4-dihydroquinoline-3-carboxylate (19)

The title compound was prepared according to procedure B from **33** (234 mg, 1.08 mmol), sodium hydride (50–65% w/w, 58 mg, 1.21 mmol) and 6-nitro-1*H*-benzo[*d*][1,3]oxazine-2,4-dione (200 mg, 0.96 mmol). After column chromatography on silica gel (*n*-hexane/ethyl acetate, 1.2/1) and recrystallization from ethyl acetate the product was isolated as a yellow solid (25 mg, 0.07 mmol, 7.3%), mp 207.6–209.0 °C. $^1$H NMR (500 MHz, DMSO-$d_6$): $\delta$ = 0.85 (t, $J$ = 7.0 Hz, 3H), 1.27–1.29 (m, 7H), 1.55 (quint, $J$ = 7.5 Hz, 2H), 3.47 (t, $J$ = 7.0 Hz, 2H), 4.26 (q, $J$ = 7.0 Hz, 2H), 4.56 (s, 2H), 7.92 (d, $J$ = 9.0 Hz, 1H), 8.47 (dd, $J$ = 2.5, 9.0 Hz, 1H), 8.81 (d, $J$ = 2.5 Hz, 1H), 12.32, (br, 1H). $^{13}$C NMR (125 MHz, DMSO-$d_6$): $\delta$ = 13.8, 14.0, 21.9, 27.5, 28.5, 60.7, 67.1, 70.7, 115.3, 120.6, 121.5, 124.2, 126.5, 142.9, 143.2, 150.1, 165.2, 173.1. LC/MS: $m/z$ 362.76 $[M+H]^+$, 98.8%.

#### 4.1.15. Ethyl 2-(4-ethoxybutyl)-6-nitro-4-oxo-1,4-dihydroquinoline-3-carboxylate (**20**)

The title compound was prepared according to procedure B from **34** (1.7 g, 7.87 mmol), sodium hydride (50–65% w/w, 360 mg, 7.50 mmol) and 6-nitro-1*H*-benzo[*d*][1,3]oxazine-2,4-dione (1.57 g, 7.55 mmol) After column chromatography on silica gel (*n*-hexane/ethyl acetate, 1.2/1) and recrystallization from ethyl acetate the product was isolated as a yellow solid (2.6 g, 7.18 mmol, 95%), mp 210.4–211.7 °C. $^1$H NMR (500 MHz, DMSO-$d_6$): $\delta$ = 1.08 (t, $J$ = 7.0 Hz, 3H), 1.28 (t, $J$ = 7.0 Hz, 3H), 1.56 (quint, $J$ = 7.0 Hz, 2H), 1.73 (quint, $J$ = 7.0 Hz, 2H), 2.67 (t, $J$ = 7.5 Hz, 2H), 3.35–3.40 (m, 4H), 4.27 (q, $J$ = 7.0 Hz, 2H), 7.75 (d, $J$ = 9.5 Hz, 1H), 8.45 (dd, $J$ = 2.5, 9.0 Hz, 1H), 8.79 (d, $J$ = 2.5 Hz, 1H), 12.30 (br, 1H). $^{13}$C NMR (125 MHz, DMSO-$d_6$): $\delta$ = 14.0, 15.1, 25.8, 29.0, 31.9, 60.7, 65.2, 69.2, 116.2, 120.1, 121.5, 123.6, 126.5, 143.0, 143.1, 153.5, 165.9, 173.1. LC/MS: $m/z$ 362.89 $[M+H]^+$, 97.9%.

#### 4.1.16. 2-Heptyl-4-oxo-1,4-dihydroquinoline-3-carboxylic acid (**21**)

The title compound was prepared according to procedure B from **17** (50 mg, 0.16 mmol). The product was isolated as a white solid (32 mg, 0.11 mmol, 69%), mp 219.4–221.7 °C. $^1$H NMR (500 MHz, DMSO-$d_6$): $\delta$ = 0.86 (t, $J$ = 7.0 Hz, 3H), 1.26–1.41 (m, 8H), 1.66 (quint, $J$ = 7.5 Hz, 2H), 3.31 (t, $J$ = 7.5 Hz, 2H, covered by water peak at 3.32), 7.56 (t, $J$ = 7.5 Hz, 1H), 7.77 (d, $J$ = 7.5 Hz, 1H), 7.87 (t, $J$ = 7.5 Hz, 1H), 8.25 (d, $J$ = 7.5 Hz, 1H), 12.96 (br, 1H). $^{13}$C NMR (125 MHz, DMSO-$d_6$): $\delta$ = 13.9, 22.0, 28.3, 29.1, 29.2, 31.1, 33.3, 105.7, 118.8, 122.9, 125.1, 125.8, 133.9, 138.2, 162.4, 166.3, 179.0. LC/MS: $m/z$ 287.92 $[M+H]^+$, 99.9%.

#### 4.1.17. 6-Nitro-4-oxo-2-(pentyloxymethyl)-1,4-dihydroquinoline-3-carboxylic acid (**23**)

The title compound was prepared according to procedure B from **19** (400 mg, 1.10 mmol). The product was isolated as a yellow solid (262 mg, 0.78 mmol, 71%), mp 149.8–150.3 °C. $^1$H NMR (500 MHz, DMSO-$d_6$): $\delta$ = 0.89 (t, $J$ = 7.0 Hz, 3H), 1.29–1.37 (m, 4H), 1.70 (quint, $J$ = 7.0 Hz, 2H), 3.69 (t, $J$ = 7.0 Hz, 2H), 5.16 (s, 2H), 8.42 (d, $J$ = 9.0 Hz, 1H), 8.61 (dd, $J$ = 2.5, 9.0 Hz, 1H), 8.91 (d, $J$ = 2.5 Hz, 1H) 12.59 (br, 1H), 15.55 (br, 1H). $^{13}$C NMR (125 MHz, DMSO-$d_6$): $\delta$ = 13.9, 21.9, 27.5, 28.3, 68.1, 71.4, 106.1, 121.1, 122.1, 123.1, 127.5, 141.5, 144.4, 160.6, 165.5, 178.1. LC/MS: $m/z$ 334.95 $[M+H]^+$, 97.7%.

#### 4.1.18. 2-(4-Ethoxybutyl)-6-nitro-4-oxo-1,4-dihydroquinoline-3-carboxylic acid (**24**)

The title compound was obtained according to procedure B from **20** (0.7 g, 1.93 mmol). The product was isolated as a yellow solid (192 mg, 0.57 mmol, 30%), mp 231.5–232.7 °C. $^1$H NMR (500 MHz, DMSO-$d_6$): $\delta$ = 1.08 (t, $J$ = 7.0 Hz, 3H), 1.62 (quint, $J$ = 7.0 Hz, 2H), 1.73 (quint, $J$ = 7.0 Hz, 2H), 3.29 (t, $J$ = 7.5 Hz, 2H. covered by water peak at 3.33), 3.37–3.41 (m, 4H), 7.92 (d, $J$ = 9.0 Hz, 1H), 8.59 (dd, $J$ = 2.5, 9.0 Hz, 1H), 8.92 (d, $J$ = 2.5 Hz, 1H), 13.24 (br, 1H), 15.67 (br, 1H). $^{13}$C NMR (125 MHz, DMSO-$d_6$): $\delta$ = 15.1, 26.2, 29.3, 33.2, 66.2, 69.3, 107.7, 120.9, 121.5, 122.8, 127.7, 141.7, 144.2, 163.7, 165.5, 178.6. LC/MS: $m/z$ 334.95 $[M+H]^+$, 97.3%.

#### 4.1.19. 2-Heptyl-4-oxo-1,4-dihydroquinoline-3-carboxamide (**25**)

*N,N′*-Carbonyldiimidazole (62 mg, 0.38 mmol, 2.0 equiv) was added to **21** (55 mg, 0.19 mmol, 1.0 equiv) in dry DMF (1 mL). After stirring at 65 °C for 5 h, the mixture was cooled to 0 °C and iced conc. $NH_3 \cdot H_2O$ (5 mL) was added. After stirring overnight at room temperature the solvent was evaporated under reduced pressure. To the residue was added iced water (5 mL) and the precipitate was isolated by filtration [35]. After purification by column chromatography on silica gel (dichloromethane/methanol, 70/1) the product was isolated as a gray solid (38 mg, 0.13 mmol, 68%), mp 215.7–216.9 °C. 1H NMR (500 MHz, DMSO-$d_6$): $\delta$ = 0.85 (t, $J$ = 7.0

Hz, 3H), 1.22–1.38 (m, 8H), 1.67 (quint, $J$ = 7.5 Hz, 2H), 3.13 (t, $J$ = 7.5 Hz, 2H), 7.15 (d, $J$ = 2.5 Hz, 1H), 7.38 (td, $J$ = 1.0, 7.5 Hz, 1H), 7.60 (d, $J$ = 7.5 Hz, 1H), 7.69 (td, $J$ = 1.5, 7.5 Hz, 1H), 8.15 (dd, $J$ = 1.5, 7.5 Hz, 1H), 9.19 (d, $J$ = 2.5 Hz, 1H), 11.94 (br, 1H). $^{13}$C NMR (125 MHz, DMSO-$d_6$): $\delta$ = 13.9, 22.0, 28.4, 29.1, 29.5, 31.2, 33.0, 111.8, 117.9, 124.0, 124.8, 125.4, 132.3, 138.4, 158.2, 167.5, 176.1. LC/MS: *m/z* 287.89 $[M+H]^+$, 99.9%.

*4.1.20. 2-Heptyl-N-hydroxy-4-oxo-1,4-dihydroquinoline-3-carboxamide (**27**)*

A mixture of **21** (55 mg, 0.19 mmol, 1.0 equiv), *N,N′*-carbonyldiimidazole (62 mg, 0.38 mmol, 2.0 equiv) and dry DMF (2 mL) was stirred for 3 h at 75 °C. The solution was cooled to 0 °C and a mixture of *N*-methylmorpholine (184 mg, 1.80 mmol, 10 equiv), hydroxylammonium chloride (130 mg, 1.90 mmol, 10 equiv) and dry DMF (1 mL) was added and the mixture was stirred overnight at room temperature [36]. The solvent was removed under reduced pressure and the residue was purified by column chromatography on silica gel (dichloromethane/methanol, 40/1) to give the product as a white solid (34 mg, 0.12 mmol, 63%), mp 161.1–161.5 °C. $^1$H NMR (500 MHz, DMSO-$d_6$): $\delta$ = 0.86 (t, $J$ = 7.0 Hz, 3H), 1.25–1.39 (m, 8H), 1.68 (quint, $J$ = 7.0 Hz, 2H), 2.95 (t, $J$ = 8.0 Hz, 2H), 7.37 (td, $J$ = 1.0, 7.5 Hz, 1H), 7.60 (d, $J$ = 8.0 Hz, 1H), 7.69 (td, $J$ = 1.5, 7.5 Hz, 1H), 8.13 (dd, $J$ = 1.0, 8.0 Hz, 1H), 8.90 (br, 1H), 11.44 (s, 1H), 11.95 (br, 1H). $^{13}$C NMR (125 MHz, DMSO-$d_6$): $\delta$ = 13.9, 22.0, 28.4, 29.1, 29.5, 31.2, 32.4, 112.0, 117.0, 123.9, 124.4, 125.3, 132.3, 138.7, 156.3, 164.0, 175.1. LC/MS: no ionization, 98.6%.

*4.1.21. 2-Heptyl-N-hydroxy-6-nitro-4-oxo-1,4-dihydroquinoline-3-carboxamide (**28**)*

The title compound was prepared using the same method as for the synthesis of **27** from **22** (250 mg, 0.75 mmol). After column chromatography on silica gel (dichloromethane/methanol, 50/1) and recrystallization from ethyl acetate the product was isolated as a yellow solid (38 mg, 0.11 mmol, 15%), mp 200.9–202.8 °C. $^1$H NMR (500 MHz, DMSO-$d_6$): $\delta$ = 0.86 (t, $J$ = 7.0 Hz, 3H), 1.26–1.37 (m, 8H), 1.69 (quint, $J$ = 7.5 Hz, 2H), 2.80 (t, $J$ = 7.5 Hz, 2H), 7.76 (d, $J$ = 9.5 Hz, 1H), 8.45 (dd, $J$ = 3.0, 9.5 Hz, 1H), 8.84 (d, $J$ = 2.5 Hz, 1H), 9.06 (s, 1H), 11.00 (s, 1H), 12.28 (br, 1H). $^{13}$C NMR (125 MHz, DMSO-$d_6$): $\delta$ = 13.9, 22.0, 28.3, 29.0, 29.1, 31.1, 32.2, 115.4, 120.0, 121.7, 123.6, 126.4, 142.8, 143.0, 155.8, 162.4, 174.3. LC/MS: *m/z* 348.00 $[M+H]^+$, 98.5%.

*4.1.22. Ethyl 2-heptyl-4-oxo-1,4-dihydro-1,6-naphthyridine-3-carboxylate (**29**)*

The title compound was prepared according to procedure B from **32** (1.6 g, 7.48 mmol), sodium hydride (50–65% w/w, 357 mg, 7.44 mmol) and 1*H*-pyrido[4,3-*d*][1,3]oxazine-2,4-dione (1.23 g, 7.50 mmol). The product was isolated as a white solid (1.36 g, 4.28 mmol, 57%), mp 172.3–174.9 °C. $^1$H NMR (500 MHz, MeOH-$d_4$): $\delta$ = 0.80 (t, $J$ = 7.0 Hz, 3H), 1.18–1.35 (m, 11H), 1.65 (quint, $J$ = 7.5 Hz, 2H), 2.66 (t, $J$ = 8.0 Hz, 2H), 4.27 (q, $J$ = 7.0 Hz, 2H), 7.38 (d, $J$ = 6.0 Hz, 1H), 8.49 (d, $J$ = 6.0 Hz, 1H), 9.21 (s, 1H). $^{13}$C NMR (125 MHz, MeOH-$d_4$): $\delta$ = 14.4, 14.5, 23.6, 30.0, 30.5, 32.8, 34.1, 62.6, 113.9, 119.3, 121.2, 146.5, 150.4, 150.8, 157.9, 167.9, 176.6. LC/MS: *m/z* 316.99 $[M+H]^+$, 96.7%.

*4.1.23. 2-Heptyl-4-oxo-1,4-dihydro-1,6-naphthyridine-3-carboxylic acid (**30**)*

The title compound was prepared according to procedure B from **29** (200 mg, 0.63 mmol). The product was isolated as a white solid (143 mg, 0.50 mmol, 79%), mp 102.3–104.5 °C. $^1$H NMR (500 MHz, DMSO-$d_6$): $\delta$ = 0.86 (t, $J$ = 7.0 Hz, 3H), 1.25–1.34 (m, 6H), 1.39 (quint, $J$ = 7.5 Hz, 2H), 1.66 (quint, $J$ = 7.5 Hz, 2H), 3.26 (t, $J$ = 7.5 Hz, 2H, covered by water peak at 3.33), 7.61 (d, $J$ = 6.0 Hz, 1H), 7.89 (d, $J$ = 6.0 Hz, 1H), 9.38 (s, 1H). $^{13}$C NMR (125 MHz, DMSO-$d_6$): $\delta$ = 13.9, 22.0, 28.3, 29.1, 31.1, 33.6, 108.7, 112.5, 118.3, 143.0, 149.2, 151.5, 164.9, 165.6, 179.0. LC/MS: *m/z* 289.06 $[M+H]^+$, 98.7%.

*4.1.24. 2-Heptyl-1,6-naphthyridin-4(1H)-one (**31**)*

The title compound was prepared using the same method as for the synthesis of **11** from **30** (292 mg, 1.01 mmol). After recrystallization from diethyl ether/methanol the product was isolated as a gray solid (150 mg, 0.61 mmol, 60%), mp 132.5–133.0 °C. $^1$H NMR (500 MHz, DMSO-$d_6$): $\delta$ = 0.85 (t, $J$ = 7.0 Hz, 3H), 1.25–1.31 (m, 8H), 1.66 (quint, $J$ = 7.5 Hz, 2H), 2.58 (t, $J$ = 7.5 Hz, 2H), 6.04 (s, 1H), 7.40 (d, $J$ = 5.5 Hz, 1H), 8.55 (d, $J$ = 5.5 Hz, 1H), 9.13 (s, 1H), 11.71 (br, 1H). $^{13}$C NMR (125 MHz, DMSO-$d_6$): $\delta$ = 13.9, 22.0, 28.0, 28.3, 28.4, 31.1, 33.2, 110.6, 111.8, 119.4, 144.6, 148.7, 149.7, 155.1, 176.7. LC/MS: *m/z* 245.01 $[M+H]^+$, 98.6%.

*4.1.25. Ethyl 3-oxo-4-(pentyloxy)butanoate (**33**)*

1-Pentanol (8.82 g, 0.10 mol, 2.0 equiv) was added to a stirred suspension of sodium hydride (8.73 g, 55% in oil, 0.20 mol, 4.0 equiv) in THF (6 mL). After stirring at room temperature for 30 min, ethyl chloroacetoacetate (8.23 g, 50 mmol, 1.0 equiv) was added slowly and stirred overnight at room temperature. Water was added carefully and the organic solvent was evaporated under reduced pressure. The residue was acidified with 1 N HCl and extracted with diethyl ether. The combined organic layers were washed with brine and evaporated under reduced pressure. After bulb-to-bulb distillation (160 °C, 5 mbar) the product was isolated as a slightly orange oil (9.82 g, 45 mmol, 90%) [37]. $^1$H NMR (300 MHz, $CDCl_3$): $\delta$ = 0.84 (t, $J$ = 7.1 Hz, 3H), 1.21 (t, $J$ = 7.1 Hz, 3H), 1.27 (m, 4H), 1.54 (m, 2H), 3.41 (t, $J$ = 6.5 Hz, 2H), 3.45 (s, 2H), 4.02 (s, 2H), 4.13 (q, $J$ = 7.1 Hz, 2H).

*4.1.26. Ethyl 7-ethoxy-3-oxoheptanoate (**34**)*

Lithium diisopropylamide (24.6 mL, 2 M in THF, 49.1 mmol, 2.4 equiv) was diluted with dry THF (25 mL) and stirred at 0 °C. A solution of ethyl acetoacetate (2.65 g, 20.4 mmol, 1.0 equiv) in THF (7 mL) was added and stirring was continued at 0 °C. After 1.5 h a solution of **35** (3.94 g, 23.7 mmol, 1.2 equiv) in THF (7 mL) was added and the mixture was stirred overnight at room temperature. At 0 °C the mixture was acidified by the addition of sat. $NH_4Cl$ solution (10 mL) and conc. HCl (19 mL). The mixture was extracted with diethyl ether (3 × 50 mL) and the combined organic layers were concentrated under reduced pressure to give the crude product [38]. After column chromatography on silica gel (*n*-hexane/ethyl acetate, 9/1) the product was obtained as a yellow oil (1.93 g, 8.92 mmol, 44%). $^1$H NMR (300 MHz, $CDCl_3$): $\delta$ = 1.12 (t, $J$ = 7.1 Hz, 3H), 1.21 (t, $J$ = 7.1 Hz, 3H), 1.46–1.66 (m, 4H), 2.51 (t, $J$ = 7.0 Hz, 2H), 3.34 (t, $J$ = 6.1 Hz, 2H), 3.36 (s, 2H), 3.39 (q, $J$ = 7.1 Hz, 2H), 4.13 (q, $J$ = 7.1 Hz, 2H).

*4.1.27. 1-Bromo-3-ethoxypropane (**35**)*

At 0 °C phosphorus tribromide (4.33 g, 16 mmol, 1.0 equiv) was added dropwise to 3-ethoxypropan-1-ol (4.90 g, 47 mmol, 2.9 equiv). The mixture was stirred overnight at room temperature. After diluting with dichloromethane the mixture was washed with sat. $NaHCO_3$ solution, dried over $MgSO_4$. After filtration and evaporation of the solvent the product was obtained as a colorless oil (3.93 g, 23.7 mmol, 50%) [39]. $^1$H NMR (300 MHz, $CDCl_3$): $\delta$ = 1.31 (t, $J$ = 7.2 Hz, 3H), 2.03 (quint, $J$ = 6.2 Hz, 2H), 3.39–3.49 (m, 6H).

*4.2. Physicochemical properties*

*4.2.1. Determination of water solubility by HPLC*

A calibration curve was made by plotting the area under the curve at 254 nm (UV by HPLC, for compound **7** at 245 nm) against the concentration of each compound injected after performing a

serial dilution (25 μM–0.781 μM in methanol). A saturated solution containing 2% DMSO was then made for each compound in PBS (pH 7.4) by performing dilution using a 10 mM DMSO stock solution of each compound. This solution was sonicated for 30 min and shaken at room temperature for 10 h, filtered and injected into the HPLC to compare the area found at wavelength 254 nm (for compound **7** at 245 nm) with the previously made calibration curve [21].

*4.2.2. CAS iron-chelation assay*

A 1.5 mL aliquot of PBS (pH 7.2) containing the relevant concentration of test compound was mixed with 1.5 mL of CAS assay solution prepared according to Schwyn and Nylands. A reference was prepared by using PBS (pH 7.2) but without test compound. The samples (s) and reference (r) absorbances at 630 nm were determined after 15 min incubation at room temperature. The percentage of iron-chelating activity was calculated by subtracting the sample $A_{630}$ from that of the reference $A_{630}$ value. Siderophore units are defined as [Ar − As/Ar]*100 = percent of siderophore units [26].

*4.3. Biology*

Yeast extract was purchased from Fluka (Neu-Ulm, Germany), peptone from casein from Merck (Darmstadt, Germany), and Bacto™ Tryptone from BD Biosciences (Heidelberg, Germany). Salts and organic solvents of analytical grade were obtained from VWR (Darmstadt, Germany). *P. aeruginosa* strain PA14 (PA14) was stored in glycerol stocks at −80 °C. The following media were used: Luria Bertani broth (LB), PPGAS medium, and modified M9 minimal medium (20 mM $NH_4Cl$; 12 mM $Na_2HPO_4$; 22 mM $KH_2PO_4$; 8.6 mM NaCl; 1 mM, $MgSO_4$; 1 mM $CaCl_2$; 11 mM glucose).

*4.3.1. Reporter gene assay in E. coli*

The ability of the compounds to either stimulate or antagonize the PqsR-dependent transcription was analysed as previously described [17] using a β-galactosidase reporter gene assay in *E. coli* expressing PqsR. Briefly, a culture of *E. coli* DH5α cells containing the plasmid pEAL08-2, which encodes PqsR under the control of the *tac* promoter and the β-galactosidase reporter gene *lacZ* controlled by the *pqsA* promoter, were co incubated with test compound. Antagonistic effects of compounds were assayed in the presence of 50 nM PQS. After incubation, β-galactosidase activity was measured spectrophotometrically at $OD_{420\ nm}$ using POLARstar Omega (BMG Labtech, Ortenberg, Germany) and expressed as percent stimulation of controls. For the determination of $IC_{50}$ values, compounds were tested at least at eight different concentrations.

*4.3.2. Quantification of extracellular PQS levels*

Extracellular levels of PQS produced by PA14 were quantified by UHPLC–MS/MS using the method of Maurer et al. [40] For each sample, cultivation and sample work-up were performed in triplicates. Inhibition values of PQS formation were normalized to $OD_{600}$.

*4.3.3. Pyocyanin assay*

For analysis of pyocyanin formation, cultivation procedure was the same as for PQS quantification with the exception of using PPGAS medium. Pyocyanin produced by PA14 was quantified using the method of Essar et al. [41] with some modifications, as described in detail by Klein et al. [42]. Briefly, 900 μL of each culture were extracted with 900 μL of chloroform and 800 μL of the organic phase re-extracted with 250 μL of 0.2 M HCl. $OD_{520}$ was measured in the aqueous phase using FLUOstar Omega (BMG Labtech, Ortenberg, Germany). For each sample, cultivation and sample work-up were performed in triplicates. Inhibition values of pyocyanin formation were normalized to $OD_{600}$.

**Acknowledgement**

For technical assistance we like to thank Simone Amann and Carina Scheid.

**Appendix A. Supplementary data**

Supplementary data related to this article can be found at http://dx.doi.org/10.1016/j.ejmech.2014.04.016.

**References**

[1] C. Koch, N. Høiby, Pathogenesis of cystic fibrosis, Lancet 341 (1993) 1065–1069.
[2] J.R. Govan, V. Deretic, Microbial pathogenesis in cystic fibrosis: mucoid *Pseudomonas aeruginosa* and *Burkholderia cepacia*, Microbiological Reviews 60 (1996) 539–574.
[3] S. Swift, J.A. Downie, N.A. Whitehead, A.M.L. Barnard, G.P.C. Salmond, P. Williams, *Quorum sensing* as a population-density-dependent determinant of bacterial physiology, Advances In Microbial Physiology 45 (2001) 199–270.
[4] E.C. Pesci, J.B.J. Milbank, J.P. Pearson, S. McKnight, A.S. Kende, E.P. Greenberg, B.H. Iglewski, Quinolone signaling in the cell-to-cell communication system of *Pseudomonas aeruginosa*, Proceedings of the National Academy of Sciences of the United States of America 96 (1999) 11229–11234.
[5] H. Cao, G. Krishnan, B. Goumnerov, J. Tsongalis, R. Tompkins, L.G. Rahme, A quorum sensing-associated virulence gene of *Pseudomonas aeruginosa* encodes a LysR-like transcription regulator with a unique self-regulatory mechanism, Proceedings of the National Academy of Sciences of the United States of America 98 (2001) 14613–14618.
[6] G. Xiao, E. Deziel, J. He, F. Lepine, B. Lesic, M.H. Castonguay, S. Milot, A.P. Tampakaki, S.E. Stachel, L.G. Rahme, MvfR, a key *Pseudomonas aeruginosa* pathogenicity LTTR-class regulatory protein, has dual ligands, Molecular Microbiology 62 (2006) 1689–1699.
[7] E. Deziel, S. Gopalan, A.P. Tampakaki, F. Lepine, K.E. Padfield, M. Saucier, G. Xiao, L.G. Rahme, The contribution of MvfR to *Pseudomonas aeruginosa* pathogenesis and *quorum sensing* circuitry regulation: multiple *quorum sensing*-regulated genes are modulated without affecting lasRI, rhlRI or the production of N-acyl-L-homoserine lactones, Molecular Microbiology 55 (2005) 998–1014.
[8] L.A. Gallagher, S.L. McKnight, M.S. Kuznetsova, E.C. Pesci, C. Manoil, Functions required for extracellular quinolone signaling by *Pseudomonas aeruginosa*, Journal of Bacteriology 184 (2002) 6472–6480.
[9] E. Deziel, F. Lepine, S. Milot, J.X. He, M.N. Mindrinos, R.G. Tompkins, L.G. Rahme, Analysis of *Pseudomonas aeruginosa* 4-hydroxy-2-alkylquinolines (HAQs) reveals a role for 4-hydroxy-2-heptylquinoline in cell-to-cell communication, Proceedings of the National Academy of Sciences of the United States of America 101 (2004) 1339–1344.
[10] J.W. Schertzer, S.A. Brown, M. Whiteley, Oxygen levels rapidly modulate *Pseudomonas aeruginosa* social behaviours via substrate limitation of PqsH, Molecular Microbiology 77 (2010) 1527–1538.
[11] S. McGrath, D.S. Wade, E.C. Pesci, Dueling *quorum sensing* systems in *Pseudomonas aeruginosa* control the production of the Pseudomonas quinolone signal (PQS), FEMS Microbiology Letters 230 (2004) 27–34.
[12] T. Bjarnsholt, M. Givskov, *Quorum sensing* blockade as a strategy for enhancing host defences against bacterial pathogens, Philosophical Transactions of the Royal Society B: Biological Sciences 362 (2007) 1213–1222.
[13] L. Cegelski, G.R. Marshall, G.R. Eldridge, S.J. Hultgren, The biology and future prospects of antivirulence therapies, Nature Reviews Microbiology 6 (2008) 17–27.
[14] W.R.J.D. Galloway, J.T. Hodgkinso, S. Bowden, M. Welch, D.R. Spring, Applications of small molecule activators and inhibitors of *quorum sensing* in Gram-negative bacteria, Trends in Microbiology 20 (2012) 449–458.
[15] A. Ilangovan, M. Fletcher, G. Rampioni, C. Pustelny1, K. Rumbaugh, S. Heeb, M. Camara, A. Truman, S.R. Chhabra, J. Emsley, P. Williams, Structural basis for native agonist and synthetic inhibitor recognition by the *Pseudomonas aeruginosa quorum sensing* regulator PqsR (MvfR), PLoS Pathogens 9 (2013) e1003508.
[16] M. Zender, T. Klein, C. Henn, B. Kirsch, C.K. Maurer, D. Kail, C. Ritter, O. Dolezal, A. Steinbach, R.W. Hartmann, Discovery and biophysical characterization of 2-amino-oxadiazoles as novel antagonists of PqsR, an important regulator of *Pseudomonas aeruginosa* virulence, Journal of Medicinal Chemistry 56 (2013) 6761–6774.
[17] C. Lu, B. Kirsch, C. Zimmer, J.C. de Jong, C. Henn, C.K. Maurer, M. Müsken, S. Häussler, A. Steinbach, R.W. Hartmann, Discovery of antagonists of PqsR, a key player in 2-alkyl-4-quinolone-dependent *quorum sensing* in *Pseudomonas aeruginosa*, Chemistry & Biology 19 (2012) 381–390.

[18] A. Cheng, K.M. Merz Jr., Prediction of aqueous solubility of a diverse set of compounds using quantitative structure-property relationships, Journal of Medicinal Chemistry 46 (2003) 3572–3580.
[19] S. Venkatesh, R.A. Lipper, Role of the development scientist in compound lead selection and optimization, Journal of Pharmaceutical Sciences 89 (2000) 145–154.
[20] M. Ishikawa, Y. Hashimoto, Improvement in aqueous solubility in small molecule drug discovery programs by disruption of molecular planarity and symmetry, Journal of Medicinal Chemistry 54 (2011) 1539–1554.
[21] R.M. Cross, A. Monastyrskyi, T.S. Mutka, J.N. Burrows, D.E. Kyle, R. Manetsch, Endochin optimization: structure-activity and structure-property relationship studies of 3-substituted 2-methyl-4(1H)-quinolones with antimalarial activity, Journal of Medicinal Chemistry 53 (2010) 7076–7094.
[22] C. Lu, C.K. Maurer, B. Kirsch, A. Steinbach, R.W. Hartmann, Overcoming unexpected functional inversion of PqsR antagonist in *Pseudomonas aeruginosa* led to the first in vivo potent anti-virulence agent targeting pqs quorum sensing, Angewandte Chemie International Edition 126 (2014) 1127–1130.
[23] R.T. Ellison 3rd, T.J. Giehl, F.M. LaForce, Damage of the outer membrane of enteric Gram-negative bacteria by lactoferrin and transferring, Infection and Immunity 56 (1988) 2774–2781.
[24] H. Nikaido, Molecular basis of bacterial outer membrane permeability revisited, Microbiology and Molecular Biology Reviews 67 (2003) 593–656.
[25] J.J. Marx, Iron and infection: competition between host and microbes for a precious element, Best Practice & Research Clinical Haematology 15 (2002) 411–426.
[26] S.P. Diggle, S. Matthijs, V.J. Wright, M.P. Fletcher, S.R. Chhabra, I.L. Lamont, X. Kong, R.C. Hider, P. Cornelis, M. Camara, P. Williams, The *Pseudomonas aeruginosa* 4-quinolone signal molecules HHQ and PQS play multifunctional roles in *quorum sensing* and iron entrapment, Chemistry & Biology 14 (2007) 87–96.
[27] J.M. Harris, S.F. Neelamkavil, B.R. Neustadt, C.D. Boyle, H. Liu, J. Hao, A. Stamford, S. Chackalamannil, W.J. Greenlee, Preparation of aminoquinazolinone derivatives and analogs for use as GPR119 modulators, PCT Int. Appl., 2009143049.
[28] I. Purcell, Bacterial Autoinducer Derived 4-quinolones as Novel Immune Modulators (PhD thesis University of Nottingham), 2006.
[29] R.M. Cross, R. Manetsch, Divergent route to access structurally diverse 4-quinolones via mono or sequential cross-couplings, Journal of Organic Chemistry 75 (2010) 8654–8657.
[30] M. Li, L. Li, H. Ge, Direct C3-Alkenylation of quinolones via palladium-catalyzed C-H functionalization with low catalyst loading, Advanced Synthesis & Catalysis 352 (2010) 2445–2449.
[31] A.L. Ruchelman, J.E. Kerrigan, T.K. Li, N. Zhou, A. Liu, L.F. Liu, E.J. LaVoie, Nitro and amino substitution within the A-ring of 5*H*-8,9-dimethoxy-5-(2-*N*,*N*-dimethylaminoethyl)dibenzo[c,h][1,6]naphthyridin-6-ones: influence on topoisomerase I-targeting activity and cytotoxicity, Bioorganic & Medicinal Chemistry 12 (2004) 3731–3742.
[32] J.P. Moerdyk, A.L. Speelman, K.E. Kuper III, B.R. Heiberger, R.P. Ter Louw, D.J. Zeller, A.J. Radler, J.G. Gillmore, Synthesis and photochemistry of two quinoline analogs of the perimidinespirohexadienone family of photochromes, Journal of Photochemistry and Photobiology A: Chemistry 205 (2009) 84–92.
[33] J. Escribano, C. Rivero-Hernández, H. Rivera, D. Barros, J. Castro-Pichel, E. Pérez-Herrán, A. Mendoza-Losana, I. Angulo-Barturen, S. Ferrer-Bazaga, E. Jiménez-Navarro, L. Ballell, 4-Substituted thioquinolines and thiazoloquinolines: potent, selective, and Tween-80 in vitro dependent families of antitubercular agents with moderate in vivo activity, ChemMedChem 6 (2011) 2252–2263.
[34] C. Pidathala, R. Amewu, B. Pacorel, G.L. Nixon, P. Gibbons, W.D. Hong, S.C. Leung, N.G. Berry, R. Sharma, P.A. Stocks, A. Srivastava, A.E. Shone, S. Charoensutthivarakul, L. Taylor, O. Berger, A. Mbekeani, A. Hill, N.E. Fisher, A.J. Warman, G.A. Biagini, S.A. Ward, P.M. O'Neill, Identification, design and biological evaluation of bisaryl quinolones targeting Plasmodium falciparum type II NADH:quinone oxidoreductase (PfNDH2), Journal of Medicinal Chemistry 55 (2012) 1831–1843.
[35] Y. Zhang, W.A. Guiguemde, M. Sigal, F. Zhu, M.C. Connelly, S. Nwaka, R.K. Guy, Synthesis and structure-activity relationships of antimalarial 4-oxo-3-carboxyl quinolones, Bioorganic & Medicinal Chemistry 18 (2010) 2756–2766.
[36] G. Giacomelli, A. Porcheddu, M. Salaris, Simple one-flask method for the preparation of hydroxamic acids, Organic Letters 5 (2003) 2715–2717.
[37] H. Schmidt, Cyclisierungsreaktionen von Ethoxymethylenmalononitril mit 4-substituierten Acetessigestern, Monatshefte fuer Chemie 120 (1989) 891–897.
[38] P.H. Lambert, M. Vaultier, R. Carrie, Application of the intramolecular aza-Wittig reaction to the synthesis of vinylogous urethanes and amides, Journal of Organic Chemistry 50 (1985) 5352–5356.
[39] M. Takakiyo, M. Hiroshi, Y. Tomoyuki, J. Masahiro, Process for the Production of an Optically Active Alcohol and a Novel Optically Active Alcohol, US6103517.
[40] C.K. Maurer, A. Steinbach, R.W. Hartmann, Development and validation of a UHPLC-MS/MS procedure for quantification of the *Pseudomonas* quinolone signal in bacterial culture after acetylation for characterization of new *quorum sensing* inhibitors, Journal of Pharmaceutical and Biomedical Analysis 86C (2013) 127–134.
[41] D.W. Essar, L. Eberly, A. Hadero, I.P. Crawford, Identification and characterization of genes for a second anthranilate synthase in *Pseudomonas aeruginosa*: interchangeability of the two anthranilate synthases and evolutionary implications, Journal of Bacteriology 172 (1990) 884–890.
[42] T. Klein, C. Henn, J.C. de Jong, C. Zimmer, B. Kirsch, C.K. Maurer, D. Pistorius, R. Müller, A. Steinbach, R.W. Hartmann, Identification of small-molecule antagonists of the *Pseudomonas aeruginosa* transcriptional regulator PqsR: biophysically guided hit discovery and optimization, ACS Chemical Biology 7 (2012) 1496–1501.

## 3.4 Evaluation of the Inhibitory Effects on Biofilm Formation

Recently, it was demostrated that blocking PqsR via small molecules indeed attenuates the biofilm development of *P. aeruginosa* (Ilangovan et al., 2013), which encouraged us to investigate the anti-biofilm activity for the most promising antagonist **I-20/II-1**. However, the results obtained from two distinct assays are ambiguous: in the crystal violet staining assay (O'Toole et al., 1999) a 10%-25% reduction of biofilm formation was observed in the presence of the compound at a concentration of 15 μM; in contrast, in the viability staining assay combined with automated confocal laser scanning microscopy (CLSM) (Musken et al., 2010) there was no inhibition recorded. In the future, further studies will be conducted to clarify the inhibitory effects of the PqsR antagonists on *P. aeruginosa* biofilm.

# 4 Summary, Conclusion and Outlook

## 4.1 Summary and Conclusion

PqsR is the receptor of the *P. aeruginosa*-specific *pqs* QS circuit, and functions as a critical regulator that fine-tunes the expression of a large set of pathogenicity-associated genes, most of which are involved in the production of virulence factors and biofilm formation. We regard this virulence regulator as an attractive drug target, and discovered anti-virulence compounds blocking PqsR (PqsR antagonists) to effectively diminish bacterial pathogenicity without provoking resistance.

### 4.1.1 Discovery of the First PqsR Antagonists

Because of the lack of an appropriate crystal structure of PqsR, we have applied a ligand-based design strategy to explore PqsR antagonists via structural modification of the natural ligands/agonists of the receptor, and subsequently identified PqsR antagonists by means of introducing strong EWGs like CN, $CF_3$ or $NO_2$ into the 6-position of HHQ. All of the antagonists **I-18, I-19** and **I-20/II-1** exhibited high activity towards PqsR with $IC_{50}$s in low nanomolar range in the *E coli*.-based reporter gene assay. This work led to the discovery of the first PqsR antagonists.

### 4.1.2 Identification of the most Potent PqsR Antagonist and the First Proof-of-concept for PqsR-targeting Therapy

Despite high activity displayed in the *E coli*.-based reporter gene assay, the first PqsR antagonist **I-20/II-1** is unable to efficiently repress the *pqs* QS activity as well as the production of virulence factor pyocynin in *P. aeruginosa*. A thorough investigation of this phenomenon revealed that the ineffectiveness of **I-20/II-1** in the pathogen is attributed to an unexpected functional inversion mediated by the bacterial enzyme PqsH that converts the strong antagonist into a potent agonist **II-2**. Consequently, we utilized medicinal-chemistry strategies to overcome the problem and reshaped the antagonist **I-20/II-1** yielding compound **II-3**, which fully protects *Galleria mellonella* larvae from lethal *P. aeruginosa* infections at a low nanomolar concentration (22 nM). To the best of our knowledge, compound **II-3** is the most active anti-virulence compound interfering with PqsR reported to date (Ilangovan et al., 2013; Klein et al., 2012; Zender et al., 2013). This work provided the first proof-of-concept for PqsR as a target for anti-virulence therapy.

### 4.1.3 Development of PqsR Antagonists with Improved Physicochemical Properties

Our PqsR antagonists turned out to be promising anti-virulence agents, however, these

compounds suffered from poor aqueous solubility that hinders them to be proper drug candidates. Thus, the antagonists were structurally modified by means of introducing polar or ionizable groups into the quinolone core or the alkyl side chain to improve their solubility. SARs as well as SPRs thus obtained were systematically studied. In this work new insights into ligand-receptor interactions were provided and a novel potent compound, **III-16**, with improved solubility was developed.

## 4.2 Outlook

In the next step the highly potent PqsR antagonists will be proceeded in mouse infection models e.g. tumor model, lung infection model and burn wound model, to investigate the *in vivo* anti-virulence efficacy in mammalian species.

Recently, the cocrystal structure of PqsR with ligands was reported by another group (Ilangovan et al., 2013), however, the resolution was poor. In cooperation with other group (Xu et al., 2012) we are also aiming at getting a high quality crystal structure of PqsR, which will assist us in elucidating the mechanism of action (MOA) of receptor activation/inactivation. This may in turn facilitate the antagonist design and optimization in the future.

Meanwhile, the existing PqsR antagonists are going to be further modified regarding activity as well as physicochemical properties. Noteworthy, the poor water solubility of this compound class can be a problem obstructing the way to drug candidates for a systemic administration (e.g. oral administration). To solve this problem, we have planned to replace the left benzene ring as well as groups at 1- or 3-position with other more polar or ionizable counterparts. Moreover, we are also investigating diverse delivery systems e.g. packing the highly lipophilic antagonists into nanoparticles or liposomes. Although further optimization is needed for the systemic application, we suggest that these compounds should be readily applicable for a topical treatment that is less affected by solubility. Application of the compounds in a form of aerosol to cure lung infections and administration as creme to deal with skin infections are promising options to achieve a local therapeutic effect.

# 5 References

Alhede, M., Bjarnsholt, T., and Givskov, M. (2014). Pseudomonas aeruginosa Biofilms: Mechanisms of Immune Evasion. Adv Appl Microbiol *86*, 1-40.
Arias, C.A., and Murray, B.E. (2009). Antibiotic-resistant bugs in the 21st century--a clinical super-challenge. N Engl J Med *360*, 439-443.
Azghani, A.O. (1996). Pseudomonas aeruginosa and epithelial permeability: role of virulence factors elastase and exotoxin A. Am J Respir Cell Mol Biol *15*, 132-140.
Azghani, A.O., Connelly, J.C., Peterson, B.T., Gray, L.D., Collins, M.L., and Johnson, A.R. (1990). Effects of Pseudomonas aeruginosa elastase on alveolar epithelial permeability in guinea pigs. Infect Immun *58*, 433-438.
Azghani, A.O., Gray, L.D., and Johnson, A.R. (1993). A bacterial protease perturbs the paracellular barrier function of transporting epithelial monolayers in culture. Infect Immun *61*, 2681-2686.
Baron, S.S., and Rowe, J.J. (1981). Antibiotic action of pyocyanin. Antimicrob Agents Chemother *20*, 814-820.
Bredenbruch, F., Geffers, R., Nimtz, M., Buer, J., and Haussler, S. (2006). The Pseudomonas aeruginosa quinolone signal (PQS) has an iron-chelating activity. Environ Microbiol *8*, 1318-1329.
Calfee, M.W., Shelton, J.G., McCubrey, J.A., and Pesci, E.C. (2005). Solubility and bioactivity of the Pseudomonas quinolone signal are increased by a Pseudomonas aeruginosa-produced surfactant. Infection and Immunity *73*, 878-882.
Cao, H., Krishnan, G., Goumnerov, B., Tsongalis, J., Tompkins, R., and Rahme, L.G. (2001). A quorum sensing-associated virulence gene of Pseudomonas aeruginosa encodes a LysR-like transcription regulator with a unique self-regulatory mechanism. P Natl Acad Sci USA *98*, 14613-14618.
Cegelski, L., Marshall, G.R., Eldridge, G.R., and Hultgren, S.J. (2008). The biology and future prospects of antivirulence therapies. Nat Rev Microbiol *6*, 17-27.
Collier, D.N., Anderson, L., McKnight, S.L., Noah, T.L., Knowles, M., Boucher, R., Schwab, U., Gilligan, P., and Pesci, E.C. (2002). A bacterial cell to cell signal in the lungs of cystic fibrosis patients. FEMS Microbiol Lett *215*, 41-46.
Costerton, J.W., Stewart, P.S., and Greenberg, E.P. (1999). Bacterial biofilms: a common cause of persistent infections. Science *284*, 1318-1322.
Costerton, W., Veeh, R., Shirtliff, M., Pasmore, M., Post, C., and Ehrlich, G. (2003). The application of biofilm science to the study and control of chronic bacterial infections. J Clin Invest *112*, 1466-1477.
D'Argenio, D.A., Calfee, M.W., Rainey, P.B., and Pesci, E.C. (2002). Autolysis and autoaggregation in Pseudomonas aeruginosa colony morphology mutants. Journal of Bacteriology *184*, 6481-6489.
Das, T., Kutty, S.K., Kumar, N., and Manefield, M. (2013). Pyocyanin Facilitates Extracellular DNA Binding to Pseudomonas aeruginosa Influencing Cell Surface Properties and Aggregation. PLoS One *8*, e58299.
Das, T., and Manefield, M. (2012). Pyocyanin Promotes Extracellular DNA Release in Pseudomonas aeruginosa. PLoS One *7*, e46718.
Davey, M.E., Caiazza, N.C., and O'Toole, G.A. (2003). Rhamnolipid surfactant production affects biofilm architecture in Pseudomonas aeruginosa PAO1. J Bacteriol *185*, 1027-1036.
Dekimpe, V., and Deziel, E. (2009). Revisiting the quorum-sensing hierarchy in Pseudomonas aeruginosa: the transcriptional regulator RhlR regulates LasR-specific factors. Microbiol-Sgm *155*, 712-723.
Deziel, E., Gopalan, S., Tampakaki, A.P., Lepine, F., Padfield, K.E., Saucier, M., Xiao, G., and Rahme, L.G. (2005). The contribution of MvfR to Pseudomonas aeruginosa pathogenesis and quorum sensing circuitry regulation: multiple quorum sensing-regulated genes are modulated without affecting lasRI, rhlRI or the production of N-acyl-L-homoserine lactones. Mol Microbiol *55*, 998-1014.
Deziel, E., Lepine, F., Milot, S., He, J., Mindrinos, M.N., Tompkins, R.G., and Rahme, L.G. (2004). Analysis of Pseudomonas aeruginosa 4-hydroxy-2-alkylquinolines (HAQs) reveals a role for 4-hydroxy-2-heptylquinoline in cell-to-cell communication. P Natl Acad Sci USA *101*, 1339-1344.
Diggle, S.P., Matthijs, S., Wright, V.J., Fletcher, M.P., Chhabra, S.R., Lamont, I.L., Kong, X., Hider, R.C., Cornelis, P., Camara, M., *et al.* (2007). The Pseudomonas aeruginosa 4-quinolone signal molecules HHQ and PQS play multifunctional roles in quorum sensing and iron entrapment. Chem Biol *14*, 87-96.
Diggle, S.P., Winzer, K., Chhabra, S.R., Chhabra, S.R., Worrall, K.E., Camara, M., and Williams, P. (2003). The Pseudomonas aeruginosa quinolone signal molecule overcomes the cell density-dependency of the quorum sensing hierarchy, regulates rhl-dependent genes at the onset of stationary phase and can be produced in the absence of LasR. Mol Microbiol *50*, 29-43.
Farrow, J.M., 3rd, Sund, Z.M., Ellison, M.L., Wade, D.S., Coleman, J.P., and Pesci, E.C. (2008). PqsE

functions independently of PqsR-Pseudomonas quinolone signal and enhances the rhl quorum-sensing system. J Bacteriol *190*, 7043-7051.
Gallagher, L.A., McKnight, S.L., Kuznetsova, M.S., Pesci, E.C., and Manoil, C. (2002). Functions required for extracellular quinolone signaling by Pseudomonas aeruginosa. Journal of Bacteriology *184*, 6472-6480.
Galloway, W.R., Hodgkinson, J.T., Bowden, S., Welch, M., and Spring, D.R. (2012). Applications of small molecule activators and inhibitors of quorum sensing in Gram-negative bacteria. Trends Microbiol *20*, 449-458.
Galloway, W.R., Hodgkinson, J.T., Bowden, S.D., Welch, M., and Spring, D.R. (2011). Quorum sensing in Gram-negative bacteria: small-molecule modulation of AHL and AI-2 quorum sensing pathways. Chem Rev *111*, 28-67.
Gambello, M.J., and Iglewski, B.H. (1991). Cloning and characterization of the Pseudomonas aeruginosa lasR gene, a transcriptional activator of elastase expression. J Bacteriol *173*, 3000-3009.
Gessard, C. (1984). Classics in infectious diseases. On the blue and green coloration that appears on bandages. Rev Infect Dis *6 Suppl 3*, S775-776.
Glick, R., Gilmour, C., Tremblay, J., Satanower, S., Avidan, O., Deziel, E., Greenberg, E.P., Poole, K., and Banin, E. (2010). Increase in rhamnolipid synthesis under iron-limiting conditions influences surface motility and biofilm formation in Pseudomonas aeruginosa. J Bacteriol *192*, 2973-2980.
Govan, J.R., and Deretic, V. (1996). Microbial pathogenesis in cystic fibrosis: mucoid Pseudomonas aeruginosa and Burkholderia cepacia. Microbiol Rev *60*, 539-574.
Hall-Stoodley, L., Costerton, J.W., and Stoodley, P. (2004). Bacterial biofilms: from the natural environment to infectious diseases. Nat Rev Microbiol *2*, 95-108.
Hartmann, R.W., Kranzfelder, G., von Angerer, E., and Schonenberger, H. (1980). Antiestrogens. Synthesis and evaluation of mammary tumor inhibiting activity of 1,1,2,2-tetraalkyl-1,2 -diphenylethanes. J Med Chem *23*, 841-848.
Haussler, S., and Becker, T. (2008). The pseudomonas quinolone signal (PQS) balances life and death in Pseudomonas aeruginosa populations. PLoS Pathog *4*, e1000166.
Heck, L.W., Morihara, K., McRae, W.B., and Miller, E.J. (1986). Specific cleavage of human type III and IV collagens by Pseudomonas aeruginosa elastase. Infect Immun *51*, 115-118.
Hentzer, M., Wu, H., Andersen, J.B., Riedel, K., Rasmussen, T.B., Bagge, N., Kumar, N., Schembri, M.A., Song, Z., Kristoffersen, P., *et al.* (2003). Attenuation of Pseudomonas aeruginosa virulence by quorum sensing inhibitors. EMBO J *22*, 3803-3815.
Ilangovan, A., Fletcher, M., Rampioni, G., Pustelny, C., Rumbaugh, K., Heeb, S., Camara, M., Truman, A., Chhabra, S.R., Emsley, J., *et al.* (2013). Structural Basis for Native Agonist and Synthetic Inhibitor Recognition by the Pseudomonas aeruginosa Quorum Sensing Regulator PqsR (MvfR). PLoS Pathog *9*, e1003508.
Irie, Y., and Parsek, M.R. (2008). Quorum sensing and microbial biofilms. Curr Top Microbiol Immunol *322*, 67-84.
Jacquot, J., Tournier, J.M., and Puchelle, E. (1985). In vitro evidence that human airway lysozyme is cleaved and inactivated by Pseudomonas aeruginosa elastase and not by human leukocyte elastase. Infect Immun *47*, 555-560.
Jander, G., Rahme, L.G., and Ausubel, F.M. (2000). Positive correlation between virulence of Pseudomonas aeruginosa mutants in mice and insects. J Bacteriol *182*, 3843-3845.
Jensen, P.O., Bjarnsholt, T., Phipps, R., Rasmussen, T.B., Calum, H., Christoffersen, L., Moser, C., Williams, P., Pressler, T., Givskov, M., *et al.* (2007). Rapid necrotic killing of polymorphonuclear leukocytes is caused by quorum-sensing-controlled production of rhamnolipid by Pseudomonas aeruginosa. Microbiology *153*, 1329-1338.
Johnson, M.K., and Boese-Marrazzo, D. (1980). Production and properties of heat-stable extracellular hemolysin from Pseudomonas aeruginosa. Infect Immun *29*, 1028-1033.
Kessler, E., Safrin, M., Gustin, J.K., and Ohman, D.E. (1998). Elastase and the LasA protease of Pseudomonas aeruginosa are secreted with their propeptides. J Biol Chem *273*, 30225-30231.
Kim, W., Tengra, F.K., Young, Z., Shong, J., Marchand, N., Chan, H.K., Pangule, R.C., Parra, M., Dordick, J.S., Plawsky, J.L., *et al.* (2013). Spaceflight promotes biofilm formation by Pseudomonas aeruginosa. PLoS One *8*, e62437.
Klein, T., Henn, C., de Jong, J.C., Zimmer, C., Kirsch, B., Maurer, C.K., Pistorius, D., Muller, R., Steinbach, A., and Hartmann, R.W. (2012). Identification of small-molecule antagonists of the Pseudomonas aeruginosa transcriptional regulator PqsR: biophysically guided hit discovery and optimization. ACS Chem Biol *7*, 1496-1501.
Koch, C., and Hoiby, N. (1993). Pathogenesis of cystic fibrosis. Lancet *341*, 1065-1069.

Kuang, Z., Hao, Y., Walling, B.E., Jeffries, J.L., Ohman, D.E., and Lau, G.W. (2011). Pseudomonas aeruginosa elastase provides an escape from phagocytosis by degrading the pulmonary surfactant protein-A. PLoS One *6*, e27091.
LaSarre, B., and Federle, M.J. (2013). Exploiting quorum sensing to confuse bacterial pathogens. Microbiol Mol Biol Rev *77*, 73-111.
Lau, G.W., Hassett, D.J., Ran, H., and Kong, F. (2004). The role of pyocyanin in Pseudomonas aeruginosa infection. Trends Mol Med *10*, 599-606.
Lee, J., Wu, J., Deng, Y., Wang, J., Wang, C., Chang, C., Dong, Y., Williams, P., and Zhang, L.H. (2013). A cell-cell communication signal integrates quorum sensing and stress response. Nat Chem Biol.
Lesic, B., Lepine, F., Deziel, E., Zhang, J.W., Zhang, Q.H., Padfield, K., Castonguay, M.H., Milot, S., Stachel, S., Tzika, A.A., *et al.* (2007). Inhibitors of pathogen intercellular signals as selective anti-infective compounds. Plos Pathogens *3*, 1229-1239.
Levy, S.B., and Marshall, B. (2004). Antibacterial resistance worldwide: causes, challenges and responses. Nat Med *10*, S122-129.
Lewis, K. (2010). Persister cells. Annu Rev Microbiol *64*, 357-372.
Lewis, K. (2012). Antibiotics: Recover the lost art of drug discovery. Nature *485*, 439-440.
Lyczak, J.B., Cannon, C.L., and Pier, G.B. (2000). Establishment of Pseudomonas aeruginosa infection: lessons from a versatile opportunist. Microbes Infect *2*, 1051-1060.
Maddocks, S.E., and Oyston, P.C.F. (2008). Structure and function of the LysR-type transcriptional regulator (LTTR) family proteins. Microbiology (Reading, England) *154*, 3609-3623.
Mahajan-Miklos, S., Tan, M.W., Rahme, L.G., and Ausubel, F.M. (1999). Molecular mechanisms of bacterial virulence elucidated using a Pseudomonas aeruginosa-Caenorhabditis elegans pathogenesis model. Cell *96*, 47-56.
Mashburn-Warren, L., Howe, J., Brandenburg, K., and Whiteley, M. (2009). Structural requirements of the Pseudomonas quinolone signal for membrane vesicle stimulation. Journal of bacteriology *191*, 3411-3414.
Mashburn-Warren, L., Howe, J., Garidel, P., Richter, W., Steiniger, F., Roessle, M., Brandenburg, K., and Whiteley, M. (2008). Interaction of quorum signals with outer membrane lipids: insights into prokaryotic membrane vesicle formation. Mol Microbiol *69*, 491-502.
Mashburn, L.M., and Whiteley, M. (2005). Membrane vesicles traffic signals and facilitate group activities in a prokaryote. Nature *437*, 422-425.
McGrath, S., Wade, D.S., and Pesci, E.C. (2004). Dueling quorum sensing systems in Pseudomonas aeruginosa control the production of the Pseudomonas quinolone signal (PQS). FEMS Microbiol Lett *230*, 27-34.
McKnight, S.L., Iglewski, B.H., and Pesci, E.C. (2000). The Pseudomonas quinolone signal regulates rhl quorum sensing in Pseudomonas aeruginosa. Journal of Bacteriology *182*, 2702-2708.
Miller, E.J., and Gay, S. (1982). Collagen: an overview. Methods Enzymol *82 Pt A*, 3-32.
Miller, M.B., and Bassler, B.L. (2001). Quorum sensing in bacteria. Annu Rev Microbiol *55*, 165-199.
Morihara, K. (1995). Pseudolysin and other pathogen endopeptidases of thermolysin family. Methods Enzymol *248*, 242-253.
Mulcahy, H., Charron-Mazenod, L., and Lewenza, S. (2008). Extracellular DNA chelates cations and induces antibiotic resistance in Pseudomonas aeruginosa biofilms. PLoS Pathog *4*, e1000213.
Muller, M. (2002). Pyocyanin induces oxidative stress in human endothelial cells and modulates the glutathione redox cycle. Free Radic Biol Med *33*, 1527-1533.
Musken, M., Di Fiore, S., Romling, U., and Haussler, S. (2010). A 96-well-plate-based optical method for the quantitative and qualitative evaluation of Pseudomonas aeruginosa biofilm formation and its application to susceptibility testing. Nat Protoc *5*, 1460-1469.
Nealson, K.H., Platt, T., and Hastings, J.W. (1970). Cellular control of the synthesis and activity of the bacterial luminescent system. J Bacteriol *104*, 313-322.
O'Malley, Y.Q., Abdalla, M.Y., McCormick, M.L., Reszka, K.J., Denning, G.M., and Britigan, B.E. (2003a). Subcellular localization of Pseudomonas pyocyanin cytotoxicity in human lung epithelial cells. Am J Physiol Lung Cell Mol Physiol *284*, L420-430.
O'Malley, Y.Q., Reszka, K.J., Rasmussen, G.T., Abdalla, M.Y., Denning, G.M., and Britigan, B.E. (2003b). The Pseudomonas secretory product pyocyanin inhibits catalase activity in human lung epithelial cells. Am J Physiol Lung Cell Mol Physiol *285*, L1077-1086.
O'Malley, Y.Q., Reszka, K.J., Spitz, D.R., Denning, G.M., and Britigan, B.E. (2004). Pseudomonas aeruginosa pyocyanin directly oxidizes glutathione and decreases its levels in airway epithelial cells. Am J Physiol Lung Cell Mol Physiol *287*, L94-103.
O'Toole, G.A., Pratt, L.A., Watnick, P.I., Newman, D.K., Weaver, V.B., and Kolter, R. (1999). Genetic

approaches to study of biofilms. Methods Enzymol *310*, 91-109.
Ochsner, U.A., Koch, A.K., Fiechter, A., and Reiser, J. (1994). Isolation and characterization of a regulatory gene affecting rhamnolipid biosurfactant synthesis in Pseudomonas aeruginosa. J Bacteriol *176*, 2044-2054.
Ochsner, U.A., and Reiser, J. (1995). Autoinducer-mediated regulation of rhamnolipid biosurfactant synthesis in Pseudomonas aeruginosa. Proc Natl Acad Sci U S A *92*, 6424-6428.
Passador, L., Cook, J.M., Gambello, M.J., Rust, L., and Iglewski, B.H. (1993). Expression of Pseudomonas aeruginosa virulence genes requires cell-to-cell communication. Science *260*, 1127-1130.
Pesci, E.C., Milbank, J.B., Pearson, J.P., McKnight, S., Kende, A.S., Greenberg, E.P., and Iglewski, B.H. (1999). Quinolone signaling in the cell-to-cell communication system of Pseudomonas aeruginosa. Proc Natl Acad Sci U S A *96*, 11229-11234.
Pesci, E.C., Pearson, J.P., Seed, P.C., and Iglewski, B.H. (1997). Regulation of las and rhl quorum sensing in Pseudomonas aeruginosa. J Bacteriol *179*, 3127-3132.
Purdy Drew, K.R., Sanders, L.K., Culumber, Z.W., Zribi, O., and Wong, G.C. (2009). Cationic amphiphiles increase activity of aminoglycoside antibiotic tobramycin in the presence of airway polyelectrolytes. J Am Chem Soc *131*, 486-493.
Rada, B., Gardina, P., Myers, T.G., and Leto, T.L. (2011). Reactive oxygen species mediate inflammatory cytokine release and EGFR-dependent mucin secretion in airway epithelial cells exposed to Pseudomonas pyocyanin. Mucosal Immunol *4*, 158-171.
Rada, B., Lekstrom, K., Damian, S., Dupuy, C., and Leto, T.L. (2008). The Pseudomonas toxin pyocyanin inhibits the dual oxidase-based antimicrobial system as it imposes oxidative stress on airway epithelial cells. J Immunol *181*, 4883-4893.
Rada, B., and Leto, T.L. (2013). Pyocyanin effects on respiratory epithelium: relevance in Pseudomonas aeruginosa airway infections. Trends Microbiol *21*, 73-81.
Rahim, R., Ochsner, U.A., Olvera, C., Graninger, M., Messner, P., Lam, J.S., and Soberon-Chavez, G. (2001). Cloning and functional characterization of the Pseudomonas aeruginosa rhlC gene that encodes rhamnosyltransferase 2, an enzyme responsible for di-rhamnolipid biosynthesis. Mol Microbiol *40*, 708-718.
Ramphal, R., Lhermitte, M., Filliat, M., and Roussel, P. (1988). The binding of anti-pseudomonal antibiotics to macromolecules from cystic fibrosis sputum. J Antimicrob Chemother *22*, 483-490.
Rampioni, G., Pustelny, C., Fletcher, M.P., Wright, V.J., Bruce, M., Rumbaugh, K.P., Heeb, S., Camara, M., and Williams, P. (2010). Transcriptomic analysis reveals a global alkyl-quinolone-independent regulatory role for PqsE in facilitating the environmental adaptation of Pseudomonas aeruginosa to plant and animal hosts. Environ Microbiol *12*, 1659-1673.
Rasko, D.A., Moreira, C.G., Li de, R., Reading, N.C., Ritchie, J.M., Waldor, M.K., Williams, N., Taussig, R., Wei, S., Roth, M., *et al.* (2008). Targeting QseC signaling and virulence for antibiotic development. Science *321*, 1078-1080.
Rasmussen, T.B., and Givskov, M. (2006a). Quorum-sensing inhibitors as anti-pathogenic drugs. Int J Med Microbiol *296*, 149-161.
Rasmussen, T.B., and Givskov, M. (2006b). Quorum sensing inhibitors: a bargain of effects. Microbiology *152*, 895-904.
Schertzer, J.W., Brown, S.A., and Whiteley, M. (2010). Oxygen levels rapidly modulate Pseudomonas aeruginosa social behaviours via substrate limitation of PqsH. Mol Microbiol *77*, 1527-1538.
Storz, M.P., Maurer, C.K., Zimmer, C., Wagner, N., Brengel, C., de Jong, J.C., Lucas, S., Musken, M., Haussler, S., Steinbach, A., *et al.* (2012). Validation of PqsD as an Anti-biofilm Target in Pseudomonas aeruginosa by Development of Small-Molecule Inhibitors. J Am Chem Soc *134*, 16143-16146.
Stover, C.K., Pham, X.Q., Erwin, A.L., Mizoguchi, S.D., Warrener, P., Hickey, M.J., Brinkman, F.S., Hufnagle, W.O., Kowalik, D.J., Lagrou, M., *et al.* (2000). Complete genome sequence of Pseudomonas aeruginosa PAO1, an opportunistic pathogen. Nature *406*, 959-964.
Strateva, T., and Yordanov, D. (2009). Pseudomonas aeruginosa - a phenomenon of bacterial resistance. J Med Microbiol *58*, 1133-1148.
Wade, D.S., Calfee, M.W., Rocha, E.R., Ling, E.A., Engstrom, E., Coleman, J.P., and Pesci, E.C. (2005). Regulation of Pseudomonas quinolone signal synthesis in Pseudomonas aeruginosa. Journal of bacteriology *187*, 4372-4380.
Wilson, R., Sykes, D.A., Watson, D., Rutman, A., Taylor, G.W., and Cole, P.J. (1988). Measurement of Pseudomonas aeruginosa phenazine pigments in sputum and assessment of their contribution to sputum sol toxicity for respiratory epithelium. Infect Immun *56*, 2515-2517.
Winzer, K., Falconer, C., Garber, N.C., Diggle, S.P., Camara, M., and Williams, P. (2000). The Pseudomonas aeruginosa lectins PA-IL and PA-IIL are controlled by quorum sensing and by RpoS. J Bacteriol *182*, 6401-6411.

Xiao, G., Deziel, E., He, J., Lepine, F., Lesic, B., Castonguay, M.-H., Milot, S., Tampakaki, A.P., Stachel, S.E., and Rahme, L.G. (2006). MvfR, a key Pseudomonas aeruginosa pathogenicity LTTR-class regulatory protein, has dual ligands. Mol Microbiol *62*, 1689-1699.

Xu, N., Yu, S., Moniot, S., Weyand, M., and Blankenfeldt, W. (2012). Crystallization and preliminary crystal structure analysis of the ligand-binding domain of PqsR (MvfR), the Pseudomonas quinolone signal (PQS) responsive quorum-sensing transcription factor of Pseudomonas aeruginosa. Acta Crystallogr Sect F Struct Biol Cryst Commun *68*, 1034-1039.

Yang, S., Abdel-Razek, O.A., Cheng, F., Bandyopadhyay, D., Shetye, G.S., Wang, G., and Luk, Y.Y. (2014). Bicyclic brominated furanones: A new class of quorum sensing modulators that inhibit bacterial biofilm formation. Bioorg Med Chem.

Zender, M., Klein, T., Henn, C., Kirsch, B., Maurer, C.K., Kail, D., Ritter, C., Dolezal, O., Steinbach, A., and Hartmann, R.W. (2013). Discovery and biophysical characterization of 2-amino-oxadiazoles as novel antagonists of PqsR, an important regulator of Pseudomonas aeruginosa virulence. J Med Chem *56*, 6761-6774.

# 6 Appendix

## 6.1 Supplemental Information for Paper I

### Table S1. Agonistic and Antagonistic Activities of PQS Analogues

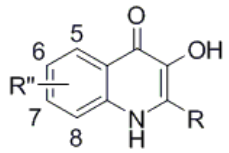


**31-42**

| | Compd. | R | R'' | PqsR stimulation induced by 50 nM test compd. compared to 50 nM PQS (= 1.00) | Inhibition of PqsR stimulation induced by 50 nM PQS in the presence of 50 nM test compd. (full inhibition = 1.00 ) |
|---|---|---|---|---|---|
| Variation of side chain | **31** | *n*-$C_5H_{11}$ | H | 0.12 | 0.08 |
| | **32** | *n*-$C_6H_{13}$ | H | 0.54* | 0.04 |
| | **33** | *n*-$C_7H_{15}$ | H | 1.00* | - |
| | **34** | *n*-$C_8H_{17}$ | H | 0.91* | n.d.[a] |
| | **35** | *n*-$C_9H_{19}$ | H | 0.81* | n.d. |
| Introduction of substituents in the carbocyclic ring | **36** | *n*-$C_7H_{15}$ | 6-$OCH_3$ | 0.04 | 0.17 |
| | **37** | *n*-$C_7H_{15}$ | 7-$OCH_3$ | 1.06* | n.d. |
| | **38** | *n*-$C_7H_{15}$ | 8-F | 0.12 | -0.07 |
| | **39** | *n*-$C_7H_{15}$ | 6-F | 1.07* | n.d. |
| | **40** | *n*-$C_7H_{15}$ | 6-$CH_3$ | 0.35 | -0.04 |
| | **41** | *n*-$C_7H_{15}$ | 6-I | 0.26* | 0.03 |
| | **42** | *n*-$C_7H_{15}$ | 6,7-benzo | 0.08 | -0.07 |

β-Galactosidase reporter gene assay was performed in *E. coli* transformed with the plasmid pEAL08-2 encoding PqsR and the reporter gene *lacZ* controlled by the *pqsA* promoter. For the agonist test, the compounds were measured at 50 nM and 5 μM (data not shown); for the antagonist test, the compounds were measured at 50 nM and 5 μM (data not shown) in the presence of 50 nM PQS. Mean value of at least two independent experiments with n=4, standard deviation less than 25%. Significance: For the agonist test, induction compared to the basal value; for the antagonist test, decrease of the PQS-induced induction. * $p < 0.05$.

[a] n.d. not determined

### Table S2. Determination of Water Solubility

| Compd. | Water solubility [μM] |
|---|---|
| **23** | >300 |
| **25** | 200-300 |
| **27** | 5-15 |
| **19** | <5 |

Aqueous solutions (containing 5% DMSO) of the test compounds were prepared with final theoretical concentrations of 5, 15, 50, 100, 200 and 300 μM. The solution clarity was examined.

## Table S3. Determination of Antibacterial Activity in *E. coli tolC*

| Compd.[a] | Mass loaded on the paper disc [µg] | Diameter of inhibition [cm] |
|---|---|---|
| Chloramphenicol | 5 | 1.9 |
| | 10 | 2.0 |
| | 15 | 2.2 |
| | 20 | 2.3 |
| **2**[b] | 25 | 1.3 |
| **3** | 25 | 1.1 |
| **4** | 25 | 1.2 |
| **5** | 25 | 1.2 |
| **6** | 25 | 1.1 |
| **11** | 25 | 1.2 |

Antibacterial activity of compounds was determined in *E. coli tolC* applying a filter disc technique. Chloramphenicol was used as the positive control. Mean value of at least two independent experiments, standard deviation less than 25%.
[a] All other compounds did not exhibit antibacterial properties.
[b] Standard deviation 28%.

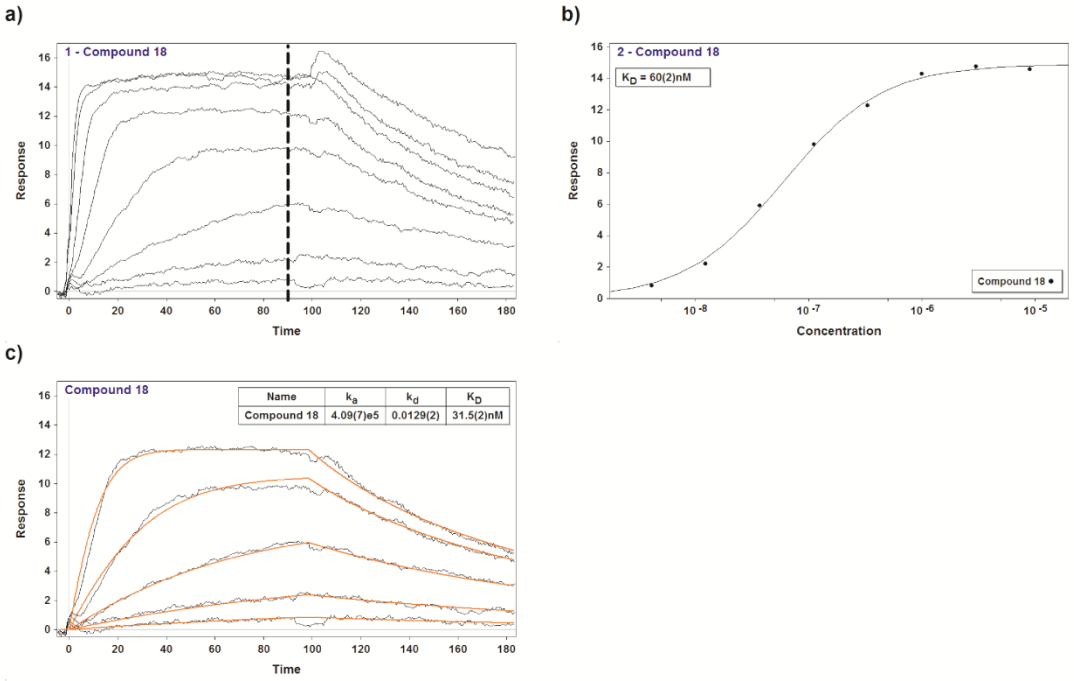


## Figure S1. Binding Affinity for Compound 18

a) Overlay of sensorgrams for compound **18** binding to $H_6$SUMO-PqsR$^{C87}$ measured at 12 ℃. The data read-out line is indicated by the dashed line. b) Fitting of compound **18** equilibrium response data from the $His_6$SUMO-PqsR$^{C87}$ surface to a steady state 1:1 model to calculate $K_d$ ((I) 54 nM, (II) 60 nM; mean 57 nM). c) Fiting of compound **18** kinetic data to a simple 1:1 interaction model including mass transport component (orange lines) to calculate $K_d$ ((I) 45 nM, (II) 32 nM; mean 38 nM).

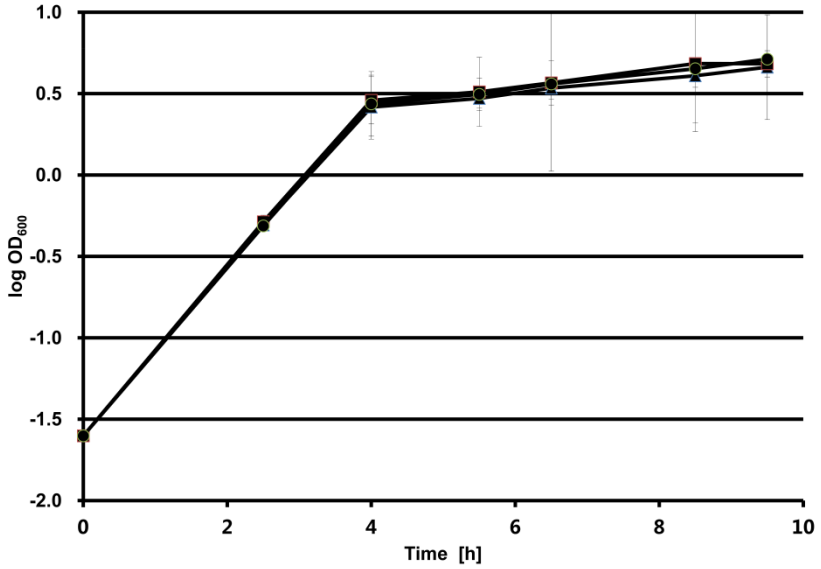


**Figure S2. Growth Curves of *P. aeruginosa* PA14**

Strains were grown in the absence (▲)/presence of 5 µM compound **18** (■) or **19** (●). Samples were taken at 0h, 2.5h, 4h, 5.5h, 6.5h, 8.5h and 9.5h to measure $OD_{600}$. Mean value of one experiment with n = 3, standard deviation less than 15%.

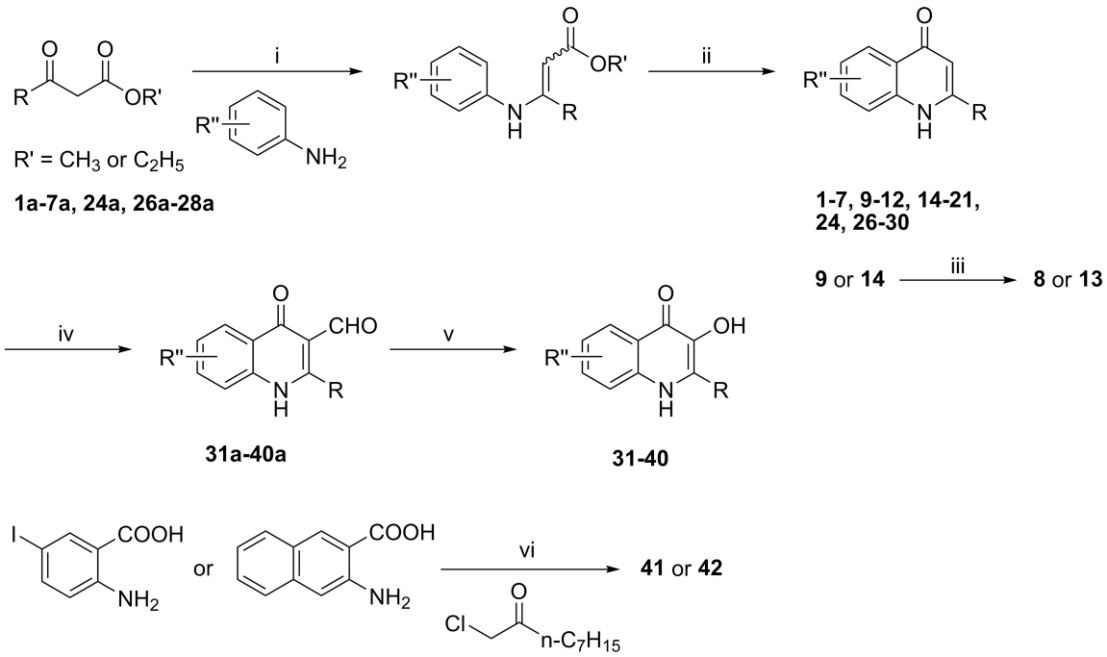


**Figure S3. Synthesis Route of HHQ and PQS Analogues**

Reagents and conditions: i) *p*-TsOH, *n*-hexane, reflux; (ii) $Ph_2O$, reflux; iii) $BF_3$• $SMe_2$, DCM, r.t., then MeOH; iv) hexamine, *p*-TsOH, AcOH, reflux, then HCl/water; v) $B(OH)_3$, conc. $H_2SO_4$, $H_2O_2$, THF, r.t.; vi) di-*iso*-propylethylamine, *N*-methylpyrrolidone, µW, 200 ℃, 30-60 min.

## Supplemental Experimental Procedures

### Syntheses of the Title Compounds 1-21, 24 and 26-42

### Procedure A1.

A solution of β-ketoester (9.24 mmol, 1 equiv), aniline (9.24 mmol, 1 equiv) and *p*-TsOH ·$H_2O$ (50 mg, 0.29 mmol, 3 mol %) in *n*-hexane (20 ml) was heated at reflux using a Dean-Stark separator for 5 h. After cooling the solution was concentrated *in vacuo* and the residue was added dropwise to

refluxing (260 °C) diphenyl ether (5 ml). Refluxing was continued for 30 min. After cooling to room temperature, $Et_2O$ (15 ml) and 2 M HCl (20 ml) were added and the mixture was left overnight at 5 °C. If a crystalline solid had formed, it was collected and washed with $Et_2O$. If no solid had formed, ammonia was added to basify the mixture. HHQ or its analogues was purified by crystallization from ethyl acetate or column chromatography on silica gel (Woschek et al., 2007).

**Procedure A2.**

A mixture of HHQ or its analogues (2.06 mmol, 1 equiv), hexamine (575 mg, 4.11 mmol, 2 equiv) and *p*-TsOH·$H_2O$ (400 mg, 2.32 mmol, 1.1 equiv) in glacial acetic acid (120 ml) was heated at reflux for 3 h under a nitrogen atmosphere. After cooling 5 M HCl (50 ml) was added and heating was continued at 105 °C for 1 h. The mixture was allowed to cool, diluted with water (200 ml), and extracted with $CH_2Cl_2$ (4 x 50 ml). The combined organic fractions were washed with brine, dried over $MgSO_4$, and concentrated under reduced pressure. The crude 3-formyl-2-alkylquinolone was purified by column chromatography on silica gel (*n*-hexane/ethyl acetate, 5/9-1/1) (Tanoue et al., 1989).

**Procedure A3.**

Boric acid (220 mg, 3.54 mmol, 5 equiv.) was suspended in THF (40 ml), followed by the addition of 30% $H_2O_2$ (in $H_2O$, 0.24 ml, 3 equiv) and conc. $H_2SO_4$ (1.0 ml). After stirring for 30 min, a solution of 3-formyl-2-alkylquinolone (0.70 mmol, 1 equiv.) in THF (20 ml) was added dropwise over 10 min. After additional stirring for 5 h, the mixture was filtered. The filtrate was neutralized by addition of a sat. $NaHCO_3$ solution (120 ml) and the aqueous layer was extracted with ethyl acetate (3 x 50 ml). After washing the combined organic fractions with brine and drying over $MgSO_4$ the organic solvent was removed *in vacuo*. PQS or its analogues was purified by column chromatography on silica gel ($CH_2Cl_2$/MeOH, 60/1) (Gross et al., 2010).

**Procedure B.**

Di-*iso*-propylethylamine (1.31 mmol, 1.2 equiv) and 1-chlorononan-2-one (1.09 mmol, 1 equiv) were added to a solution of the appropriate substituted anthranilic acid (1.09 mmol, 1 equiv) in anhydrous *N*-methylpyrrolidone (2.25 ml) contained in a 10 ml microwave vial. The solution was then heated under microwave irradiation to 200 °C for 30-60 min. The reaction mixture was allowed to cool to room temperature, added to an ice/water mixture and left to settle for 20 min. The precipitate thus formed was isolated by filtration, dried *in vacuo* overnight and the PQS analogues was purified by recrystallization from ethyl acetate (Hodgkinson et al., 2011).

**Procedure C.**

To a solution of methoxy-substituted HHQ (0.36 mmol, 1 equiv) in anhydrous $CH_2Cl_2$ (8 ml) was added $BF_3$·$SMe_2$ complex (10 mmol, 30 equiv) at 0 °C and the reaction mixture was stirred at room temperature overnight. The reaction was quenched with MeOH, evaporated, and the residue was

purified by column chromatography on silica gel ($CH_2Cl_2$/MeOH, 40/1~25/1) (Konieczny et al., 2005).

**2-Methylquinolin-4(1*H*)-one (1).** Compound **1** was obtained according to procedure A1 from aniline (357 mg, 3.84 mmol) and **1a** (500 mg, 3.84 mmol, commercial available) after crystallization as a brown solid (241 mg, 1.51 mmol, 39%), mp 234-235 °C. $^1$H-NMR (500 MHz, DMSO-$d_6$): δ = 2.50 (s, 3H), 6.06 (s, 1H), 7.42 (t, *J* = 8.0 Hz, 1H), 7.65 (d, *J* = 8.0 Hz, 1H), 7.76 (dt, *J* = 1.5 Hz, 8.0 Hz, 1H), 8.19 (dd, *J* = 1.0 Hz, 8.0 Hz, 1H), 11.69 (brs, 1H). $^{13}$C-NMR (125 MHz, DMSO-$d_6$): δ = 19.4, 108.3, 117.6, 122.6, 124.4, 124.7, 131.3, 140.0, 149.5, 176.6. LC/MS *m/z* 160.12 ($MH^+$), 99.9%.

**2-Pentylquinolin-4(1*H*)-one (2).** Compound **2** was obtained according to procedure A1 from aniline (405 mg, 4.36 mmol) and **2a** (811 mg, 4.36 mmol) after crystallization as a white solid (287 mg, 1.33 mmol, 30%), mp 175-178 °C. $^1$H-NMR (500 MHz, DMSO-$d_6$): δ = 0.87 (t, *J* = 7.0 Hz, 3H), 1.32-1.35 (m, 4H), 1.76 (quint, *J* = 7.5 Hz, 2H), 2.99 (t, *J* = 7.5 Hz, 2H), 7.04 (s, 1H), 7.68 (t, *J* = 7.5 Hz, 1H), 7.96 (t, *J* = 7.5 Hz, 1H), 8.12 (d, *J* = 8.5 Hz, 1H), 8.25 (d, *J* = 7.0 Hz, 1H), 14.77 (brs, 1H). $^{13}$C-NMR (125 MHz, DMSO-$d_6$): δ = 13.8, 21.7, 28.4, 30.6, 33.2, 105.2, 119.3, 119.8, 123.4, 126.6, 133.8 139.4, 159.8, 170.1. LC/MS: *m/z* 217.32 ($MH^+$), 99.9%.

**2-Hexylquinolin-4(1*H*)-one (3).** Compound **3** was obtained according to procedure A1 from aniline (785 mg, 8.44 mmol) and **3a** (1.69 g, 8.44 mmol) after crystallization as a grey solid (933 mg, 4.07 mmol, 48%), mp 142-143 °C. $^1$H-NMR (500 MHz, DMSO-$d_6$): δ = 0.82 (t, *J* = 7.0 Hz, 3H), 1.24-1.32 (m, 6H), 1.72 (quint, *J* = 7.5 Hz, 2H), 2.98 (t, *J* = 7.5 Hz, 2H), 7.07 (s, 1H), 7.68 (t, *J* = 8.0 Hz, 1H), 7.96 (t, *J* = 7.5 Hz, 1H), 8.13 (d, *J* = 8.5 Hz, 1H), 8.23 (d, *J* = 8.5 Hz, 1H), 14.91 (brs, 1H). $^{13}$C-NMR (125 MHz, DMSO-$d_6$): δ = 13.8, 21.9, 28.1, 28.7, 30.8, 33.3, 105.1, 119.4, 119.6, 123.4, 126.8, 133.9, 139.3, 160.1, 169.8. LC/MS: *m/z* 230.27 ($MH^+$), 99.9%.

**2-Heptylquinolin-4(1*H*)-one (4).** Compound **4** was obtained according to procedure A1 from aniline (859 mg, 9.24 mmol) and **4a** (1.98 g, 9.24 mmol) after crystallization as a white solid (1320 mg, 5.43 mmol, 59%), mp 149-151 °C. $^1$H-NMR (500 MHz, MeOH-$d_4$): δ = 0.91 (t, *J* = 7.0 Hz, 3H), 1.32-1.47 (m, 8H), 1.87 (quint, *J* = 7.5 Hz, 2H), 3.069 (t, *J* = 7.5 Hz, 2H), 7.04 (s, 1H), 7.78 (dt, *J* = 1.0 Hz, 8.5 Hz, 1H), 8.00 (d, *J*= 8.0 Hz, 1H), 8.04 (dt, *J* = 1.0 Hz, 8.5 Hz, 1H), 8.40 (d, *J* = 7.5 Hz, 1H). $^{13}$C-NMR (125 MHz, MeOH-$d_4$): δ = 14.4, 23.6, 30.0, 30.2, 30.4, 32.8, 35.4, 106.0, 120.3, 120.9 125.0, 128.7, 135.9, 141.0, 162.7, 171.6. LC/MS: *m/z* 244.276 ($MH^+$), 95.0%.

**2-Octylquinolin-4(1*H*)-one (5).** Compound **5** was obtained according to procedure A1 from aniline (711 mg, 7.65 mmol) and **5a** (1.744 g, 7.65 mmol) after crystallization as a white solid (537 mg, 2.09 mmol, 27%), mp 132-135 °C. $^1$H-NMR (500 MHz, DMSO-$d_6$): δ = 0.80 (t, *J* = 7.0 Hz, 3H), 1.19-1.32 (m, 10H), 1.71 (quint, *J* = 7.5 Hz, 2H), 2.97 (t, *J* = 7.5 Hz, 2H), 7.04 (s, 1H), 7.66 (t, *J* =

7.5 Hz, 1H), 7.94 (t, *J* = 7.0 Hz, 1H), 8.11 (d, *J* = 7.5 Hz, 1H), 8.22 (d, *J* = 7.5 Hz, 1H), 14.84 (brs, 1H). $^{13}$C-NMR (125 MHz, DMSO-$d_6$): δ = 14.4, 22.5, 28.9, 28.9, 29.0, 29.2, 31.6, 33.7, 105.6, 119.8, 120.1, 123.9, 127.2, 134,3, 139.8, 160.5, 170.4. LC/MS: *m/z* 258.22 ($MH^+$), 99.9%.

**2-Nonylquinolin-4(1*H*)-one (6).** Compound **6** was obtained according to procedure A1 from aniline (960 mg, 10.33 mmol) and **6a** (2.50 g, 10.33 mmol) after crystallization as a white solid (1.61 g, 5.96 mmol, 57%), mp 101-103 ℃. $^1$H-NMR (500 MHz, DMSO-$d_6$): δ = 0.83 (t, *J* = 7.0 Hz, 3H), 1.15-1.37 (m, 12H), 1.74 (quint, *J* = 7.5 Hz, 2H), 2.99 (t, *J* = 7.5 Hz, 2H), 7.04 (s, 1H), 7.69 (dt, *J* =1.0 Hz, 7.5 Hz, 1H), 7.97 (dt, *J* = 1.0 Hz, 7.5 Hz, 1H), 8.12 (d, *J* = 8.5 Hz, 1H), 8.25 (dd, *J* =1.0 Hz, 8.5 Hz, 1H), 14.76 (brs, 1H). $^{13}$C-NMR (125 MHz, DMSO-$d_6$): δ = 13.0, 22.0, 28.4, 28.59, 28.62, 28.7, 28.8, 31.2, 33.3, 105.2, 119.3, 119.8, 123.5, 126.7, 133.8, 139.4, 159.9, 170.1. LC/MS: *m/z* 272.27 ($MH^+$), 99.9%.

**2-(3-Phenylpropyl)quinolin-4(1*H*)-one (7).** Compound **7** was obtained according to procedure A1 from aniline (79 mg, 0.85 mmol) and **7a** (200 mg, 0.85 mol). After cooling the reaction mixture was extracted with ethyl acetate. The combined organic phases were dried with $MgSO_4$, and evaporated *in vacuo*. The residue was purified by chromatography on silica gel ($CH_2Cl_2$/MeOH, 25/1~30/1) yielding compound **7** (18 mg, 0.07 mmol, 8%) as a yellow solid, mp 168-170 ℃. $^1$H-NMR (500 MHz, MeOH-$d_4$): δ = 2.04 (quint, *J* = 7.5 Hz, 2H), 2.69 (dt, *J* = 3.0 Hz, 7.5 Hz, 4H), 6.19 (s ,1H), 7.12 (t, *J* = 7.5 Hz, 1H), 7.17 (d, *J* = 7.0 Hz, 2H), 7.23 (dt, *J* = 1.5 Hz, 7.5 Hz, 2H), 7.35 (dt, *J* = 1.5 Hz, 7.5 Hz, 1H), 7.53 (d, *J* = 7.5 Hz, 1H), 7.64 (dt, *J* = 1.5 Hz, 7.5 Hz, 1H), 8.17 (dd, *J* = 0.5 Hz, 8.0 Hz, 1H). $^{13}$C-NMR (125 MHz, MeOH-$d_4$): δ = 30.3, 33.0, 34.8, 107.5, 117.6, 123.6, 124.1, 124.5, 125.6, 128.0, 131.9, 140.2, 141.1, 155.2, 179.2. LC/MS: *m/z* 264.16 ($MH^+$), 97.3%.

**2-Heptyl-7-hydroxyquinolin-4(1*H*)-one (8).** Compound **8** was obtained according to procedure C from **9** (100 mg, 0.37 mol) after chromatography on silica gel as a white solid (42 mg, 0.17 mmol, 46%), mp 138-141 ℃. $^1$H-NMR (500 MHz, DMSO-$d_6$): δ = 0.86 (t, *J* = 6.5 Hz, 3H), 1.26-1.31 (m, 8H), 1.64 (quint, *J* = 6.5 Hz, 2H), 2.53 (t, 3H), 5.76 (s, 1H), 6.72 (dd, *J* = 2.0 Hz, 9.0 Hz, 1H), 6.81 (s, 1H), 7.85 (d, *J* = 8.5 Hz, 1H), 10.18 (s, 1H), 11.13 (s, 1H). $^{13}$C-NMR (125 MHz, DMSO-$d_6$): δ = 13.9, 22.0, 28.2, 28.3, 28.4, 31.1, 33.1, 100.8, 106.8, 113.2, 118.0, 126.6, 141.9, 152.7, 160.1, 176.5. LC/MS: *m/z* 260.20 ($MH^+$), 99.9%.

**2-Heptyl-7-methoxyquinolin-4(1*H*)-one (9).** Compound **9** was obtained according to procedure A1 from 3-methoxyaniline (260 mg, 2.11 mmol) and **4a** (450 mg, 2.10 mmol) after chromatography on silica gel ($CH_2Cl_2$/MeOH, 20/1) as a yellow solid (171 mg, 0.63 mmol, 30%), mp 152-154 ℃. $^1$H-NMR (500 MHz, DMSO-$d_6$): δ = 0.91 (t, *J* = 7.0 Hz, 3H), 1.29-1.37 (m, 8H), 1.68-1.74 (quint, *J* = 7.5 Hz, 2H), 2.59 (t, *J* = 7.5 Hz, 2H), 3.90 (s, 3H), 5.87 (s, 1H), 6.92 (dd, *J* = 2.5 Hz, 9.0 Hz, 1H), 6.98 (d, *J* = 7.5 Hz, 1H), 7.98 (d, *J* = 9.0 Hz, 1H), 11.34 (brs, 1H). $^{13}$C-NMR (125 MHz, DMSO-$d_6$):

δ = 13.8, 22.0, 28.2, 28.3, 28.4, 31.1, 33.1, 55.2, 98.8, 107.3, 112.5, 118.9, 126.5, 141.8, 152.9, 161.6, 176.4. LC/MS: *m/z* 274.27 ($MH^+$), 99.9%.

**2-Heptyl-8-methoxyquinolin-4(1*H*)-one (10).** Compound **10** was obtained according to procedure A1 from 2-methoxyaniline (516 mg, 4.20 mmol) and **4a** (900 mg, 4.20 mmol) after crystallization as a white solid (435 mg, 1.59 mmol, 38%), mp 105-108 °C. $^1$H-NMR (500 MHz, DMSO-$d_6$): δ = 0.86 (t, *J* = 7.0 Hz, 3H), 1.25-1.31 (m, 8H), 1.62 (quint, *J* = 7.5 Hz, 2H), 2.66 (t, *J* = 7.5 Hz, 2H), 3.98 (s, 3H), 5.91 (s, 1H), 7.19-7.21 (m, 2H), 7.60 (t, *J* = 8.0 Hz, 1H), 10.86 (brs, 1H). $^{13}$C-NMR (125 MHz, DMSO-$d_6$): δ = 13.9, 22.0, 28.4, 28.5, 29.0, 31.2, 32.7, 56.1, 108.1, 111.0, 116.0, 117.1, 122.4, 125.6, 130.8, 148.3, 153.7, 176.,5. LC/MS: *m/z* 274.26 ($MH^+$), 96.3%.

**8-Ethyl-2-heptylquinolin-4(1*H*)-one (11).** Compound **11** was obtained according to procedure A1 from 2-ethylaniline (339 mg, 2.80 mmol) and **4a** (600 mg, 2.80 mmol) after crystallization as a white solid (101 mg, 0.37 mmol, 13%), mp 103-104 °C. $^1$H-NMR (500 MHz, DMSO-$d_6$): δ = 0.85 (t, *J* = 7.0 Hz, 3H), 1.21-1.32 (m, 11H), 1.65 (quint, *J* = 7.5 Hz, 2H), 2.70 (t, *J* = 7.5 Hz, 2H), 2.95 (q, *J* = 7.5 Hz, 2H), 5.94 (s, 1H), 7.22 (t, *J* = 7.5 Hz, 1H), 7.46 (d, *J* = 7.0 Hz, 1H), 7.93 (d, *J* = 9.5 Hz, 1H), 10.27 (brs, 1H). $^{13}$C-NMR (125 MHz, DMSO-$d_6$): δ = 13.9, 14.2, 22.0, 23.1, 28.4, 28.5, 28.9, 31.2, 32.9, 107.7, 122.6, 122.7, 125.0, 130.6, 131.8, 137.9, 154.2, 177.1. LC/MS: *m/z* 272.41 ($MH^+$), 99.9%.

**8-Fluoro-2-heptylquinolin-4(1*H*)-one (12).** Compound **12** was obtained according to procedure A1 from 2-fluoroaniline (520 mg, 4.67 mmol) and **4a** (1.00 g, 4.67 mmol) after crystallization as a yellow solid (371 mg, 1.42 mmol, 30%), mp 151-154 °C. $^1$H-NMR (500 MHz, DMSO-$d_6$): δ = 0.85 (t, *J* = 7.0 Hz, 3H), 1.24-1.31 (m, 8H), 1.64 (quint, *J* = 7.0 Hz, 2H), 2.64 (t, *J* = 7.0 Hz, 2H), 5.98 (s, 1H), 7.25 (dt, *J* = 4.5 Hz, 8.0 Hz, 1H), 7.52 (m, 1H), 7.85 (dd, *J* = 1.0 Hz, 8.0 Hz, 1H), 11.42 (brs, 1H). $^{13}$C-NMR (125 MHz, DMSO-$d_6$): δ = 13.8, 22.0, 28.3, 28.5, 28.7, 31.1, 32.9, 108.3, 116.1 (d, $J_{CF}$ = 16.8 Hz), 120.4, 122.3 (d, $J_{CF}$ = 6.9 Hz), 126.7, 129.5, 151.5 (d, $J_{CF}$ = 249.6 Hz), 154,5, 175.8. LC/MS: *m/z* 262.21 ($MH^+$), 97.8%.

**2-Heptyl-6-hydroxyquinolin-4(1*H*)-one (13).** Compound **13** was obtained according to procedure C from **14** (100 mg, 0.37 mol) after chromatography on silica gel as a yellow solid (45 mg, 0.17 mmol, 46%), mp 215-218 °C. $^1$H-NMR (500 MHz, DMSO-$d_6$): δ = 0.85 (t, *J* = 7.0 Hz, 3H), 1.24-1.30 (m, 8H), 1.64 (quint, *J* = 7.0 Hz, 2H), 2.53 (t, *J* = 7.5 Hz, 2H), 5.79 (s, 1H), 7.09 (dd, *J* = 3.0 Hz, 9.0 Hz, 1H), 7.351 (d, *J* = 3.5 Hz, 1H), 7.39 (d, *J* = 9.0 Hz, 1H), 9.54 (brs, 1H), 11.31 (brs, 1H). $^{13}$C-NMR (125 MHz, DMSO-$d_6$): δ =13.9, 22.0, 28.3, 28.4, 31.1, 33.1, 106.0, 107.3, 119.3, 121.4, 126.0, 133.6, 152.1, 153.2, 176.2. LC/MS: *m/z* 260.23 ($MH^+$), 99.9%.

**2-Heptyl-6-methoxyquinolin-4(1*H*)-one (14).** Compound **14** was obtained according to procedure A1 from 4-methoxyaniline (517 mg, 4.20 mmol) and **4a** (900 mg, 4.20 mmol) after crystallization ($Et_2O$/MeOH) as a yellow solid (455 mg, 1.67 mmol, 40%), mp 140-141 °C. $^1$H-NMR (500 MHz,

DMSO-$d_6$): δ = 0.85 (t, *J* = 7.0 Hz, 3H), 1.24-1.32 (m, 8H), 1.70 (quint, *J* = 7.0 Hz, 2H), 2.77 (t, *J* = 8.0 Hz, 2H), 3.87 (s, 3H), 6.46 (s, 1H), 7.45 (dd, *J* = 2.5 Hz, 9.0 Hz, 1H), 7.50 (d, *J* = 3.0 Hz, 1H), 7.77 (d, *J* = 9.0 Hz, 1H), 13.10 (brs, 1H). $^{13}$C-NMR (125 MHz, DMSO-$d_6$): δ = 13.9, 22.0, 28.3, 28.4, 28.6, 31.1, 33.2, 55.6, 102.9, 105.7, 120.4, 123.1, 123.7, 134.7, 156.4, 170.8. LC/MS: *m/z* 274.27 ($MH^+$), 97.5%.

**2-Heptyl-6-methylquinolin-4(1*H*)-one (15).** Compound **15** was obtained according to procedure A1 from *p*-toluidine (400 mg, 3.74 mmol) and **4a** (800 mg, 3.74 mmol) after chromatography on silica gel ($CH_2Cl_2$/MeOH, 30/1) as a yellow solid (194 mg, 0.74 mmol, 20%), mp 179-182 ℃. $^1$H-NMR (500 MHz, DMSO-$d_6$): δ = 0.96 (t, *J* = 7.0 Hz, 3H), 1.35-1.42 (m, 8H), 1.77 (quint, *J* = 7.0 Hz, 2H), 2.50 (s, 3H), 2.68 (t, *J* = 7.5 Hz, 2H), 6.00 (s, 1H), 7.55 (d, *J* = 1.0 Hz, 2H), 7.94 (s, 1H), 11.53 (brs, 1H). $^{13}$C-NMR (125 MHz, DMSO-$d_6$): δ = 13.8, 20.6, 22.0, 28.3, 28.4, 31.1, 33.1, 107.3, 117.7, 124.0, 124.5, 131.8, 132.7, 138.1, 153.1, 176.7. LC/MS: *m/z* 258.27 ($MH^+$), 99.9%.

**6-Fluoro-2-heptylquinolin-4(1*H*)-one (16).** Compound **16** was obtained according to procedure A1 from 4-fluoroaniline (233 mg, 2.10 mmol) and **4a** (450 mg, 2.10 mmol) after chromatography on silica gel ($CH_2Cl_2$/MeOH, 30/1~40/1) as a white solid (208 mg, 0.80 mmol, 38%), mp 175-177 ℃. $^1$H-NMR (500 MHz, DMSO-$d_6$): δ = 0.85 (t, *J* = 7.0 Hz, 3H), 1.25-1.32 (m, 8H), 1.67 (quint, *J* = 7.5 Hz, 2H), 2.59 (t, *J* = 7.5 Hz, 2H), 5.94 (s, 1H), 7.52 (dt, *J* = 3.0 Hz, 8.0 Hz, 1H), 7.60 (dd, *J* = 4.5 Hz, 9.0 Hz, 1H), 7.68 (dd, *J* = 3.0 Hz, 9.5 Hz, 1H), 11.62 (brs, 1H). $^{13}$C-NMR (125 MHz, DMSO-$d_6$): δ = 13.8, 21.9, 28.3, 18.4, 31.0, 33.2, 106.8, 108.7(d, $J_{CF}$ = 22.2 Hz), 120.1 (d, $J_{CF}$ = 25.6 Hz), 120.5 (d, $J_{CF}$ = 8.2 Hz), 125.6 (d, $J_{CF}$ = 6.3 Hz), 136.8, 153.7, 158.0 (d, $J_{CF}$ = 240.8 Hz), 175.9. LC/MS: *m/z* 262.23 ($MH^+$), 99.9%.

**6-Chloro-2-heptylquinolin-4(1*H*)-one (17).** Compound **17** was obtained according to procedure A1 from 4-chloroaniline (474 mg, 3.73 mmol) and **4a** (800 mg, 3.74 mmol) after chromatography on silica gel ($CH_2Cl_2$/MeOH, 110/1) as a yellow solid (70 mg, 0.25 mmol, 7%), mp 220-223 ℃. $^1$H-NMR (500 MHz, DMSO-$d_6$): δ = 0.84 (t, *J* = 7.0 Hz, 3H), 1.22-1.31 (m, 8H), 1.65 (quint, *J* = 7.0 Hz, 2H), 2.58 (t, *J*= 7.5 Hz, 2H), 5.96 (s, 1H), 7.56 (d, *J* = 9.0 Hz, 1H), 7.64 (dd, *J* = 2.5 Hz, 9.0 Hz, 1H), 7.96 (d, *J* = 2.5 Hz, 1H) 11.66 (brs, 1H). $^{13}$C-NMR (125 MHz, DMSO-$d_6$): δ = 13.8, 21.9, 28.2, 28.3, 28.4, 31.1, 33.2, 107.8, 120.3, 123.6, 125.5, 127.3, 131.5, 138.7, 154.1, 175.5. LC/MS: *m/z* 278.28 ($MH^+$), 96.4%.

**2-Heptyl-8-methoxy-6-(trifluoromethyl)quinolin-4(1*H*)-one (21).** Compound **21** was obtained according to procedure A1 from 2-methoxy-4-(trifluoromethyl)aniline (535 mg, 2.80 mmol) and **4a** (600 mg, 2.80 mmol) after chromatography on silica gel ($CH_2Cl_2$/MeOH, 120/1~90/1) as a yellow solid (40 mg, 0.11 mmol, 4%), mp 168 ℃. $^1$H-NMR (500 MHz, DMSO-$d_6$): δ = 1.66 (t, *J* = 7.0 Hz, 3H), 2.03-2.12 (m, 8H), 2.43 (quint, *J* = 7.5 Hz, 2H), 3.50 (t, *J* = 7.5 Hz, 2H), 4.88(s, 3H), 6.86 (s, 1H), 8.22 (d, *J* = 2.0 Hz, 1H), 8.71 (s, 1H), 12.07 (brs, 1H). $^{13}$C-NMR (125 MHz, DMSO-$d_6$): δ =

16.6, 24.7, 31.1, 31.2, 31.6, 33.9, 35.4, 59.5, 109.3, 112.1, 116.2, 116.3, 116.3, 116.3, 125.5, 125.8, 125.8, 127.3, 128.0, 136.0, 152.0, 157.8, 178.6. LC/MS: *m/z* 342.10 ($MH^+$), 99.9%.

**2-Ethyl-6-(trifluoromethyl)quinolin-4(1*H*)-one (24).** Compound **24** was obtained according to procedure A1 from 4-(trifluoromethyl)aniline (1.61 g, 10.0 mmol) and **24a** (1.30 g, 10.0 mmol) after crystallization as a white solid (0.40 g, 1.66 mmol, 16%), mp 293-296 °C. $^1$H-NMR (500 MHz, DMSO-$d_6$): δ = 1.26 (t, *J* = 7.6 Hz, 3H), 2.65 (q, *J* = 7.6 Hz, 2H), 6.05 (s, 1H), 7.71 (d, *J* = 8.9 Hz, 1H), 7.91 (dd, *J* = 8.9 Hz, 2.1 Hz, 1H), 8.30 (s, 1H), 11.81 (brs, 1H). $^{13}$C-NMR (125 MHz, DMSO-$d_6$): δ = 12.7, 26.4, 107.8, 119.4, 122.4 (q, $J_{CF}$ = 4.4 Hz), 123.0 (q, $J_{CF}$ = 32.0 Hz), 123.8, 124.3 (q, $J_{CF}$ = 272.0 Hz), 127.4 (q, $J_{CF}$ = 3.5 Hz), 142.3, 156.0, 176.3. LC/MS: *m/z* 242.22 ($MH^+$), 99.4%.

**2-Butyl-6-(trifluoromethyl)quinolin-4(1*H*)-one (26).** Compound **26** was obtained according to procedure A1 from 4-(trifluoromethyl)aniline (1.61 g, 10.0 mmol) and **26a** (1.58 g, 10.0 mmol) after crystallization as a white solid (1.87 g, 6.95 mmol, 69%), mp 225-226 °C. $^1$H-NMR (500 MHz, DMSO-$d_6$): δ = 0.88 (t, *J* = 7.4 Hz, 3H), 1.32 (sextet, *J* = 7.5 Hz, 2H), 1.63 (quint, *J* = 7.6 Hz, 2H), 2.59 (t, *J* = 7.7 Hz, 2H), 6.02 (s, 1H), 7.70 (d, *J* = 8.7 Hz, 1H), 7.87 (dd, *J* = 8.9 Hz, 2.1 Hz, 1H), 8.30 (s, 1H), 11.80 (brs, 1H). $^{13}$C-NMR (125 MHz, DMSO-$d_6$): δ = 13.5, 21.6, 30.2, 32.9, 108.7, 119.5, 122.4 (q, $J_{CF}$ = 4.3 Hz), 123.0 (q, $J_{CF}$ = 32.0 Hz), 123.8, 124.2 (q, $J_{CF}$ = 272.0 Hz), 127.4 (q, $J_{CF}$ = 3.5 Hz), 142.2, 154.7, 176.2. LC/MS: *m/z* 270.28 ($MH^+$), 99.7%.

**2-Pentyl-6-(trifluoromethyl)quinolin-4(1*H*)-one (27).** Compound **27** was obtained according to procedure A1 from 4-(trifluoromethyl)aniline (1.61 g, 10.0 mmol) and methyl **27a** (1.72 g, 10.0 mmol) after crystallization as a white solid (1.23 g, 4.34 mmol 43%), mp 197-198 °C. $^1$H-NMR (500 MHz, DMSO-$d_6$): δ = 0.86 (t, *J* = 7.1 Hz, 3H), 1.28-1.33 (m, 4H), 1.67 (m, 2H), 2.59 (t, *J* = 7.7 Hz, 2H), 6.03 (s, 1H), 7.71 (d, *J* = 8.9 Hz, 1H), 7.89 (dd, *J* = 9.0 Hz, 2.1 Hz, 1H), 8.30 (d, *J* = 1.6 Hz, 1H), 11.80 (brs, 1H). $^{13}$C-NMR (125 MHz, DMSO-$d_6$): δ = 13.7, 21.7, 27.8, 30.6, 33.2, 108.7, 119.5, 122.4 (q, $J_{CF}$ = 4.3 Hz), 123.0 (q, $J_{CF}$ = 32.0 Hz), 123.8, 124.3 (q, $J_{CF}$ = 272.0 Hz), 127.4 (q, $J_{CF}$ = 3.4 Hz), 142.3, 154.8, 176.2. LC/MS: *m/z* 284.27 ($MH^+$), 97.2%.

**2-Hexyl-6-(trifluoromethyl)quinolin-4(1*H*)-one (28).** Compound **28** was obtained according to procedure A1 from 4-(trifluoromethyl)aniline (1.61 g, 10.0 mmol) and **28a** (1.86 g, 10.0 mmol) after crystallization as a white solid (1.55 g, 5.22 mmol, 52%), mp 185 °C. $^1$H-NMR (500 MHz, DMSO-$d_6$): δ = 0.83 (t, *J* = 7.1 Hz, 3H), 1.23-1.35 (m, 6H), 1.66 (quint, *J* = 7.5 Hz, 2H), 2.59 (t, *J* = 7.7 Hz, 2H), 6.03 (d, J = 1.2 Hz, 1H), 7.71 (d, *J* = 8.5 Hz, 1H), 7.89 (dd, *J* = 8.9 Hz, 2.2 Hz, 1H), 8.30 (d, *J* = 1.7 Hz, 1H), 11.80 (brs, 1H). $^{13}$C-NMR (125 MHz, DMSO-$d_6$): δ = 13.8, 21.9, 28.1, 30.9, 33.2, 108.7, 119.5, 122.4 (q, $J_{CF}$ = 4.6 Hz), 123.0 (q, $J_{CF}$ = 32.0 Hz), 123.8, 124.3 (q, $J_{CF}$ = 272.0 Hz), 127.4 (q, $J_{CF}$ = 3.6 Hz), 142.3, 154.8, 176.2. LC/MS: *m/z* 298.32 ($MH^+$), 99.5%.

**2-Heptyl-7-(trifluoromethyl)quinolin-4(1*H*)-one (29).** Compound **29** was obtained according to

procedure A1 from 3-(trifluoromethyl)aniline (415 mg, 2.58 mmol) and **4a** (600 mg, 2.80 mmol) after crystallization as a white solid (133 mg, 0.43 mmol, 16%), mp 218-220 °C. $^{1}$H-NMR (500 MHz, DMSO-$d_6$): δ = 0.84 (t, *J* = 7.0 Hz, 3H), 1.23-1.35 (m, 8H), 1.73 (quint, *J* = 7.5 Hz, 2H), 2.85 (t, *J* = 7.5 Hz, 2H), 6.65 (s, 1H), 7.79 (d, *J* = 8.5 Hz, 1H), 8.27(s, 1H), 8.36 (d, *J* = 8.5 Hz, 1H) $^{13}$C-NMR (125 MHz, DMSO-$d_6$): δ = 13.9, 21.9, 28.3, 28.4, 31.0, 33.4, 107.6, 116.6 (q, $J_{CF}$ = 3.6 Hz), 120.5(q, $J_{CF}$ = 3.6 Hz), 123.5(q, $J_{CF}$ = 272.0 Hz), 124.0, 126.2, 132.1 (q, $J_{CF}$ = 32.0 Hz), 139.2, 158.8, 172.6. LC/MS: *m/z* 311.98 ($MH^+$), 99.9%.

**2-Heptyl-8-(trifluoromethyl)quinolin-4(1*H*)-one (30).** Compound **30** was obtained according to procedure A1 from 2-(trifluoromethyl)aniline (415 mg, 2.58 mmol) and **4a** (600 mg, 2.80 mmol) after chromatography on silica gel ($CH_2Cl_2$/MeOH, 100/1) as a yellow solid (191 mg, 0.61 mmol, 24%), mp 85-86 °C. $^{1}$H-NMR (500 MHz, DMSO-$d_6$): δ = 0.83 (t, *J* = 7.0 Hz, 3H), 1.22-1.33 (m, 8H), 1.87 (s, 2H), 2.78 (t, *J* = 7.5 Hz, 2H), 6.67 (brs, 1H), 7.49 (t, *J* = 7.5 Hz, 1H), 8.03 (d, *J* = 7.5 Hz, 1H), 8.37 (*J* = 8.0 Hz, 1H). $^{13}$C-NMR (125 MHz, DMSO-$d_6$): δ = 13.8, 21.9, 28.4, 28.5, 31.2, 122.6 (not all signals of carbons were observed). LC/MS: *m/z* 311.99 ($MH^+$), 99.3%.

**3-Hydroxy-2-pentylquinolin-4(1*H*)-one (31).** Compound **31** was obtained according to procedure A3 from **31a** (95 mg, 0.39 mmol) after chromatography on silica gel as a white solid (25 mg, 0.11 mmol, 28%), mp 259-263 °C. $^{1}$H-NMR (500 MHz, DMSO-$d_6$): δ = 0.93 (t, *J* = 7.0 Hz, 3H), 1.37-1.40 (m, 4H), 1.73 (quint, *J* = 6.5 Hz, 2H), 2.78 (t, *J* = 7.5 Hz, 2H), 7.27 (quint, *J* = 9.0 Hz, 1H), 7.58 (d, *J* = 3.5 Hz, 2H), 8.14 (d, *J* = 7.5 Hz, 1H), 11.46 (brs, 1H). $^{13}$C-NMR (125 MHz, DMSO-$d_6$): δ = 13.8, 21.8, 27.4, 28.0, 30.9, 117.7, 121.4, 122.1, 124.4, 129.9, 135.3, 137.3, 137.7, 168.8. LC/MS: *m/z* 232.24 ($MH^+$), 96.4%.

**2-Hexyl-3-hydroxyquinolin-4(1*H*)-one (32).** Compound **32** was obtained according to procedure A3 from **32a** (288 mg, 1.12 mmol) after chromatography on silica gel as a light brown solid (86 mg, 0.35 mmol, 31%), mp 203-205 °C. $^{1}$H-NMR (500 MHz, DMSO-$d_6$): δ = 0.81 (t, *J* = 7.0 Hz, 3H), 1.21-1.32 (m, 6H), 1.62 (quint, *J* = 7.5 Hz, 2H), 2.69 (t, *J* = 7.5 Hz, 2H), 7.17 (quint, *J* = 4.0 Hz, 1H), 7.49 (d, *J* = 4.0 Hz, 2H), 8.05 (d, *J* = 8.0 Hz, 1H), 11.36 (brs, 1H). $^{13}$C-NMR (125 MHz, DMSO-$d_6$): δ = 14.4, 22.5, 28.2, 28.6, 28.9, 31.5, 118.2, 121.9, 122.6, 124.9, 130.4, 135.9, 137.8, 138.3, 169.3. LC/MS: *m/z* 246.23 ($MH^+$), 98.7%.

**2-Heptyl-3-hydroxyquinolin-4(1*H*)-one (33).** Compound **33** was obtained according to procedure A3 from **33a** (190 mg, 0.70 mmol) after chromatography on silica gel as a white solid (73 mg, 0.28 mmol, 40%), mp 195-198 °C. $^{1}$H-NMR (500 MHz, DMSO-$d_6$): δ = 0.84 (t, *J* = 7.0 Hz, 3H), 1.22-1.34 (m, 8H), 1.66 (quint, *J* = 7.0 Hz, 2H), 2.72 (t, *J* = 7.5 Hz, 2H), 7.21 (quint, *J* = 4.0 Hz, 1H), 7.52 (d, *J* = 3.5 Hz, 2H), 8.08 (d, *J* = 8.0 Hz, 1H), 11.41 (brs, 1H). $^{13}$C-NMR (125 MHz, DMSO-$d_6$): δ = 13.9, 22.0, 27.8, 28.1, 28.4, 28.7, 31.2, 117.7, 121.5, 122.1, 124.4, 129.9, 135.5, 137.3, 137.8, 168.8. LC/MS: *m/z* 260.25 ($MH^+$), 97.1%.

**3-Hydroxy-2-octylquinolin-4(1*H*)-one (34).** Compound **34** was obtained according to procedure A3 from **34a** (243 mg, 0.85 mmol) after chromatography on silica gel as a light brown solid (116 mg, 0.42 mmol, 49%), mp 192-194 °C. $^{1}$H-NMR (500 MHz, DMSO-$d_6$): δ = 0.84 (t, *J* = 7.0 Hz, 3H), 1.24-1.34 (m, 10H), 1.66 (quint, *J* = 7.5 Hz, 2H), 2.72 (t, *J* = 7.5 Hz, 2H), 7.21 (quint, *J* = 4.0 Hz, 1H), 7.52 (d, *J* = 4.0 Hz, 2H), 8.08 (d, *J* = 8.0 Hz, 1H), 11.38 (brs, 1H). $^{13}$C-NMR (125 MHz, DMSO-$d_6$): δ = 13.9, 22.0, 27.7, 28.0, 28.6, 28.7, 28.8, 31.2, 117.7, 121.4, 122.1, 124.4, 129.9, 135.4, 137.3, 137.8, 168.8. LC/MS: *m/z* 274.29 ($MH^+$), 99.9%.

**3-Hydroxy-2-nonylquinolin-4(1*H*)-one (35).** Compound **35** was obtained according to procedure A3 from **35a** (240 mg, 0.80 mmol) after chromatography on silica gel as a white solid (113 mg, 0.42 mmol, 39%), mp 167-169 °C. $^{1}$H-NMR (500 MHz, DMSO-$d_6$): δ = 0.84 (t, *J* = 7.0 Hz, 3H), 1.18-1.35 (m, 12H), 1.66 (quint, *J* = 7.5 Hz, 2H), 2.72 (t, *J* = 7.5 Hz, 2H), 7.21 (quint, *J* = 4.0 Hz, 1H), 7.52 (d, *J* = 3.5 Hz, 2H), 8.08 (d, *J* = 8.5 Hz, 1H), 11.38 (brs, 1H). $^{13}$C-NMR (125 MHz, DMSO-$d_6$): δ = 13.9, 22.0, 27.7, 28.1, 28.6, 28.8, 28.9, 31.2, 117.7, 121.4, 122.1, 124.4, 129.9, 135.4, 137.3, 137.8, 168.8. LC/MS *m/z* 288.37 ($MH^+$), 99.9%.

**2-Heptyl-3-hydroxy-6-methoxyquinolin-4(1*H*)-one (36).** Compound **36** was obtained according to procedure A3 from **36a** (210 mg, 0.70 mmol) after chromatography on silica gel as a brown solid (79 mg, 0.27 mmol, 38%), mp 211-214 °C. $^{1}$H-NMR (500 MHz, DMSO-$d_6$): δ = 0.84 (t, *J* = 7.0 Hz, 3H), 1.23-1.31 (m, 8H), 1.65 (quint, 2H), 2.71 (t, 2H), 3.82 (s, 3H), 7.18 (dd, *J* = 2.0 Hz, 6.0 Hz, 1H), 7.4-7.48 (br, 2H), 11.40 (brs, 1H). $^{13}$C-NMR (125 MHz, DMSO-$d_6$): δ = 13.8, 22.0, 27.8, 28.1, 28.4, 28.7, 31.1, 55.2, 102.8, 119.5, 121.2, 122.8, 132.3, 134.8, 137.3, 154.3, 167.8. LC/MS: *m/z* 290.24 ($MH^+$), 99.9%.

**2-Heptyl-3-hydroxy-7-methoxyquinolin-4(1*H*)-one (37).** Compound **37** was obtained according to procedure A3 from **37a** (240 mg, 0.80 mmol) after chromatography on silica gel as a brown solid (218 mg, 0.75 mmol, 94%), mp 222-224 °C. $^{1}$H-NMR (500 MHz, DMSO-$d_6$): δ = 0.85 (t, *J* = 7.0 Hz, 3H), 1.25-1.31 (m, 8H), 1.65 (m, 2H), 2.68 (m, 2H), 3.83 (s, 3H), 6.82 (d, *J* = 9.0 Hz, 1 H), 6.91 (br. 1H), 7.82 (br, 1H), 7.97 (d, *J* = 9.0 Hz, 1H), 11.18 (brs, 1H). $^{13}$C-NMR (125 MHz, DMSO-$d_6$): δ = 13.8, 22.0, 27.7, 27.9, 28.4, 28.6, 31.1, 55.2, 97.8, 112.5, 116.6, 126.1, 134.3, 137.2, 139.0, 160.7, 168.7. LC/MS: *m/z* 290.24 ($MH^+$), 99.9%.

**8-Fluoro-2-heptyl-3-hydroxyquinolin-4(1*H*)-one (38).** Compound **38** was obtained according to procedure A3 from **38a** (68 mg, 0.23 mmol) after chromatography on silica gel as a brown solid (21 mg, 0.08 mmol, 35%), mp 167-169 °C. $^{1}$H-NMR (500 MHz, DMSO-$d_6$): δ = 0.84 (t, *J* = 7.0 Hz, 3H), 1.23-1.35 (m, 8H), 1.63 (quint, *J*= 7.5 Hz, 2H), 2.79 (t, *J* = 7.5 Hz, 2H), 7.16-7.20 (m ,1H), 7.43-7.46 (m, 1H), 7.91 (d, *J* = 8.0 Hz, 1H), 8.20 (brs, 1H), 11.93 (s 1H). $^{13}$C-NMR (125 MHz, DMSO-$d_6$): δ = 13.893, 22.023, 27.710, 27.998, 28.428, 28.823, 31.181, 114.1, 114.2, 117.1, 117.7,

120.2, 120.3, 121.0, 124.4,125.9, 125.9, 126.6, 126.8, 136.4, 138.5, 151.4(d, $J_{CF}$ = 247.8 Hz), 168.3. LC/MS: *m/z* 278.23, 99.0%.

**6-Fluoro-2-heptyl-3-hydroxyquinolin-4(1*H*)-one (39).** Compound **39** was obtained according to procedure A3 from **39a** (172 mg, 0.59 mmol) after chromatography on silica gel as a pink solid (140 mg, 0.50 mmol, 85%), mp 228-231 °C. $^1$H-NMR (500 MHz, DMSO-$d_6$): δ = 0.84 (t, *J* = 7.0 Hz, 3H), 1.24-1.32 (m, 8H), 1.66 (quint, *J* = 6.5 Hz, 2H), 2.72 (t, *J* = 6.5 Hz, 2H), 7.44 (t, *J* = 6.5 Hz, 1H), 7.60 (brs, 1H), 7.70 (dd, *J* = 3.0 Hz, 6.5 Hz, 1H), 8.13 (brs, 1H). $^{13}$C-NMR (125 MHz, DMSO-$d_6$): δ = 13.8, 22.0, 27.7, 28.1, 28.4, 28.7, 31.1, 107.8 (d, $J_{CF}$ = 21.9 Hz), 119.1(d, $J_{CF}$ = 25.8 Hz), 120.4(d, $J_{CF}$ = 8.2 Hz), 122.9(d, $J_{CF}$ = 6.8 Hz), 134.1, 136.1, 137.5, 157.2 (d, $J_{CF}$ = 240.1 Hz), 167.9, 167.9. LC/MS: *m/z* 278.22 ($MH^+$), 99.9%.

**2-Heptyl-3-hydroxy-6-methylquinolin-4(1*H*)-one (40).** Compound **40** was obtained according to procedure A3 from **40a** (150 mg, 0.52 mmol) after chromatography on silica gel as a white solid (118 mg, 0.43 mmol, 83%), mp 221-222 °C. $^1$H-NMR (500 MHz, DMSO-$d_6$): δ = 0.95 (t, *J* = 7.0 Hz, 3H), 1.34-1.45 (m, 8H), 1.76 (quint, *J* = 7.5 Hz, 2H), 2.50 (s, 3H), 2.82 (t, *J*= 7.5 Hz, 2H), 7.47 (dd, *J* = 2.0 Hz, 8.5 Hz, 1H), 7.55 (d, *J* = 8.5 Hz, 1H), 7.98 (s, 1H) 11.46 (br, 1H). $^{13}$C-NMR (125 MHz, DMSO-$d_6$): δ = 13.8, 20.6, 22.0, 27.7, 28.4, 28.7, 31.1, 117.6, 122.0, 123.3, 130.6, 131.6, 135.2, 135.5, 137.6, 168.4. LC/MS: *m/z* 274.32 ($MH^+$), 95.4%.

**2-Heptyl-3-hydroxy-6-iodoquinolin-4(1*H*)-one (41).** Compound **41** was obtained according to procedure B from 1-chlorononan-2-one (192 mg, 1.10 mmol) and 2-amino-5-iodobenzoic acid (288 mg, 1.10 mmol) after recrystallisation as a grey solid (70 mg, 0.18 mmol, 16%), mp 275-279 °C. $^1$H-NMR (500 MHz, DMSO-$d_6$): δ = 0.83 (t, *J* = 7.0 Hz, 3H), 1.23-1.31 (m, 8H), 1.64 (quint, *J* = 7.5 Hz, 2H), 2.70 (t, *J*= 7.5 Hz, 2H), 7.36 (d, *J* = 6.0 Hz, 1H), 7.77 (dd, *J* = 2.0 Hz, 8.5 Hz, 1H), 8.38 (d, *J* = 2.5 Hz, 1H) 11.57 (brs, 1H). $^{13}$C-NMR (125 MHz, DMSO-$d_6$): δ = 13.8, 21.9, 27.6, 28.1, 28.3, 28.6, 31.1, 85.6, 120.2, 124.1, 132.8, 136.2, 136.3, 137.8, 138.2, 167.4. LC/MS: *m/z* 386.19 ($MH^+$), 99.1%.

**2-Heptyl-3-hydroxybenzo[g]quinolin-4(1*H*)-one (42).** Compound **42** was obtained according to procedure B from 1-chlorononan-2-one (192 mg, 1.10 mmol) and 3-amino-2-naphthoic acid (151 mg, 1.10 mmol) after chromatography on silica gel as a yellow solid (15mg, 0.05 mmol, 4%), mp 250-253 °C. $^1$H-NMR (500 MHz, DMSO-$d_6$): δ = 0.90 (t, *J* = 7.0 Hz, 3H), 1.29-1.49 (m, 8H), 1.84 (quint, *J* = 7.5 Hz, 2H), 2.95 (t, *J*= 7.5 Hz, 2H), 7.44 (t, *J* = 7.5 Hz, 1H), 7.52 (t, *J* = 7.5 Hz, 1H), 7.92 (d, *J* = 8.5 Hz, 1H), 8.05 (m, 2H). $^{13}$C-NMR (125 MHz, DMSO-$d_6$): δ = 14.3, 23.6, 29.3, 30.1, 30.2, 30.5, 32.8, 114.9, 123.5, 125.6, 126.0, 128.0, 128.6, 130.1, 130.6, 135.7, 142.6, 171.6. LC/MS: *m/z* 310.35 ($MH^+$), 96.6%.

For synthesis of compounds **18-20** see the experimental procedures of the paper.

Compounds **22**, **23** and **25** were commercially available.

**Syntheses of the Intermediates 2a-7a, 27a-28a and 31a-40a**
**Procedure D.**

Sythesis of ethyl β-ketoester. To a THF solution of 2M LDA (20 ml, 40 mmol 2.4 equiv) was added ethyl acetoacetate (16.6 mmol, 1.0 equiv) at 0 ℃. The deep yellow clear solution was stirred at 0 ℃ for 1 h. To this solution the alkyl halide was added (20.0 mmol 1.2 equiv) at -78 ℃. The temperature was allowed to reach an ambient temperature over 14 h and the solution was stirred at r.t. for 2 h. To the solution was added 10% HCl (200 ml) and the mixture was extracted with $Et_2O$ (4 × 250 ml). The combined organic layers were dried over $Na_2SO_4$, filtered, and the filtrate was concentrated *in vacuo*. The residue was purified by column chromatography (*n*-hexane/ethyl acetate, 30/1) to give ethyl β-ketoester (Nguyen et al., 2006).

**Procedure E.**

Sythesis of methyl β-ketoester. A solution of methyl akylnyl ester (30.0 mmol, 1 equiv) and piperidine (30.0 mmol, 1 equiv) in benzene (10 ml) was heated overnight under reflux. After evaporation of the solvent under reduced pressure the residue was purified by flash column chromatography on silica (ethyl acetate/*n*-hexanes 15/85) twice to yield methyl β-ketoester (Bestmann et al., 1977).

**Ethyl 3-oxooctanoate (2a).** Compound **2a** was obtained according to procedure D from ethyl acetoacetate (2.57 g, 16.60 mmol) and 1-iodobutane (3.68 g, 19.89 mmol) after chromatography on silica gel as a yellow oil (811 mg, 4.36 mmol, 26%). $^1$H-NMR (500 MHz, $CDCl_3$): δ = 0.82 (t, *J* = 7.0 Hz, 3H), 1.17-1.28 (m, 7H), 1.53 (quint, *J* = 7.5 Hz, 2H), 2.46 (t, *J* = 7.5 Hz, 2H), 3.35 (s, 2H), 4.12 (q, *J* = 8.0 Hz 2H). $^{13}$C-NMR (125 MHz, $CDCl_3$): δ = 13.8, 14.0, 22.3, 23.1, 31.1, 42.9, 49.2, 61.2, 167.2, 202.9. LC/MS: *m/z* 344.39, 93.3%.

**Ethyl 3-oxononanoate (3a).** Compound **3a** was obtained according to procedure D from ethylacetoactate (2.57 g, 16.60 mmol) and 1-iodopentane (3.96 g, 20.00 mmol) after chromatography on silica gel as a yellow oil (1.69 g, 9.08 mmol, 55%). $^1$H-NMR (500 MHz, $CDCl_3$): δ = 0.81 (t, *J* = 7.0 Hz, 3H), 1.19-1.25 (m, 9H), 1.52 (quint, *J* = 7.5 Hz, 2H), 2.46 (t, *J* = 7.5 Hz, 2H), 3.35 (s, 2H), 4.11 (m, 2H). $^{13}$C-NMR (125 MHz, $CDCl_3$): δ = 13.9, 14.0, 22.4, 23.4, 28.6, 31.5, 43.0, 49.2, 61.2, 167.2, 202.9. LC/MS: *m/z* 372.44, 94.1%.

**Ethyl 3-oxodecanoate (4a).** Compound **4a** was obtained according to procedure D from ethylacetoactate (2.16 g, 16.60 mmol) and 1-iodohexane (4.20 g, 19.81 mmol) after chromatography on silica gel as a yellow oil (1.98 g, 9.24 mmol, 55%). $^1$H-NMR (500 MHz, $CDCl_3$): δ = 0.84 (t, *J* = 7.0 Hz, 3H), 1.23-1.28 (m, 11H), 1.54 (quint, *J* = 7.0 Hz, 2H), 2.49 (t, *J* = 7.0 Hz, 2H), 3.39 (s, 2H), 4.16 (m, 2H). $^{13}$C-NMR (125 MHz, $CDCl_3$): δ = 13.9, 14.0, 22.5, 23.4, 28.9, 31.5, 43.0, 49.2, 61.2, 167.2, 202.9. LC/MS: *m/z* 457.98, 87.1%.

**Ethyl 3-oxoundecanoate (5a).** Compound **5a** was obtained according to procedure D from ethylacetoactate (2.57 g, 16.60 mmol) and 1-iodoheptane (4.48 g, 19.83 mmol) after

chromatography on silica gel as a yellow oil (1.74 g, 7.65 mmol, 46%). $^{1}$H-NMR (500 MHz, $CDCl_3$): δ = 0.80 (t, *J* = 7.0 Hz, 3H), 1.19-1.25 (m, 13H), 1.52 (quint, *J* = 7.5 Hz, 2H), 2.45 (t, *J* = 7.5 Hz, 2H), 3.35 (s, 2H), 4.12 (q, *J* = 7.5 Hz, 2H). $^{13}$C-NMR (125 MHz, $CDCl_3$): δ = 14.0, 14.0, 22.6, 23.4, 29.0, 29.0, 29.2, 31.7, 43.0, 49.3, 61.3, 167.2, 202.9. LC/MS: *m/z* 237.31, 99.9%.

**Ethyl 3-oxododecanoate (6a).** Compound **6a** was obtained according to procedure D from ethylacetoactate (2.57 g, 16.60 mmol) and 1-iodooctane (7.40 g, 20.00 mmol) after chromatography on silica gel as a yellow oil (2.50 g, 10.33 mmol, 62%). $^{1}$H-NMR (500 MHz, DMSO-$d_6$): δ = 0.85 (t, *J* = 7.0 Hz, 3H), 1.16-1.28 (m, 15H), 1.45 (quint, *J* = 7.0 Hz, 2H), 2.49 (t, *J* = 7.0 Hz, 2H, overlapped with peak of solution), 3.55 (s, 2H), 4.08 (q, *J* = 7.0 Hz, 2H). $^{13}$C-NMR (125 MHz, DMSO-$d_6$): δ = 13.8, 13.9, 22.0, 22.8, 28.3, 28.6, 28.7, 28.8, 31.2, 42.1, 48.7, 60.4, 167.2, 203.5. LC/MS: *m/z* 372.41, 96.4%.

**Ethyl 3-oxo-6-phenylhexanoate (7a).** To a stirred solution of 4-phenylbutyric acid (800 mg, 4.88 mmol, 1 equiv) and $SOCl_2$ (4 ml, 54.69 mmol, 11.2 equiv) was added pyridine (0.3 ml, 3.71 mmol, 0.76 equiv). The solution was stirred at room temperature for 30 min and at 40 ℃ for an additional 1 h before it was concentrated to give 4-phenylbutanoylchloride as a yellow oil, which was used in the next step without further purification (Muhlman et al., 2001). Under a nitrogen atmosphere monoethyl malonate (1.20 g, 9.09 mmol) and 2,2'-bipyridyl (8 mg, as an indicator) were added to a solution of THF (25 ml). After cooling to -70 ℃, *n*-butyllithium (1.6 M, in *n*-hexane, 12 ml, 19.2 mmol) was added slowly while allowing the temperature to rise to ca. -5 ℃ near the end of the addition. After the pink color persisted at -5 ℃ the heterogeneous solution was recooled to -70 ℃ and 4-phenylbutanoylchloride (4.88 mmol) was added over 5 min. Stirring was continued at -70 ℃ for 1 h. The reaction solution was poured into a mixture of ether (40 ml) and HCl (1.0 M, 20 ml). After mixing and separating the aqueous phase, the organic phase was washed with saturated sodium bicarbonate and water, dried over $Na_2SO_4$, and concentrated *in vacuo* to yield **7a** (150 mg, 0.64 mmol, 13%) as a yellow oil (Wierenga et al., 1979). $^{1}$H-NMR (500 MHz, DMSO-$d_6$): δ = 1.14 (t, *J* = 7.0 Hz, 3H), 1.73 (quint, *J* = 7.5 Hz, 2H), 2.50 (q, *J* = 7.5 Hz, 4H), 3.28 (s, 1H), 3.52 (s, 2H), 4.04 (q, *J* = 7.0 Hz, 2H), 7.13-7.15 (m, 3H), 7.23-7.26 (m, 2H). $^{13}$C-NMR (125 MHz, DMSO-$d_6$): δ = 13.9, 24.6, 34.2, 41.5, 48.7, 60.4, 125.7, 128.2, 141.5, 167.2, 203.3. LC/MS: *m/z* 415.26, 97.7%.

**Methyl 3-oxooctanoate ester (27a).** Compound was obtained according to procedure E from methyl 2-octynoate (4.63 g, 30.0 mmol) after chromatography on silica gel as a colorless oil (3.00 g, 17.44 mmol, 58%). $^{1}$H-NMR (500 MHz, $CDCl_3$): δ = 0.88 (t, *J* = 7.1 Hz, 3H), 1.29 (m, 4H), 1.59 (m, 2H), 2.52 (t, *J* = 7.4 Hz, 2H), 3.44 (s, 2H), 3.73 (s, 3H).

**Methyl 3-oxononanoate (28a).** Compound was obtained according to procedure E from methyl 2-nonynoate (5.05 g, 30 mmol) after chromatography on silica gel as a colorless oil (2.96 g, 15.91 mmol, 53%). $^{1}$H-NMR (500 MHz, $CDCl_3$): δ = 0.85 (t, *J* = 6.9 Hz, 3H), 1.25 (m, 6H), 1.56 (m, 2H),

2.50 (t, *J* = 7.4 Hz, 2H), 3.42 (s, 2H), 3.71 (s, 3H).

**4-Oxo-2-pentyl-1,4-dihydroquinoline-3-carbaldehyde (31a).** Compound **31a** was obtained according to procedure A2 from **2** (224 mg, 1.03 mmol) after chromatography on silica gel as a yellow solid (105 mg, 0.43 mmol, 42%). $^{1}$H-NMR (500 MHz, DMSO-$d_6$): δ = 0.88 (t, *J* = 7.0 Hz, 3H), 1.32-1.37 (m, 4H), 1.60 (quint, *J* = 7.5 Hz, 2H), 3.04 (t, *J*= 7.5 Hz, 2H), 7.42 (t, *J* = 7.0 Hz, 1H), 7.59 (d, *J* = 8.0 Hz, 1H), 7.73 (m, 1H), 8.14 (dd, *J* = 1.5 Hz, 8.5 Hz, 1H), 10.38 (s, 1H), 12.11 (brs, 1H). $^{13}$C-NMR (125 MHz, DMSO-$d_6$): δ = 13.7, 21.7, 28.4, 31.1, 314, 113.3, 118.7, 124.9, 126.1, 133.0, 139.1, 160.0, 178.0, 190.7. LC/MS: 244.23 ($MH^+$), 99.9%

**2-Hexyl-4-oxo-1,4-dihydroquinoline-3-carbaldehyde (32a).** Compound **32a** was obtained according to procedure A2 from **3** (500 mg, 2.18 mmol) after chromatography on silica gel as a yellow solid (298 mg, 1.16 mmol, 53%). $^{1}$H-NMR (500 MHz, DMSO-$d_6$): δ = 0.86 (t, *J* = 7.0 Hz, 3H), 1.27-1.41 (m, 6H), 1.59 (quint, *J* = 7.5 Hz, 2H), 3.04 (t, *J*= 8.0 Hz, 2H), 7.42 (t, *J* = 8.0 Hz, 1H), 7.59 (d, *J* = 8.0 Hz, 1H), 7.73 (m, 1H), 8.14 (dd, *J* = 1.0 Hz, 8.0 Hz, 1H) 10.38 (s, 1H) 12.13 (brs, 1H). $^{13}$C-NMR (125 MHz, DMSO-$d_6$): δ = 13.8, 21.9, 28.6, 28.7, 30.8, 31.5, 113.3, 118.6, 124.9, 126.1, 133.0, 139.1, 160.0, 178.0, 190.7. LC/MS: 258.24 ($MH^+$), 99.9%

**2-Heptyl-4-oxo-1,4-dihydroquinoline-3-carbaldehyde (33a).** Compound **33a** was obtained according to procedure A2 from **4** (500 mg, 2.06 mmol) after chromatography on silica gel as a yellow solid (310 mg, 1.14 mmol, 55%). Compound **33a** was unstable, decomposition was observed in $^{1}$H-NMR test. LC/MS: 272.22 ($MH^+$), 99.9%.

**2-Octyl-4-oxo-1,4-dihydroquinoline-3-carbaldehyde (34a).** Compound **34a** was obtained according to procedure A2 from **5** (500 mg, 1.94 mmol) after chromatography on silica gel as a yellow solid (243 mg, 0.85 mmol, 44%). $^{1}$H-NMR (500 MHz, DMSO-$d_6$): δ = 0.84 (t, *J* = 7.0 Hz, 3H), 1.15-1.40 (m, 10H), 1.59 (quint, *J* = 7.5 Hz, 2H), 3.06 (t, *J*= 8.0 Hz, 2H), 7.42 (t, *J* = 8.0 Hz, 1H), 7.59 (d, *J* = 8.0 Hz, 1H), 7.73 (m, 1H), 8.14 (dd, *J* = 1.5 Hz, 8.5 Hz, 1H), 10.38 (s, 1H), 12.11 (brs, 1H). $^{13}$C-NMR (125 MHz, DMSO-$d_6$): δ = 13.9, 22.0, 28.5, 28.6, 28.8, 29.0, 31.2, 31.5, 113.3, 118.6, 124.9, 126.1, 133.0, 139.1, 160.0, 178.1, 190.8. LC/MS: 286.29 ($MH^+$), 99.9%.

**2-Nonyl-4-oxo-1,4-dihydroquinoline-3-carbaldehyde (35a).** Compound **35a** was obtained according to procedure A2 from **6** (500 mg, 1.84 mmol) after chromatography on silica gel as a yellow solid (252 mg, 0.84 mmol, 46%). $^{1}$H-NMR (500 MHz, DMSO-$d_6$): δ = 0.84 (t, *J* = 7.0 Hz, 3H), 1.24-1.27 (m, 12H), 1.59 (quint, *J* = 7.5 Hz, 2H), 3.04 (t, *J*= 7.5 Hz, 2H), 7.42 (t, *J* = 8.0 Hz, 1H), 7.59 (d, *J* = 8.0 Hz, 1H), 7.73 (m, 1H), 8.14 (dd, *J* = 1.5 Hz, 8.5 Hz, 1H), 10.38 (s, 1H), 12.11 (brs, 1H). $^{13}$C-NMR (125 MHz, DMSO-$d_6$): δ = 13.9, 22.0, 28.6, 28.6, 28.8, 28.9, 31.3, 113.3, 118.6, 124.9, 126.1, 133.0, 139.1, 160.0, 178.0, 190.7. LC/MS: 300.28 ($MH^+$), 98.3%.

**2-Heptyl-6-methoxy-4-oxo-1,4-dihydroquinoline-3-carbaldehyde (36a).** Compound **36a** was obtained according to procedure A2 from **14** (350 mg, 1.28 mmol) after chromatography on silica

gel as a yellow solid (210 mg, 0.70 mmol, 54%). $^{1}$H-NMR (500 MHz, DMSO-$d_6$): δ = 0.85 (t, *J* = 7.0 Hz, 3H), 1.25-1.38 (m, 8H), 1.58 (quint, *J* = 7.5 Hz, 2H), 3.02 (t, *J* = 8.0 Hz, 2H), 3.85 (s, 3H), 7.36 (dd, J = 3.0 Hz, 9.0 Hz, 1H), 7.54-7.56 (m, 2H), 10.39 (s, 1H), 12.10 (brs, 1H). $^{13}$C-NMR (125 MHz, DMSO-$d_6$): δ =13.8, 22.0, 28.3, 28.8, 28.9, 31.1, 31.5, 55.4, 104.9, 112.5, 120.4, 122.6, 127.4, 133.5, 156.6, 158.4, 177.5, 190.7. LC/MS: 302.25 ($MH^+$), 99.9%.

**2-Heptyl-7-methoxy-4-oxo-1,4-dihydroquinoline-3-carbaldehyde (37a).**Compound **37a** was obtained according to procedure A2 from **9** (580 mg, 2.13 mmol) after chromatography on silica gel as a yellow solid (250 mg, 0.83 mmol, 39%). $^{1}$H-NMR (500 MHz, DMSO-$d_6$): δ = 1.06 (t, *J* = 7.0 Hz, 3H), 1.46-1.59 (m, 8H), 1.79 (quint, *J* = 7.5 Hz, 2H), 3.22 (t, *J*= 7.5 Hz, 2H), 4.08 (s, 3H), 7.18-7.22 (m, 2H), 8.24 (d, *J* = 7.5 Hz, 1H), 10.56 (s, 1H), 12.15 (brs, 1H). $^{13}$C-NMR (125 MHz, DMSO-$d_6$): δ = 13.8, 21.9, 28.2, 28.7, 28.9, 31.0, 31.4, 55.5, 100.2, 113.1, 114.2, 120.0, 126.8, 140.9, 159.9, 162.7, 177.4, 190.8, 190.9. LC/MS: 302.22 ($MH^+$), 99.9%.

**8-Fluoro-2-heptyl-4-oxo-1,4-dihydroquinoline-3-carbaldehyde (38a).** Compound **38a** was obtained according to procedure A2 from **12** (305 mg, 1.17 mmol) after chromatography on silica gel as a yellow solid (68 mg, 0.23 mmol, 20%).Compound **27a** was unstable, decomposition was observed in $^{1}$H-NMR test. LC/MS: 264.17 ($MH^+$), 98.0%.

**6-Fluoro-2-heptyl-4-oxo-1,4-dihydroquinoline-3-carbaldehyde (39a).** Compound **39a** was obtained according to procedure A2 from **16** (290 mg, 1.11 mmol) after chromatography on silica gel as a yellow solid (182 mg, 0.63 mmol, 56%). $^{1}$H-NMR (500 MHz, DMSO-$d_6$): δ = 0.86 (t, *J* = 7.0 Hz, 3H), 1.23-1.42 (m, 8H), 1.60 (quint, *J* = 7.5 Hz, 2H), 3.04 (t, *J*= 7.5 Hz, 2H), 7.62-7.69 (m, 2H), 7.80 (dd, *J* = 3.0 Hz, 9.5 Hz, 1H) 10.38 (s, 1H), 12.26 (brs, 1H). $^{13}$C-NMR (125 MHz, DMSO-$d_6$): δ = 13.8, 21.9, 28.2, 28.7, 28.9, 31.0, 31.6, 109.5, 111.9, 112.7, 121.5, 127.6, 136.0, 158.9 (d, $J_{CF}$ = 244.1 Hz), 177.2, 190.6. LC/MS: 290.22 ($MH^+$), 95.7%.

**2-Heptyl-6-methyl-4-oxo-1,4-dihydroquinoline-3-carbaldehyde (40a).** Compound **40a** was obtained according to procedure A2 from **15** (300 mg, 1.17 mmol) after chromatography on silica gel as a yellow solid (161 mg, 0.56 mmol, 48%). $^{1}$H-NMR (500 MHz, DMSO-$d_6$): δ = 0.93 (t, *J* = 7.0 Hz, 3H), 1.30-1.48 (m, 8H), 1.66 (quint, *J* = 7.5 Hz, 2H), 2.50 (s, 3H), 3.10 (t, *J* = 8.0 Hz, 2H), 7.57 (d, *J* = 8.0 Hz, 1H), 7.64 (dd, J = 2.0 Hz, 8.5 Hz, 1H), 8.01 (s, 1H), 10.458 (s, 1H). $^{13}$C-NMR (125 MHz, DMSO-$d_6$): δ = 13.8, 20.7, 21.9, 28.2, 28.8, 28.9, 31.0, 31.5, 113.1, 118.6, 124.3, 126.1, 134.2, 134.5, 137.1, 159.4, 177.9, 190.7. LC/MS: 286.33 ($MH^+$), 99.7%.

Intermediates **1a**, **24a** and **26a** were commercially available.

## Supplemental References

Bestmann, H.J. and Geismann, C. Justus Liebigs Annalen der Chemie. (1977). 2, 282-287.

Cross, R.M. and Manetsch, R. Divergent route to access structurally diverse 4-quinolones via mono or sequential cross-couplings. (2010). J. Org. Chem. 75, 8654-8657.

Gross, P.J., Hartmann, C.E., Nieger, M. and Brase, S. Synthesis of methoxyfumimycin with 1,2-addition to ketimines. (2010). J. Org. Chem. 75, 229-232.

Hodgkinson, J.T., Galloway, W.R., Saraf, S., Baxendale, I.R., Ley, S.V., Ladlow, M., Welch, M., and Spring, D.R.

Microwave and flow syntheses of *Pseudomonas* quinolone signal (PQS) and analogues. (2011). Org. Biomol. Chem. 9, 57-61.

Konieczny, M.T., Maciejewski, G. and Konieczny, W. Selectivity adjustment in the cleavage of allyl phenyl and methyl phenyl ethers with boron trifluoride– methyl sulfide complex. (2005). Synthesis 10, 1575-1577.

Muhlman, A., Lindberg, J., Classon, B., Unge, T., Hallberg, A. and Samuelsson, B. Synthesis of novel, potent, diol-based HIV-1 protease inhibitors via intermolecular pinacol homocoupling of (2S)-2- benzyloxymethyl- 4-phenylbutanal. (2001). J. Med. Chem. 44, 3407-3416.

Nguyen, V.T.H., Bellur, E., Appel, B. and Langer, P. Synthesis of 4-Alkyl- and 4-(w-Chloroalkyl)-3-hydroxy-5-alkylidenebutenolidesbased on cyclizations of 4-alkyl- and 4-(-chloroalkyl)-1,3-bis(trimethylsilyloxy)buta-1,3-dienes with oxalyl chloride. (2006). Synthesis 17, 2865-2872.

Tanoue, Y., Terada, A. and Matsumoto, Y. A synthetic route of 1,4,8- trimethoxy -2-naphthalenecarbaldehyde via Duff formylation of 4,8-dimethoxy-1-Naphthol. (1989). B. Chem. Soc. Jpn. 62, 2736-2738.

Wierenga., W. and Skulnick, H.I. General, efficient, one-step synthesis of beta- keto esters. (1979). J. Org. Chem. 44, 310-311

Woschek, A., Mahout, M., Mereiter, K. and Hammerschmidt, F. Synthesis of 2-heptyl-1-hydroxy-4(1H)-quinolone - Unexpected rearrangement of 4-(alkoxycarbonyloxy)quinoline *N*-oxides to 1-(alkoxycarbonyloxy)-4(1*H*)-quinolones. (2007). Synthesis 10, 1517-1522.

# 6.2 Supplemental Information for Paper II

## General Experimental Information-Chemistry

### Chemicals and Analytical Methods

$^{1}H$ and $^{13}C$ NMR spectra were recorded on a Bruker DRX-500 instrument. Chemical shifts are given in parts per million (ppm) with the solvent resonance as internal standard for spectra obtained in $CDCl_3$, MeOH-$d_4$ and DMSO-$d_6$. All coupling constants ($J$) are given in hertz. Mass spectrometry (LC/MS) was performed on a MSQ® electro spray mass spectrometer (Thermo Fisher). The system was operated by the standard software Xcalibur®. A RP C18 NUCLEODUR® 100-5 (125 × 3 mm) column (Macherey-Nagel GmbH) was used as stationary phase with water/acetonitrile mixtures as eluent. All solvents were HPLC grade. Reagents were used as obtained from commercial suppliers without further purification. Flash chromatography was performed on silica gel 60, 70-230 mesh (Fluka) and the reaction progress was determined by thin-layer chromatography (TLC) analyses on silica gel 60, $F_{254}$ (Merck). Visualization was accomplished with UV light and staining with basic potassium permanganate ($KMnO_4$). The melting points were measured using melting point apparatus SMP3 (Stuart Scientific). The apparatus is uncorrected.

The following compounds were prepared according to previously described procedures: HHQ, PQS, **1** and **7**.[1]

### Synthesis of Title Compounds

**2-Heptyl-3-hydroxy-6-nitroquinolin-4(1*H*)-one (compound 2).**

A solution of **4** (200 mg, 0.63 mmol, 1.0 equiv) in dry THF (50 mL) was added dropwise to pure activated $MnO_2$ (540 mg, 6.21 mmol, 9.9 equiv) at room temperature. The mixture was then stirred overnight. After filtration through Celite the solvent was removed under reduced pressure and the residue was purified by column chromatography on silica gel (dichloromethane:methanol, 80:1 v/v) to give 2-heptyl-6-nitro-4-oxo-1,4-dihydroquinoline-3-carbaldehyde as a yellow solid (80 mg, 0.25 mmol), which was unstable and used immediately in the next step. Boric acid (80 mg, 1.30 mmol, 5.0 equiv) was suspended in THF (20 mL), followed by the addition of 30% $H_2O_2$ (90 µL, 3.0 equiv) and conc. $H_2SO_4$ (0.5 mL). After stirring for 30 min a solution of the aldehyde (80 mg, 0.25 mmol) in THF (10 mL) was added dropwise over 10 min. After additional stirring for 5 h, the mixture was filtered. The filtrate was neutralized by addition of a sat. $NaHCO_3$ solution (120 mL) and the aqueous layer was extracted with ethyl acetate (3 x 30 mL). After drying of the combined

organic layers over $MgSO_4$ the solvent was removed under reduced pressure. The residue was purified by preparative thin layer chromatography on silica gel (dichloromethane:methanol, 30:1 v/v) to give **2** as a yellow solid (60 mg, 0.20 mmol, 32% for 2 steps). mp: 217.1-219.7 ℃; $^1$H-NMR (500 MHz, DMSO-$d_6$): δ 0.85 (t, *J* = 7.0 Hz, 3H), 1.24-1.39 (m, 8H), 1.67 (quint, *J* = 7.5 Hz, 2H), 2.74 (t, *J* = 7.5 Hz, 2H), 7.70 (d, *J* = 9.0 Hz, 1H), 8.29 (dd, *J* = 2.5, 9.0 Hz, 1H), 8.71 (br, 1H), 8.90 (d, *J* = 2.5 Hz, 1H), 11.99 (br, 1H); $^{13}$C-NMR (125 MHz, DMSO-$d_6$): δ 13.9, 22.0, 27.6, 28.0, 28.4, 28.7, 31.1, 119.5, 121.1, 121.8, 123.8, 136.8, 139.2, 140.2, 141.4, 169.2; LC/MS: *m/z* 305.03 $[M + H]^+$, 99.9%.[1]

**2-Heptyl-6-nitro-4-oxo-1, 4-dihydroquinoline-3-carboxamide (compound 3).**

*N*,*N*'-Carbonyldiimidazole (62 mg, 0.38 mmol, 2.0 equiv) was added to **5** (62 mg, 0.19 mmol, 1.0 equiv) in dry DMF (1 mL). After stirring at 65 ℃ for 5 h, the mixture was cooled to 0 ℃ and iced conc. $NH_3$•$H_2O$ (5 mL) was added. After stirring overnight at room temperature the solvent was evaporated under reduced pressure. To the residue was added iced water (5 mL) and the pricipitate was isolated by filtration. After purification by column chromatography on silica gel (dichloromethane:methanol, 70:1 v/v) **3** was isolated as a white solid (43 mg, 0.13 mmol, 68%), mp: 237.6-239.1 ℃; $^1$H-NMR (500 MHz, DMSO-$d_6$): δ 0.86 (t, *J* = 7.0 Hz, 3H), 1.23-1.39 (m, 8H), 1.69 (quint, *J* = 7.5 Hz, 2H), 3.00 (t, *J* = 8.0 Hz, 2H), 7.36 (br, 1H), 7.76 (d, *J* = 9.0 Hz, 1H), 8.45 (dd, *J* = 2.5, 9.0 Hz, 1H), 8.54 (br, 1H), 8.86 (d, *J* = 2.5 Hz, 1H), 12.30 (br, 1H); $^{13}$C-NMR (125 MHz, DMSO-$d_6$): δ 13.9, 22.0, 28.3, 29.0, 29.2, 31.1, 32.7, 115.3, 119.9, 121.9, 123.9, 126.4, 142.4, 143.1, 157.7, 166.7, 175.0; LC/MS: *m/z* 332.92 $[M + H]^+$, 96.8%.[2]

**2-Heptyl-3-(hydroxymethyl)-6-nitroquinolin-4(1*H*)-one (compound 4).**

At 0 ℃ $LiAlH_4$ (90 mg, 2.37 mmol, 2.0 equiv) was added to a stirred solution of **6** (420 mg, 1.17 mmol, 1.0 equiv) in dry THF (20 mL). After stirring at room temperature for 2 h water (8 drops) and NaOH (2 drops, 15%) were added at 0 ℃ and after filtration the solvent was removed under reduced pressure. The residue was purified by column chromatography (dichloromethane:methanol, 60:1 v/v) and washed with *n*-hexane to give **4** as a yellow solid (35 mg, 0.11 mmol, 9%), mp: >350 ℃; $^1$H-NMR (500 MHz, DMSO-$d_6$): δ 0.86 (t, *J* = 7.0 Hz, 3H), 1.23-1.42 (m, 8H), 1.70 (quint, *J* = 7.5 Hz, 2H), 2.77 (t, *J* = 7.5 Hz, 2H), 4.48 (d, *J* = 5.5 Hz, 2H), 4.68 (t, *J* = 5.5 Hz, 1H), 7.70 (d, *J* = 9.0 Hz, 1H), 8.39 (dd, *J* = 2.5, 9.0 Hz, 1H), 8.84 (d, *J* = 3.0 Hz, 1H), 11.93 (br, 1H); $^{13}$C-NMR (125 MHz, DMSO-$d_6$): δ 13.9, 22.0, 28.4, 29.0, 29.2, 31.1, 53.4, 119.6, 119.9, 121.9, 122.9, 125.6, 142.3, 143.2, 153.9, 175.6; LC/MS: *m/z* 319.06 $[M + H]^+$, 99.9%.[3]

**2-Heptyl-6-nitro-4-oxo-1, 4-dihydroquinoline-3-carboxylic acid (compound 5).**

**6** (250 mg, 0.69 mmol) was suspended in 10% NaOH (50 mL) solution and heated at reflux for 4 h. After cooling to 0 ℃ on an ice water bath and extraction with ethyl acetate, the water phase was acidified with conc. HCl to reach a pH of 4.0-6.0. **5** was isolated by filtration, washed with water

and dried under vacuum as a gray solid (32 mg, 0.10 mmol, 14%). mp: 192.7-194.9 ℃; $^{1}$H-NMR (500 MHz, DMSO-$d_6$): δ 0.86 (t, *J* = 7.0 Hz, 3H), 1.27-1.44 (m, 8H), 1.67 (quint, *J* = 7.5 Hz, 2H), 3.26 (t, *J* = 7.5 Hz, 2H), 7.91 (d, *J* = 9.0 Hz, 1H), 8.58 (dd, *J* = 2.5, 9.0 Hz, 1H), 8.90 (d, *J* = 2.5 Hz, 1H), 13.22 (br, 1H), 15.64 (br, 1H); $^{13}$C-NMR (125 MHz, DMSO-$d_6$): δ 13.9, 22.0, 28.3, 29.1, 31.1, 33.3, 107.6, 120.8, 121.5, 122.7, 127.7, 141.6, 144.2, 163.9, 165.4, 178.6; LC/MS: *m/z* 332.90 [M + H]$^{+}$, 98.8%.

**Ethyl 2-heptyl-6-nitro-4-oxo-1, 4-dihydroquinoline-3-carboxylate (compound 6).**

Under nitrogen atmosphere **7** (3.40 g, 15 mmol, 1.0 equiv) was added to a suspension of sodium hydride (50-65% w/w, 0.75 g, 15 mmol, 1.0 equiv) in dry DMF (50 mL), causing the liberation of hydrogen gas. A solution of 6-nitro-1*H*-benzo[*d*][1,3]oxazine-2,4-dione (3.0 g, 14 mmol, 0.9 equiv) in dry DMF (30 mL) was added dropwise and stirred overnight. Most of the solvent was removed under reduced pressure and the remaining solvent treated with 1M HCl, yielding the crude product as a yellow solid. After recrystallization from ethyl acetate/methanol **6** was isolated as a yellow solid (1.8 g, 5.71 mmol, 41%). mp: 239.6-241.8 ℃; $^{1}$H-NMR (500 MHz, MeOH-$d_4$): δ 0.91 (t, *J* = 7.0 Hz, 3H), 1.29-1.47 (m, 11H), 1.78 (quint, *J* = 7.5 Hz, 2H), 2.80 (t, *J* = 8.0 Hz, 2H), 4.39 (q, *J* = 8.0 Hz, 2H), 7.72 (d, *J* = 9.0 Hz, 1H), 8.49 (dd, *J* = 2.5, 9.0 Hz, 1H), 9.04 (d, *J* = 2.5 Hz, 1H); $^{13}$C-NMR (125 MHz, MeOH-$d_4$): δ 14.4, 14.6, 23.3, 30.3, 30.5, 30.6, 32.8, 33.8, 62.6, 117.6, 120.8, 123.1, 125.4, 127.8, 144.3, 145.4, 156.8, 167.8, 176.4. LC/MS; *m/z* 360.77 [M + H]$^{+}$, 96.3%.[4]

**General Experimental Information-Biology**

**Chemicals, Bacterial Strains, and Media**

Yeast extract was purchased from Fluka (Neu-Ulm, Germany), peptone from casein from Merck (Darmstadt, Germany), Bacto™ Tryptone from BD Biosciences (Heidelberg, Germany), and Gibco® phosphate-buffered saline (PBS) from Life Technologies (Darmstadt, Germany). Salts and organic solvents of analytical grade were obtained from VWR (Darmstadt, Germany).

*P. aeruginosa* strain PA14 (PA14), the isogenic *pqsH* and *pqsA* transposon mutants, and the isogenic *pqsR* knockout mutant were stored in glycerol stocks at - 80 ℃.

The following media were used: Luria Bertani broth (LB), PPGAS medium,[5] and modified M9 minimal medium (20 mM $NH_4Cl$; 12 mM $Na_2HPO_4$; 22 mM $KH_2PO_4$; 8.6 mM NaCl; 1 mM, $MgSO_4$; 1 mM $CaCl_2$; 11 mM glucose).[6]

**Reporter Gene Assay in *E. coli***

The ability of the compounds to either stimulate or antagonize the PqsR-dependent transcription was analysed as previously described[1] using a β-galactosidase reporter gene assay in *E. coli*

expressing PqsR. Briefly, a culture of *E. coli* DH5α cells containing the plasmid pEAL08-2, which encodes PqsR under the control of the *tac* promoter and the β-galactosidase reporter gene *lacZ* controlled by the *pqsA* promoter, were co incubated with test compound. Antagonistic effects of compounds were assayed in the presence of 50 nM PQS. After incubation, β- galactosidase activity was measured spectralphotometrically at $OD_{420nm}$ using POLARstar Omega (BMG Labtech, Ortenberg, Germany) and expressed as percent stimulation of controls. For the determination of $IC_{50}$ values, compounds were tested at least at eight different concentrations. The given data represent mean values of two experiments with n = 4.

**Reporter Gene Assay in *P. aeruginosa***

In order to study the antagonistic and agonistic properties of compounds **1**, **2** and **3** in *P. aeruginosa*, the PqsR-dependent transcription was evaluated using a β-galactosidase reporter gene assay system. A PA14 strain carrying a non-functional *pqsA* gene to eliminate intracellular HHQ and PQS production was transformed with the plasmid pEAL08-2 and incubated with test compound in the presence or absence of 50 nM PQS and proceeded analogously to reporter gene assay in *E. coli*.

**Measurement of Compound 2 Levels**

In order to strengthen the theory of a possible biotransformation of the antagonistic compound **1** levels of compound **2** produced by *P. aeruginosa* were investigated for PA14, *pqsA* and *pqsH* mutants. Cultures were inoculated with a starting $OD_{600}$ = 0.1 in 100 mL Erlenmeyer flasks containing 50 mL LB medium. DMSO as a control or a DMSO solution of **1** (5 µM) was added to the cultures to a final DMSO concentration of 0.5%. The flasks were incubated at 37 °C, 200 rpm for 16 h. Every 60 min, samples of 995 µL of each culture were taken and supplemented with 15 µL of methanol containing 50 µM of the internal standard (HHQ-$d_4$). The cells were lysed via sonification (amplitude 80%, 1 min) and compound **2** was extracted with 995 µL of ethyl acetate for 1 min. After centrifugation (42,000 *g*, 2 min) 800 µL of the organic phase were transferred to a glass vial for vacuum evaporation. The residues were redissolved in 200 µL of methanol and subjected to UHPLC-MS/MS analysis. For each sample, cultivation and extraction were performed in triplicates.

**UHPLC-MS/MS Analysis of Extracted Compound 2 Levels**

UHPLC-MS/MS analysis was carried out on a TSQ Quantum Access Max mass spectrometer equipped with an HESI-II source and a triple quadrupole mass detector (Thermo Scientific, Dreieich, Germany). For analysis of compound **2**, the following chromatographic conditions were used: 0.00-1.20 min, solvent gradient from 60% A up to 99% A, 1.21-1.80 min, isocratic 99% A,

1.81-2.00 min 60% A. Monitored ions were (mother ion [m/z], product ion [m/z], scan time [s], scan width [m/z], collision energy [V], tube lens offset [V], polarity): compound **2**: 303.088, 217.959, 0.2, 0.010, 32, 114, negative; internal standard (HHQ-$d_4$): 248.340, 163.360, 0.2, 0.010, 32, 113, positive. Samples were injected with a volume of 25 µL. The mobile phase consisted of acetonitrile containing 1‰ TFA (*v/v*; A) and 10 mM ammonium acetate buffer containing 1‰ TFA (*v/v*; B) and a flow rate of 0.8 mL/min. Xcalibur software was used for data acquisition and quantification using a calibration curve relative to the area of the IS.

**Determination of Extracellular HHQ and PQS Levels**

For determination of extracellular levels of HHQ and PQS produced by PA14, cultivation was performed in the following way: cultures (initial $OD_{600}$ = 0.02) were incubated with or without inhibitor (final DMSO concentration 1%, *v/v*) at 37 °C, 200 rpm and a humidity of 75% for 16 h in 24-well Greiner Bio-One (Frickenhausen, Germany) Cellstar plates containing 1.5 mL of LB medium per well. For HHQ analysis, according to the method of Lepine *et al.*,[7] 500 µL of the cultures supplemented with 50 µL of a 10 µM methanolic solution of the internal standard (IS) 5,6,7,8-tetradeutero-2-heptyl-4(1*H*)-quinolone (HHQ-$d_4$) were extracted with 1 mL of ethyl acetate. After centrifugation (18,620 *g*, 12 min), 400 µL of the organic phase were evaporated to dryness and redissolved in methanol. UHPLC-MS/MS analysis was carried out as described in detail by Storz *et al.*.[8] The monitored ions were (mother ion [m/z], product ion [m/z], scan time [s], scan width [m/z], collision energy [V], tube lens offset [V]): HHQ: 244, 159, 0.5, 0.01, 30, 106; HHQ-*d4* (IS): 248, 163, 0.1, 0.01, 32, 113. Quantification of PQS produced by PA14 was performed according to the method of Maurer *et al.*[9] For each sample, cultivation and sample work-up were performed in triplicates. Inhibition values of HHQ and PQS formation were normalized to $OD_{600}$.

**Pyocyanin Assay**

For analysis of pyocyanin formation, cultivation procedure was the same as for HHQ determination with the exception of using PPGAS medium. Pyocyanin produced by PA14 was quantified using the method of Essar *et al.*[10] with some modifications, as described in detail by Klein *et al.*.[11] Briefly, 900 µL of each culture were extracted with 900 µL of chloroform and 800 µL of the organic phase re-extracted with 250 µL of 0.2 M HCl. $OD_{520}$ was measured in the aqueous phase using FLUOstar Omega (BMG Labtech, Ortenberg, Germany). For each sample, cultivation and sample work-up were performed in triplicates. Inhibition values of HHQ and PQS formation were normalized to $OD_{600}$.

**Determination of Growth Curves of PA14 in Minimal Medium**

Cultures of PA14 adjusted to a starting $OD_{600}$ of 0.05 were grown in triplicates in 100 mL Erlenmeyer flasks containing 10 mL modified M9 minimal medium at 37 °C, 200 rpm and a humidity of 75%. DMSO alone or 15 µM DMSO solutions of compound **3** were added to the cultures to a final DMSO concentration of 1% (*v/v*). Bacterial growth was measured as a function of $OD_{600}$ using Thermo Spectronic Helios Epsilon UV-VIS Spectrophotometer (Thermo Scientific, Dreieich, Germany).

***Caenorhabditis elegans* Fast Killing Assay**

*C. elegans* nematodes (Bristol *N2*, wild type, German Center for Neurodegenerative Diseases, Bonn, Germany) were synchronized at fourth larval stage (L4) according to the protocol of *Worm Book* (www.wormbook.org). PA14 was incubated overnight in LB medium in the presence or absence of 15 µM antagonist **3** containing 1% DMSO. After spreading of 10 µL of an overnight bacterial culture, the PGS plates with or without 15 µM antagonist **3** containing 1% DMSO were incubated at 37 °C for 24 h and placed at room temperature for further 16 h. After transfer of 15-20 L4 *C. elegans* onto each plate, the mortality was scored every hour.[12] The nematodes were considered dead or alive based on movements elicited by touching their heads gently with a thin wire or shaking the plates. For each condition, data from three independent experiments were combined.

***Galleria mellonella* Virulence Assay**

*G. mellonella* larvae were purchased from local supplier (Angelsport Becker, Saarbrücken, Germany). For infection of the larvae, bacterial cultures were grown to exponential growth phase, adjusted to an $OD_{600}$ of 1.6 in sterile PBS (pH 7.2), and serially diluted in PBS to obtain a lethal cell density ($7 \pm 1$ CFUs/20 µL). CFUs were determined according to the method of Miles and Misra.[13] Aliquots of 5 µL were injected into the *Galleria mellonella* larvae (average weight $450 \pm 50$ mg) via the hindmost left proleg using a 10 µL Hamilton syringe. Larvae were incubated in Petri-dishes in the dark at 37 °C. Survival rates were monitored in time intervals of 12 h for 108 h post infection. Larvae were considered dead when no movement was observed in response to touch or when melanization of the cuticle occurred.[14] Groups of 15 larvae each were subjected to the following treatments: injection of a) PA14 suspension diluted as described above, b) 10 pmol of compound **3** dissolved in a), c) 5 pmol of compound **3** dissolved in a), d) PA14 isogenic *pqsA* transposon mutant suspension diluted as mentioned above, and e) PA14 isogenic *pqsR* knockout mutant suspension prepared as described above. For each treatment, data from at least two independent experiments were combined.

**Statistical Analysis**

For the animal experiments, statistical analysis was performed using GraphPad Prism 5.04 software. Survival curves were generated by the Kaplan-Meier method and analyzed by the log-rank (Mantel-Cox) test. $IC_{50}$ values were calculated with Origin 8 software.

**Supplementary Results**

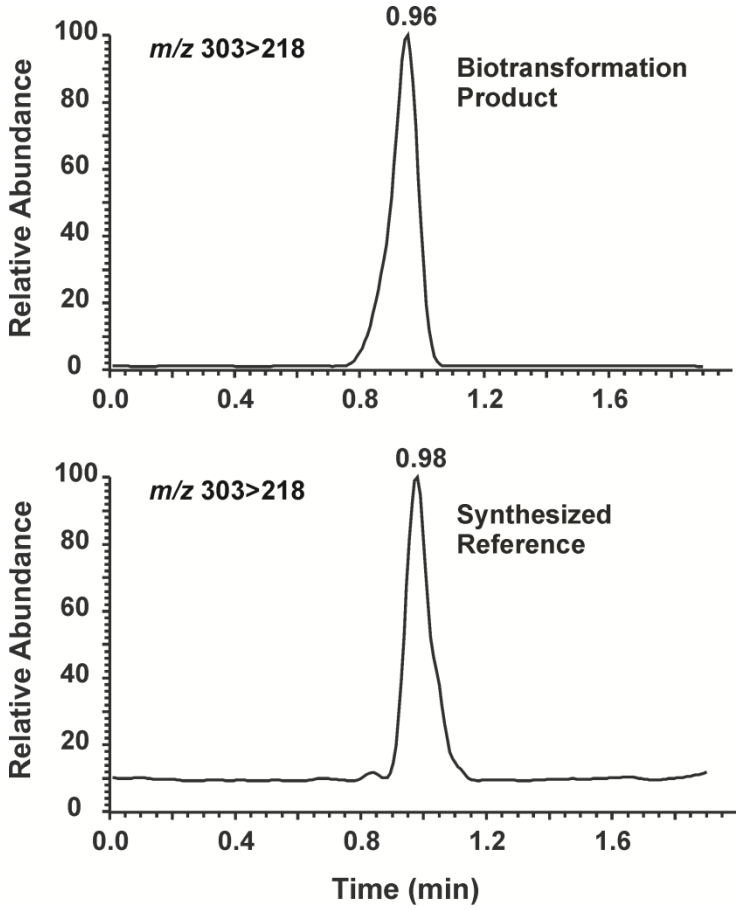


**Figure S1. Chromatograms of SRM transition *m/z* 303>218 indicating biotransformation product (upper diagram) and chemically synthesized reference 2 (lower diagram).**

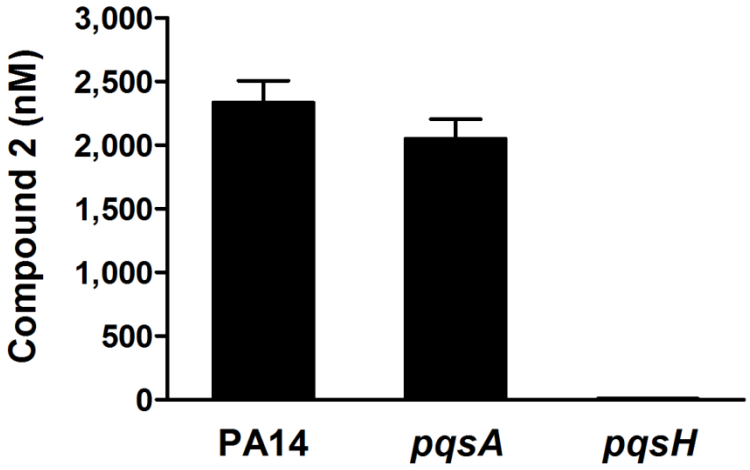

**Figure S2. Production of compound 2 in PA14, *pqsA* and *pqsH* mutants after 16 hours. Strains were incubated with 1 at 5 µM.**

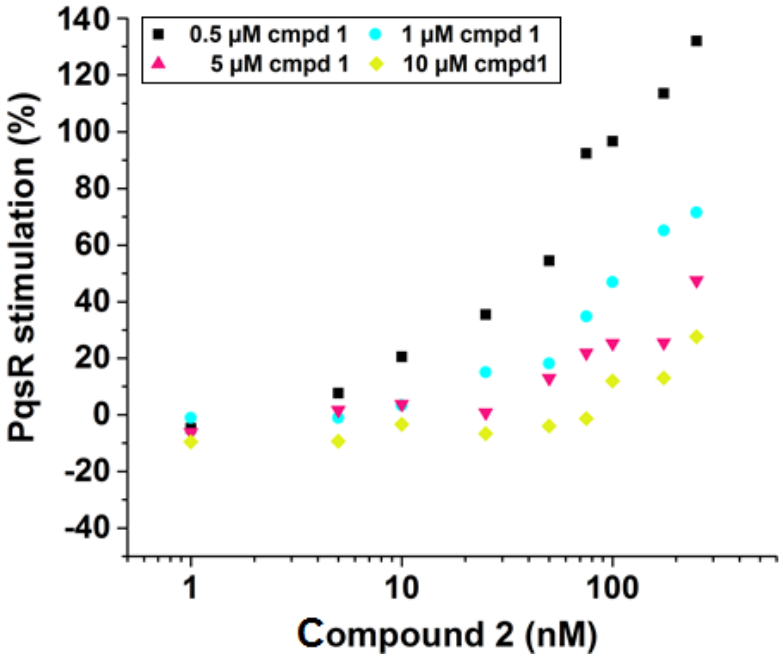


**Figure S3. Competition experiment with PqsR antagonist 1 and agonist 2 in *E. coli* β-galactosidase reporter gene assay.** The assay was performed in the presence of 50 nM PQS. For Y axis, 0% is defined as the basal PqsR stimulation without ligands and 100% is defined as the PqsR stimulation by 50 nM PQS.

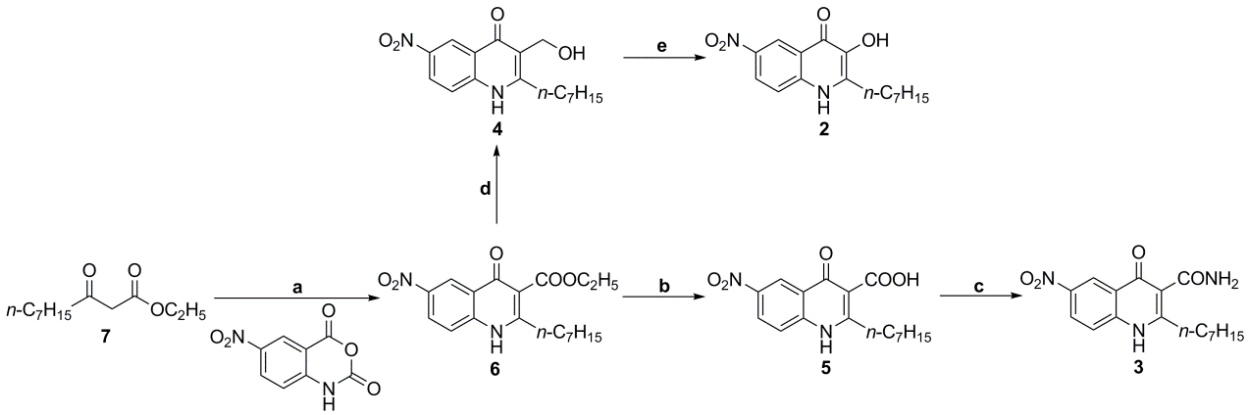


**Figure S4. Synthetic route of compounds 2 and 3.** Reagents and conditions: a) NaH, dry DMF, r.t. then HCl; b) NaOH, $H_2O$, reflux then HCl; c) *N*,*N*'-carbonyldiimidazole, $NH_3$•$H_2O$, dry DMF, 0 ℃ – r.t.; d) $LiAlH_4$, dry THF, 0 ℃ – r.t.; e) $MnO_2$, dry THF, r.t. then $B(OH)_3$, conc. $H_2SO_4$, $H_2O_2$, THF, r.t.

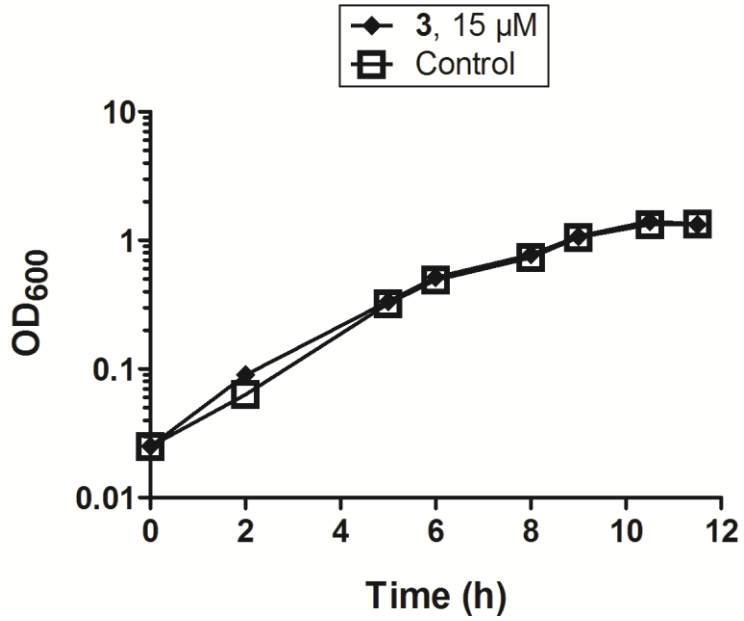


**Figure S5. Growth curves of PA14 in modified M9 minimal medium in the absence (control) and presence of 15 µM of compound 3.**

## References


[1]. C. Lu, B. Kirsch, C. Zimmer, J. C. de Jong, C. Henn, C. K. Maurer, M. Müsken, S. Häussler, A. Steinbach, R. W. Hartmann, *Chem. Biol.* **2012**, *19*, 381-390

[2]. Y. Zhang, W. A. Guiguemde, M. Sigal, F. Zhu, M. C. Connelly, S. Nwaka, R. K. Guy, *Bioorg. Med. Chem.* **2010**, *18*, 2756-2766.

[3]. C. Pidathala, R. Amewu, B. Pacorel, G. L. Nixon, P. Gibbons, W. D. Hong, S. C. Leung, N. G. Berry, R. Sharma, P. A. Stocks, A. Srivastava, A. E. Shone, S. Charoensutthivarakul, L. Taylor, O. Berger, A. Mbekeani, A. Hill, N. E. Fisher, A. J. Warman, G. A. Biagini, S.A. Ward, P.M. O'Neill. *J. Med. Chem.* **2012**, *55*, 1831-1843.

[4]. Purcell, I.C. thesis, University of Nottingham **2007**.

[5]. Y. Zhang, R. M. Miller, *Appl. Environ. Microbiol.* **1992**, *58*, 3276-3282.

[6]. J. Tremblay, E. Deziel, *J. Basic Microbiol.* **2008**, *48*, 509-515.

[7]. F. Lepine, S. Milot, E. Deziel, J. He, L. G. Rahme, *J. Am. Soc. Mass Spectrom.* **2004**, *15*, 862-869.

[8]. M. P. Storz, C. K. Maurer, C. Zimmer, N. Wagner, C. Brengel, J. C. de Jong, S. Lucas, M. Müsken, S. Häussler, A. Steinbach, R. W. Hartmann, *J. Am. Chem. Soc.* **2012**, *134*, 16143-16146.

[9]. C. K. Maurer, A. Steinbach, R. W. Hartmann, *J. Pharm. Biomed. Anal.* **2013**, http://dx.doi.org/10.1016/j.jpba.2013.07.047.

[10]. D. W. Essar, L. Eberly, A. Hadero, I. P. Crawford, *J. Bacteriol.* **1990**, *172*, 884-890.

[11]. T. Klein, C. Henn, J.C. de Jong, C. Zimmer, B. Kirsch, C. K. Maurer, D. Pistorius, R. Müller, A. Steinbach, R. W. Hartmann, *ACS Chem. Biol.* **2012**, *7*, 1496-1501.

[12]. S. Mahajan-Miklos, M. Tan, L. G. Rahme, F. M. Ausubel, *Cell* **1999**, *96*, 47-56.

[13]. A. A. Miles, S. S. Misra, J. O. Irwin, *J. Hyg. (Lond)* **1938**, *38*, 732-749.

[14]. G. Jander, L. G. Rahme, F. M. Ausubel, *J. Bacteriol.* **2000**, *182*, 3843-3845.

# 6.3 Curriculum Vitae

## Persönliche Daten

**Name:** Cenbin Lu

**E-Mail:** c.lu@mx.uni-saarland.de

**Geschlecht:** männlich

**Geburtsjahr:**1984

**Geburtsort:** Changsha, Provinz Hunan,V.R. China

**Staatsangehörigkeit:** chinesisch

**Familienstand:** verheiratet

## Schulausbildung

| | |
|---|---|
| 09/1990–06/1996 | Grundschule |
| 09/1996–06/2002 | Gymnasium |
| 2002 | Abitur |

## Berufsausbildung/Studium

| | |
|---|---|
| 09/2002–06/2006 | Institut für Pharmazie, Central South University, V.R. China |
| 2006 | Abschluss als Bachelor |
| 09/2006–06/2009 | Institut für Pharmazie, Central South University, V.R. China |
| 2009 | Abschluss als Master |
| 09/2009– | Helmholtz-Institut für Pharmazeutische Forschung Saarland (HIPS) und Institut Pharmazeutische und Medizinische Chemie, Universität des Saarlandes, Deutschland, Doktorand |